1-1-1976

Application of neutron noise analysis and pattern recognition techniques to in-core surveillance of nuclear reactors

Kevin Carl Holthaus
Iowa State University

Application of neutron noise analysis and pattern recognition techniques to in-core surveillance of nuclear reactors

by

Kevin Carl Holthaus

A Thesis Submitted to the
Graduate Faculty in Partial Fulfillment of
The Requirements for the Degree of
MASTER OF SCIENCE

Department: Chemical Engineering and Nuclear Engineering
Major: Nuclear Engineering

Iowa State University
Ames, Iowa

1976

TABLE OF CONTENTS

LIST OF FIGURES

LIST OF TABLES

I. INTRODUCTION

A. Preamble

In-core neutron detectors provide sensor signals essential to the operation of a nuclear power station. These sensor signals consist of a mean value component (d-c level) and a superimposed randomly fluctuating component (noise signal). In monitoring reactor parameters such as power or neutron flux levels, utilities operating the nuclear units primarily use the sensor's mean value component, ignoring or even attempting to eliminate the fluctuating portion. The extraction of useful information from the fluctuating component of the sensor signal is not a new technique, but it has not been routinely applied to operating commercial power reactors.

In a noise analysis system the randomly fluctuating signals under investigation are often transformed into power spectral density (PSD) estimates in the frequency domain using Fourier transform techniques. In-core vibrations usually occur at specific frequencies and are easily detected with a noise analysis surveillance system.

Neutron noise analysis surveillance systems have recently become of interest to the owners and operators of boiling water reactors (BWR's), specifically those incorporating bypass flow holes for cooling the in-core instrument tubes. The reason for this interest was prompted by the discovery of significant wear on the corners of some fuel assembly channels adjacent to in-core neutron monitor and startup source locations. Out-of-reactor testing by the vendor showed wear to be caused by flow induced vibrations of the in-core instrument tubes

against the channel corners. Use of noise analysis equipment in the BWR's confirmed these postulated vibrations. Forced plant outages of five weeks or more were required in some instances for plant modification designed to reduce the vibration amplitude.

Thus the need has arisen for a system which will monitor the core of the reactor for vibrations or other anomalous behavior. An efficient method of in-core surveillance which requires a minimal amount of human interpretation and decision making is that of a neutron noise analysis-pattern recognition system. Pattern recognition requires the use of a computer to determine the normality of a new "noise signature" or PSD data set based upon the previous operating history of the reactor. This history consists of data files with normal and abnormal (if present) noise signature sets of earlier PSD data.

B. Statement of the Problem and Its Importance

The source of data for this research project was the Duane Arnold Energy Center (DAEC) reactor which is operated by Iowa Electric Light and Power Company. The DAEC unit is a 550 Mw(e) boiling water reactor located near Palo, Iowa.

The purpose of the study was to:

(1) collect a library of noise signatures for the DAEC BWR,

(2) develop and demonstrate an off-line system capable of detecting abnormal operating conditions,

(3) examine the effects on PSD of changing reactor conditions such as power and coolant flow rate, and

(4) evaluate the effectiveness of blocking bypass flow holes to reduce in-core vibrations.

In addition to safety related aspects of plant operation, economic considerations are perhaps the most important factor in determining the need for a surveillance system. If a system can provide warnings of an incipient component failure the utility may undertake repair of the component during a scheduled shutdown or limit the extent of repairs that would be required under a forced shutdown situation.

Forced shutdown costs for 100% emergency power replacement during peak demand periods average $400,000 per day. Even "planned" forced outages (such as the bypass flow hole plugging shutdown) require the purchase of discounted (~ 35%) emergency power. Assumption of this discount rate during a nonpeak demand period and a requirement for only 50% power still result in a cost of over $100,000 per day.

With downtime cost penalties of several hundred thousand dollars per day for replacement of electrical power, the incentive for employing surveillance systems (capable of reducing the number of forced outages or outage time) increases. Elimination of wasteful deratings based on inadequate information concerning component conditions is also possible in specific situations.

II. LITERATURE REVIEW

Methods for the extraction of useful information from noise signals in the time, amplitude, and frequency domains are adequately described in several current texts [1-3]. Useful descriptors in the time domain include RMS levels and auto- and cross-correlations. Probability density and distribution functions feature amplitude analysis. Frequency domain variables include auto- and cross-spectral densities and coherence. Frequency domain analysis currently has wider use and is more suitable for vibration surveillance. The fast Fourier transform [4], a computational technique for conversion of data into the frequency domain, has become a necessary step in the analysis of reactor neutron noise.

Surveillance of nuclear reactors using neutron noise analysis techniques has been used in the successful diagnosis of incipient component failure in control rod bearings at the HFIR [5], detection of core-barrel motion of the Palisades pressurized water reactor [6], and confirmation of in-core instrument tube vibration in a number of BWR/4's [7, 8]. Identification of the sources of abnormal behavior is not immediately obvious. Thie [9] discusses the main signals of importance which can be identified.

Thie [9] summarizes reactor monitoring instrumentation and the associated parameters which can be used to provide noise signals for a surveillance system. These include temperature sensors (thermocouples), vibration transducers (linear differential transformers, velocity

sensors, and accelerometers), acoustic monitors (acelerometers), strain gauges, and pressure and flow sensors.

Since neutron noise surveillance requires "normal" noise signatures for the determination of current abnormalities, a trained noise analyst is often required. Computer oriented pattern recognition applied to noise analysis measurements offers the advantage of machine decision-making and efficiency. Gonzalez et al. [10, 11] and Kryter et al. [12] used the ISODATA algorithm [13] in their noise analysis-pattern recognition surveillance system for the HFIR to show how noise signatures changed with time. Piety and Robinson [14] and Piety [15] demonstrated the use of an on-line reactor surveillance system, using an algorithm based on the multi-variate analysis of noise.

In most nuclear power plants in-core neutron sensors now being utilized are adequate and capable of supplying the signals needed for noise analysis systems. Process computers used for reactor operations may be suitable for use with a pattern recognition system although additional equipment such as FFT analyzers will be needed for a complete surveillance system.

III. THEORY

A. Introduction to Reactor Malfunction Monitoring

Mechanical and structural integrity of nuclear reactor components and systems are initially insured by the manufacturer's quality-assurance programs. Once reactor operation has commenced, however, dynamic conditions may alter the mechanical and hydraulic integrity of various components making it difficult to continue assurance of these systems.

Some of the potential mechanical/hydraulic malfunctions are given by Thie [9] to be:

(1) fatigue or cracks in the metal of the vessel internal structure or piping,

(2) bolts or other means of fastening which have come loose,

(3) wearing away of metal,

(4) control-rod-movement abnormalities,

(5) flow blockage caused by accumulations, foreign materials in the system, or structure that has broken loose,

(6) excessive vibrations, and

(7) instabilities or other departures from normal cooling.

With the high costs of reactor down-time, forced shutdowns due to unexpected complications comprised of any of the above seven conditions must be minimized. Thus the need exists for reactor surveillance systems capable of detecting abnormal operating conditions and providing operational quality assurance.

The traditional methods of monitoring reactor operation rely primarily upon mean value measurements, and the associated circuitry is often designed to smooth or remove any randomly fluctuating component (noise) superimposed upon this mean value component. The mean value measurements yield little if any information concerning dynamic changes taking place (such as low-amplitude in-core vibration).

A specific group of BWR's, incorporating one-inch diameter bypass flow holes in the core support plate to allow a high velocity jet of coolant flow past in-core instrument tubes, have recently come under the scrutiny of the Nuclear Regulatory Commission. Early warning of vibrational problems were encountered during refueling of the Tokyo Electric Power Company's Fukushima 1 reactor when fuel assembly channels were found to exhibit severe corner wear adjacent to the in-core neutron monitor and startup source locations. Other reactors designed by the same vendor and of the BWR/4 product line (which incorporated the bypass flow holes) were immediately suspected of having similar in-core vibrational problems. The jet of coolant passing through the bypass flow holes caused cross-flow-induced vibrations of the in-core instrument tubes against the surrounding structure. Wear created by these vibrations was sufficient to change normal flow patterns which would alter the performance of the reactor during the design base accident (DBA), i.e. the loss of coolant accident (LOCA), when removal of fission product decay heat is necessary. The use of noise analysis equipment by the reactor vendor corroborated the postulated vibrations in the other BWR/4's with bypass flow holes. Modification to significantly reduce the in-core vibrations of the

BWR/4's was made by plugging all the bypass flow holes, however, this lead to derating of the nuclear units due to changes in the thermal hydraulic margins for the DBA.

In retrospect, if noise surveillance systems had been used during startup of the first BWR/4, design modifications could have been incorporated into later-built units eliminating the in-core high-amplitude vibration problems.

B. Neutron Noise Analysis in the Frequency Domain

1. Review of neutron noise analysis principles

Before proceeding further it will be necessary to briefly review the random process theory essential to the work performed in this project. One of the first steps is the development of appropriate terminology to be employed in describing the characteristics of any given process. A convenient approach is to use descriptors, arranged in pairs, and to select one name from each pair to describe the process. Descriptor pairs appropriate to reactor noise analysis are:

(1) continuous; discrete,

(2) deterministic; nondeterministic,

(3) stationary; nonstationary, and

(4) ergodic; nonergodic.

A continuous random process is one in which the random variables can assume any value within a specified range of possible values. This range may be finite, infinite, or semi-infinite. This definition

implies that the probability density function is continuous and has no delta functions in it. A discrete random process is one in which the random variable can assume only certain isolated values and no others. The probability density function for a discrete random process will consequently consist of a series of delta functions.

A process for which the future values of any sample function can be exactly predicted from past values is said to be deterministic. A nondeterministic sample function is a random function of time and its future values cannot be predicted from previous values.

If all marginal and joint density functions of a process do not depend upon the choice of the time origin, the process is said to be stationary. This implies that all mean values and moments are constants independent of the absolute value of time. The above requirements for determining if a process is stationary are usually more stringent than necessary. A more relaxed requirement is that the mean value and autocorrelation function be independent of the time origin. Processes satisfying these criteria are said to be stationary in the wide sense. It will further be assumed in this work that "stationary" will mean stationary in the wide sense. A process whose mean and autocorrelation function vary with different choices of time origin are nonstationary.

Some stationary random processes possess the property that almost every member of the ensemble exhibits the same statistical behavior that the whole ensemble has. Ergodic processes are those which allow this determination of the statistical behavior by examination of only one sample function. The mean values and moments can be determined

by time averages as well as by ensemble averages. Thus the nth moment for variable X is given by

$$\hat{\overline{X}} \triangleq \frac{1}{T}\int_0^T X^n(t)dt \approx \int_{-\infty}^{\infty} x^n p(x)dx \tag{3.1}$$

where x is the true function and p(x) is its probability density function. If $\hat{\overline{X^n}}$, the nth moment of a sample, is to be a good estimate of $\overline{X^n}$, the two should be equal. Upon further examination the expected value of $\hat{\overline{X^n}}$ is

$$\begin{aligned} E[\hat{\overline{X^n}}] &= E[\frac{1}{T}\int_0^T X^n(t)dt] = \frac{1}{T}\int_0^T E[X^n(t)]dt \\ &= \frac{1}{T}\int_0^T \overline{X^n}\, dt = \frac{1}{T}\,[\overline{X^n}\, t\Big|_0^T] \\ &= \overline{X^n} \end{aligned} \tag{3.2}$$

It is clear from Equation 3.2 that $E[\hat{\overline{X^n}}]$ has the proper nth moment. Nonergodic processes are those who do not possess the property of Equation 3.1.

Before applying the random process descriptors to neutron detector noise, it will first be necessary to examine the components of a neutron sensor signal output as shown in Figure 3.1.

As previously stated, the output signal from a neutron detector consists of a randomly fluctuating component (noise) superimposed on a mean value or d-c level. Removal of the d-c component is necessary to examine only the noise (which has a mean value of zero). Figure 3.2 shows an ensemble or collection of noise sample functions

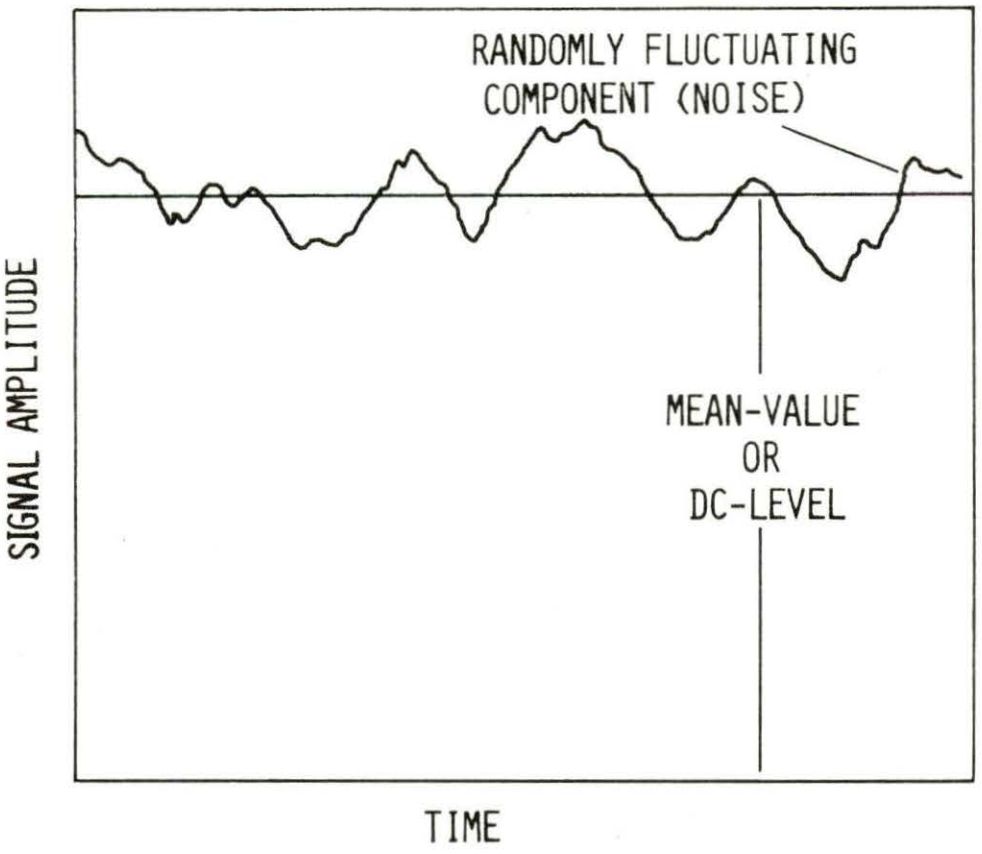

Figure 3.1. Components of a neutron sensor signal.

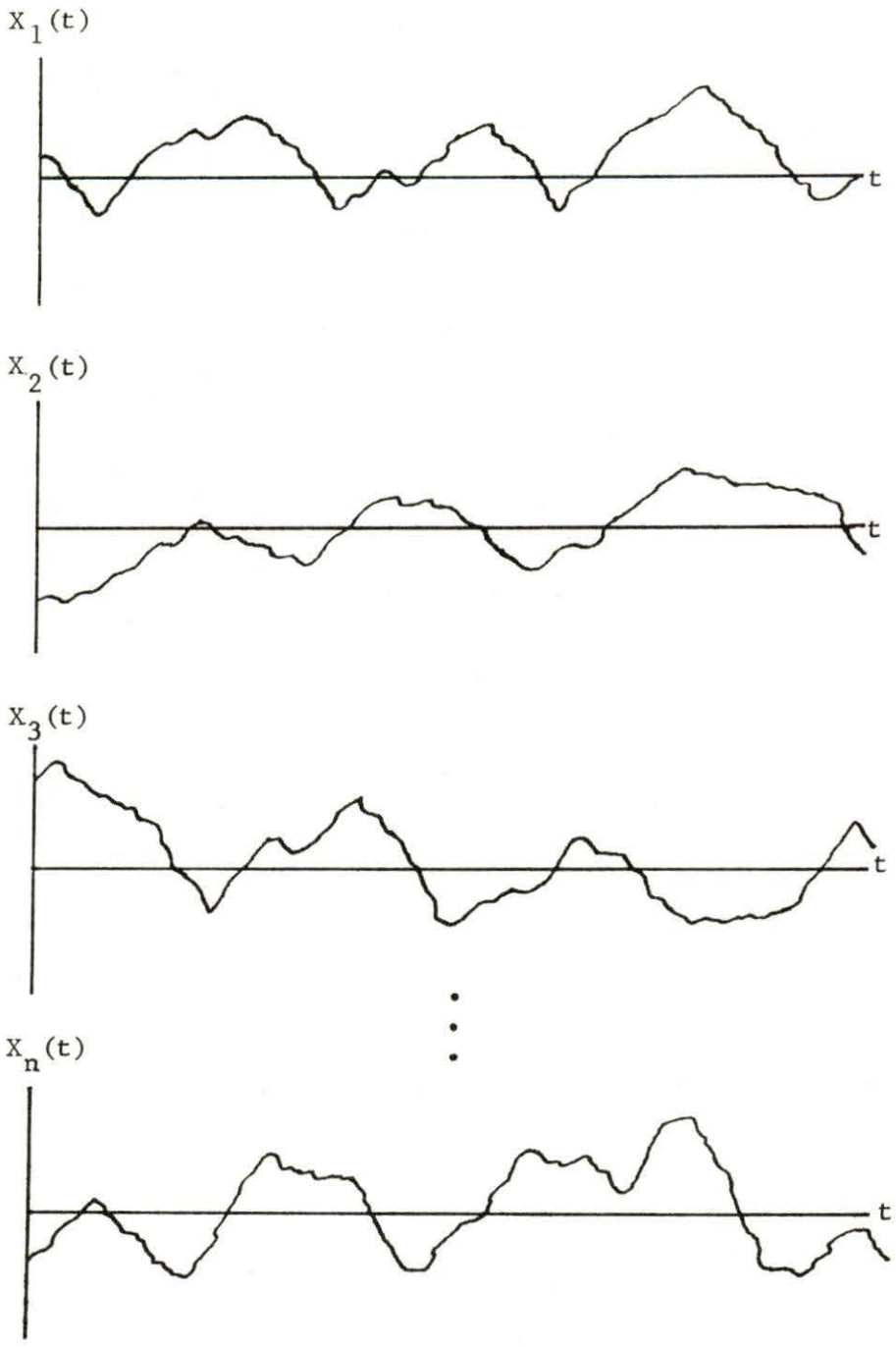

Figure 3.2. Ensemble of sample functions from a neutron sensor forming a random process.

similar to what might be obtained from a neutron sensor. Using the descriptors previously defined the process is:

(1) continuous: it can assume any value within a specified range,

(2) nondeterministic: exact future values cannot be determined from random time functions,

(3) stationary: choice of time origin has no effect on the statistical properties, and

(4) ergodic: Equations 3.1 and 3.2 are applicable.

It is very important that the ensemble data be obtained over a period of time in which the reactor operating parameters, such as power or flow rate, are not changing. If changes do take place over the data measurement period, the ensemble will be comprised of nonstationary and consequently nonergodic data as shown for two sample functions in Figure 3.3. Sample function $X_1(t)$ might have been obtained at some initial power level P_0. An increase in power to $P_0 + \delta P$ results in two changes shown in $X_n(t)$. First there is an increase in the d-c level to $\overline{X} + \delta\overline{X}$ (where $\overline{X}$ has already been removed), and secondly there should be a change in the noise characteristics with power.

Time domain descriptors of random data are not used in the data analysis of this research, but it is important to briefly review the autocorrelation function. The autocorrelation function of random data describes the general dependence of the data at a given time on the values at another time. One would expect random variables separated by very small time increments to be highly correlated and those widely

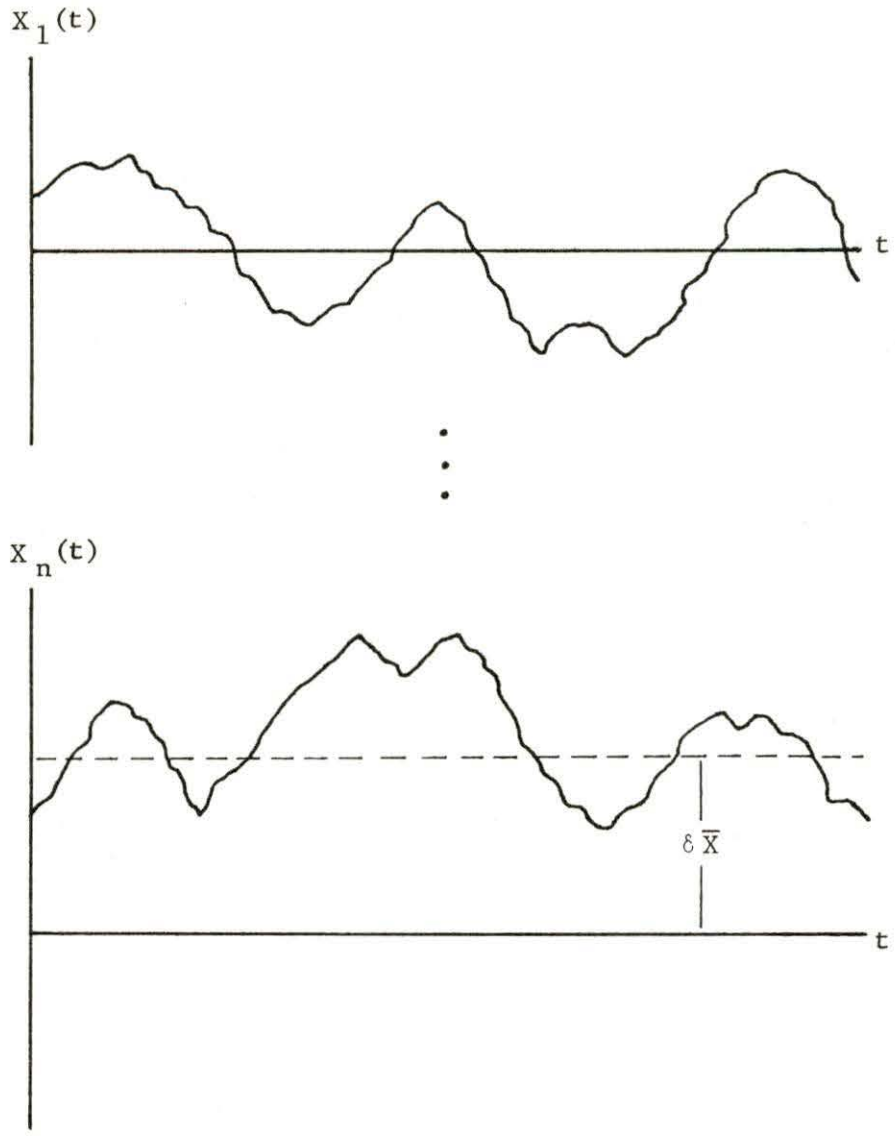

Figure 3.3. Effects of nonstationary data in the nth record due to changing reactor operating conditions (power).

separated to be uncorrelated. If X(t) is a sample function from a random process, and the random variables are defined to be

$$X_1 = X(t_1)$$

$$X_2 = X(t_2) = X(t_1 + \tau)$$

where τ is the time interval spacing ($\tau = t_2 - t_1$), the autocorrelation function is defined by

$$R_x(t_1, t_2) = E[X_1X_2] = \int_{-\infty}^{\infty} dx_1 \int_{-\infty}^{\infty} x_1x_2p(x_1, x_2)dx_2 \qquad (3.3)$$

For stationary processes all ensemble averages are independent of the choice of the time axis, so the autocorrelation function may be written as

$$R_x(t, t + \tau) = E[x(t)x(t + \tau)]$$

or simply

$$R_x(\tau) = E[x(t)x(t + \tau)] \qquad (3.4)$$

The analysis of noise data is most conveniently done after it has been transformed into the frequency domain. The most natural representation of this sort is the Fourier transform which leads to the concept of spectral density. For a nonrandom time function, x(t), its Fourier transform is given by

$$X(\omega) = \int_{-\infty}^{\infty} x(t)e^{-j\omega t}dt$$

or

$$X(f) = \int_{-\infty}^{\infty} x(t)e^{-j2\pi ft}dt \tag{3.5}$$

where the units of ω and f are radians per second and hertz, respectively. If x(t) is a voltage then X(f) has the units of volts per hertz and represents the relative magnitude and phase of steady state sinusoids that can be summed to produce the original x(t). The physical significance of the Fourier transform is that it gives an indication of how the energy of x(t) is distributed with respect to frequency.

The two-sided power spectral density, $S_x(\omega)$ is given by

$$S_x(\omega) = \lim_{T\to\infty} \frac{E[|X(\omega)|^2]}{2T} \tag{3.6}$$

If x(t) is a voltage, then $S_x(\omega)$ has the units of volts^2/hertz, and its integral leads to the mean-square value

$$\overline{x^2} = \frac{1}{2\pi}\int_{-\infty}^{\infty} S_x(\omega)d\omega \tag{3.7}$$

In the application to reactor noise analysis only positive frequency components of power spectral density exist, and a one-sided PSD is utilized. This one-sided spectral density, $G_x(f)$ is related to $S_x(\omega)$ by

$$G_x(f) = 2S_x(\omega) = 2S_x(2\pi f) \tag{3.8}$$

and Equation 3.7 becomes

$$\overline{x^2} = \int_0^{\infty} G_x(f)df \tag{3.9}$$

Another useful relationship known as the Wiener-Khinchine relation states that the power spectral density of a stationary random process is just the Fourier transform of the autocorrelation function; that is,

$$G_x(f) = \mathcal{F}\{R_x(\tau)\}$$

$$= 2\int_0^\infty R_x(\tau)e^{-j2\pi f\tau}d\tau \tag{3.10}$$

Direct calculation of the power spectral density estimate, $\hat{G}_x(f)$, is performed through the use of digital computers and the fast Fourier transform using the equation

$$\hat{G}_x(f) = \frac{2h}{N}|X(f)|^2 \tag{3.11}$$

where N is the number of data points used, h is the spacing between successive sampled points ($1.0/f_s$), and X(f) is the Fourier transform consisting of real and imaginary parts.

2. At-power reactor noise

The power spectral density obtained from an at-power nuclear reactor is very much different from the classical zero-power reactor PSD. The neutron signal PSD obtained using an ionization chamber in a reactor operating at power is given by [16]

$$PSD(\omega) = w_n\overline{Fq^2} + w_n^2\overline{Fq}^2 D|H_0(\omega)|^2$$

$$+ w_n^2\overline{F}^2\overline{q}^2|H_0(\omega)|^2|\rho_{dr}(\omega)|^2 \tag{3.12}$$

where the first term represents white noise from the detection process, the second term represents neutron power spectral density due to internal or noise equivalent source [17], and the last term is the neutron noise caused by external reactivity driving forces (perturbations) such as in-core component vibrations. w_n is the detector efficiency, $\bar{q}$ is the mean charge transferred per neutron absorbed in the detector, $\overline{q^2}$ is the mean square value of q, F is the fission rate or power level, D is the Diven factor $(\frac{\overline{\nu(\nu - 1)}}{\bar{\nu}^2})$, $H_0(\omega)$ is the at-power reactor transfer function, and $|\rho_{dr}(\omega)|^2$ stands for the power spectrum of all normal and abnormal (anomalous) reactivity driving forces, that is,

$$\rho_{dr} = \sum_i \rho_{dr_i}(\omega)$$

The first two terms of Equation 3.12, being proportional to the power level (fission rate), become insignificant in a reactor operating at even a few megawatts (provided $|\rho_{dr}|^2$ is not equal to zero). The PSD is now approximately equal to the third term, the noise due to external reactivity fluctuations, which is proportional to the power squared. Equation 3.12 may now be rewritten as

$$PSD(\omega) \simeq w_n^2 F^2 \overline{q}^2 |H_0(\omega)|^2 |\rho_{dr}(\omega)|^2 \qquad (3.13)$$

The average ion chamber current I_{dc} is given by

$$I_{dc} = F w_n \bar{q}$$

so Equation 3.13 becomes

$$PSD(\omega) \simeq I_{dc}^2 |H_0(\omega)|^2 |\rho_{dr}(\omega)|^2$$

It should be noted that I_{dc} is proportional to the neutron flux, so the PSD is proportional to the flux squared. Denoting the flux as ϕ the previous equation can be written

$$PSD(\omega) \propto \phi^2 |H_0(\omega)|^2 |\rho_{dr}(\omega)|^2 \tag{3.14}$$

For experimental work at DAEC, in-core fission chambers were utilized for neutron detection, and the voltage output was analyzed. Since the voltage output of a fission chamber is proportional to neutron flux, Equation 3.14 can be modified for use with the equipment used at DAEC; that is

$$PSD(\omega) \propto v_{fc}^2 |H_0(\omega)|^2 |\rho_{dr}(\omega)|^2 \tag{3.15}$$

where v_{fc} represents a fission chamber mean voltage.

Normalization of all noise signatures is necessary to permit comparison of frequency spectra from various power levels and for noise magnitude as well as shape differences. This normalization corrects both the detector sensitivity and neutron density at the detector location. Equation 3.15 shows that v_{fc}^2 may be used as the normalization factor when the PSD's are divided by it. It should be noted that the units of the normalized PSD's are hertz^{-1}, and it is $|\rho_{dr}(\omega)|$, the external reactivity driving perturbations, that is being examined.

Since $|H_0(\omega)|^2$ is essentially a smooth function over the range in which flow-induced component vibrations take place, the shape of the normalized noise signature is that of $|\rho_{dr}(\omega)|^2$. The effect of

the $|H_0(\omega)|^2$ term is to amplify $|\rho_{dr}(\omega)|^2$, so it is easily observed during the normal operation of the reactor. Detection of abnormal conditions requires that the power spectrum of the anomalous reactivity be at least of the same order as the power spectrum of the normal driving reactivities at the frequencies being sampled.

Neutron noise in BWR's is believed to be separable into global and local components [18]. Fry [8] states that the global noise due to core reactivity changes dominates in the frequency range from 0.0 to approximately 2.0 hertz, whereas the local noise is caused by voids, vibrations, and other perturbing conditions in the vicinity of the detector and is significant from approximately 1.0 to 10.0 hertz. Since the global noise is much lower in amplitude above 1.0 hertz, mechanical vibrations greater than 1.0 hertz should be detectable. If a local noise component is present, it will appear as an additional term in Equation 3.12.

C. Pattern Recognition Techniques

1. Introduction

Determination of anomalous reactor behavior, such as in-core component vibration, through the use of neutron noise analysis requires standards (baseline data) of normal reactor behavior for comparison. Since the noise signatures vary with fuel burnup and operating conditions it is necessary to keep and maintain an operating history or library of PSD data. In addition to the normal records, abnormal data should also be kept for reference as a standard of abnormality. Thus a library of noise signatures define normal reactor operation and

provide a standard for the identification and source of degree of difficulty should any abnormalities be detected.

The collection and analysis of large groups of PSD data require the use of a trained noise analyst for determination of abnormal reactor behavior. Computer-based pattern recognition offers the advantage of being able to perform the analyst's tasks in less time, at a relatively low price, and yet with a sufficiently high reliability for the detection of abnormal reactor operation.

2. Terminology

A pattern is a mathematical representation of a physical quantity and can be considered as a column vector in n-dimensional Euclidean space. A noise signature may be represented as an n-dimension pattern vector such that

$$\underline{PSD} = (PSD(f_1), PSD(f_2), PSD(f_3), \ldots, PSD(f_n))^T \qquad (3.16)$$

where the "T" indicates transposition. In the above equation $PSD(f_1)$ represents the power spectral density at frequency f_1.

Pattern recognition theory is simply that body of knowledge which pertains to the design of pattern recognition systems. The recognition process is one of assigning given patterns to one of several predefined groups or categories based on pattern similarities. When using noise signature patterns from nuclear reactors one may be concerned with classification into either normal or abnormal categories. The normal category contains several classes corresponding to different reactor operating conditions. When examining patterns which have been

categorized as being abnormal, the degree of abnormality is important in determination of how close a component is to failure.

Two basic approaches exist which may be followed during the development of a pattern recognition system. The supervised approach consists of gathering representatives of each normal class and using these patterns to adaptively train the system to recognize and classify the sample sets. This approach requires supervision by indicating to the system the class of each sample during the training process.

The unsupervised approach utilizes techniques which accomplish learning without prior knowledge of the characteristics and classes present in the data sets. Thus categorization and classification of large groups of data containing unknown characteristics is possible. Since no extensive libraries of noise signature patterns exist for any commercial operating nuclear reactor, this approach offers the greatest potential for the development of a noise analysis-pattern recognition surveillance system. Another feature of this technique is that it requires a minimal amount of human intervention for its operation.

The basis for classification of patterns in this research is a univariate, hyperspace Euclidean distance. For an n-dimensional pattern, the distance between it and any cluster center (or the "mean vector" of a pattern class) is given by

$$D_{ij} = \left\{ \sum_{k=1}^{n} [PSD_i(f_k) - Z_j(f_k)]^2 \right\}^{1/2} \qquad (3.17)$$

where i represents the ith pattern, j represents the jth cluster center, f_k is the kth dimensional frequency, and Z_j is the jth cluster center vector. A pattern is assigned to a cluster center (pattern class)

$j = m$ when its hyperspace distance is less than any other distance; that is,

$$D_{im} < D_{ij} \text{ for all } j \neq m$$

3. The pattern recognition algorithm

The algorithm used for the pattern recognition portion of the off-line reactor surveillance system is based on the ISODATA (Iterative Self Organizing Data Analysis Technique A, the A being added to make the word pronouncable) algorithm [13] developed at the Stanford Research Institute. Many of the steps in the algorithm resulted from experience gained through experimentation. Since patterns of higher dimensionality are needed in the analysis of reactor noise (more than intended in the original algorithm), modifications of ISODATA were required. A listing and brief explanation of the modified algorithm (MISODATA) used in the pattern recognition system is presented in Appendix A.

Further discussion of the algorithm and its use are included in the experimental work.

IV. EXPERIMENTAL WORK

A. Data Analysis Procedures

1. Data acquisition

The neutron noise signals monitored at DAEC were obtained from fission chambers located at various radial and axial positions in the core of the reactor. The signals were obtained from the Local Power Range Monitor (LPRM) circuitry associated with each detector. These are 20 vertical strings of fission chambers (or instrument tubes), each containing four fixed position detectors and one traversing in-core probe (TIP), dispersed at regular intervals in the core. The four fixed position detectors labeled A, B, C, and D in each string are located at 18, 54, 90, and 126 in. from the bottom of the core, respectively. A cross sectional view of the LPRM in-core assembly showing its location in the coolant channel is shown in Figure 4.1. It should be noted that it was these instrument tubes containing the LPRM fission chambers that were severely vibrating against the surrounding structure prior to bypass flow hole plugging.

Initial selection of the LPRM strings to be monitored in this study was based on the following criteria:

(1) the 16-09 LPRM exhibited a large amount of noise (in tests by the reactor vendor) due to vibration of the instrument tube in the coolant channel prior to the bypass hole plugging (June-July 1975),

(2) the 40-17 LPRM string was quiet and exhibited a very small amount of the (1) above problems, and

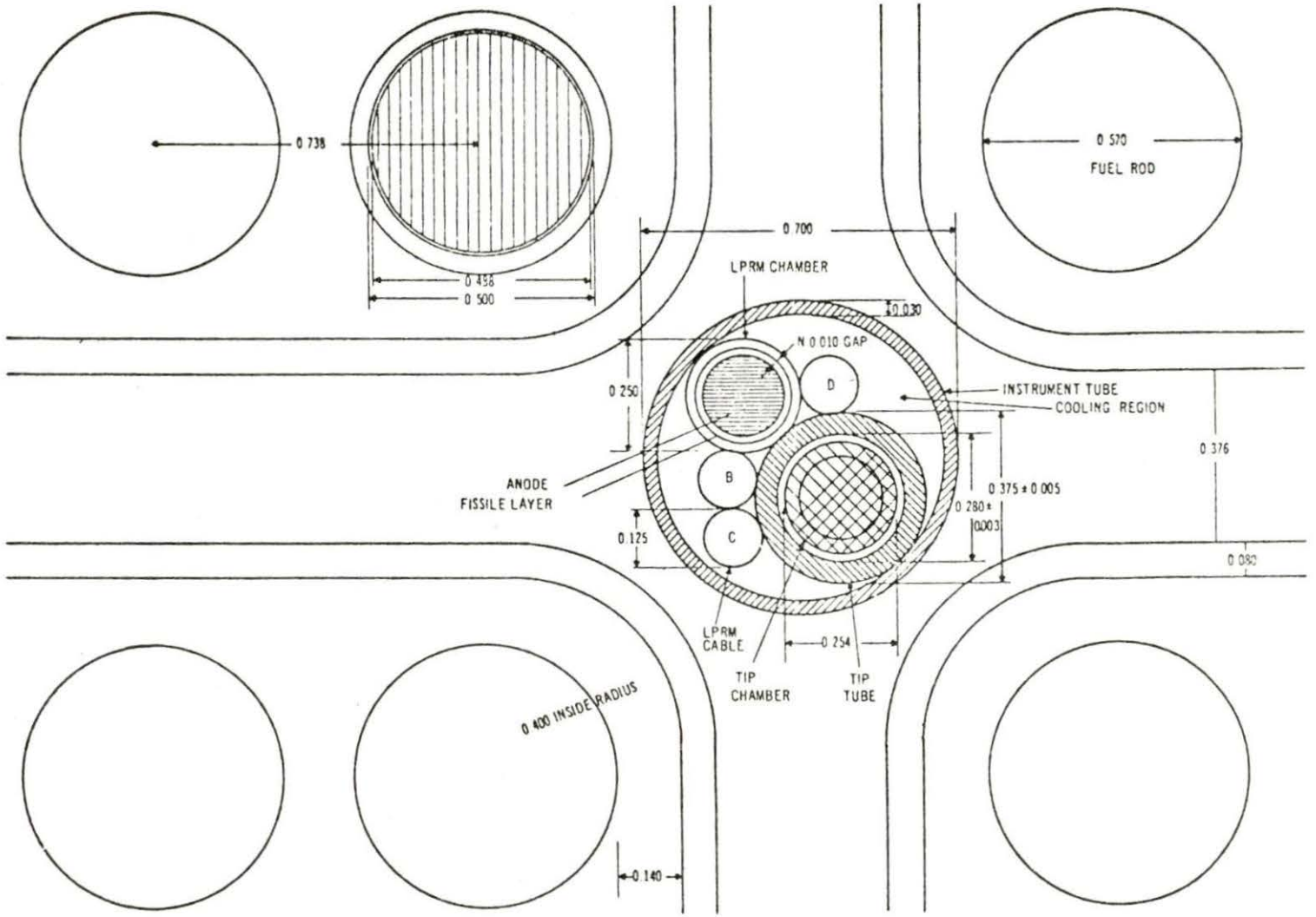

Figure 4.1. LPRM in-core instrument tube cross section.

(3) the 24-25 LPRM string was located near the center of the core where the radial neutron flux has the highest value.

Figure 4.2 shows the layout of the DAEC reactor core and the locations of the LPRM strings monitored in this research. Due to time factors involved in data analysis and processing only the most interesting LPRM's, the 16-09 string, will be examined in this research project.

Prior to plugging, the number of bypass flow holes located in the core support plate near each LPRM string varied depending upon the location in the core. There were five LPRM's with no bypass flow holes, three with one hole, two with three holes, and ten with four holes. The 16-09 LPRM string contained three bypass flow holes while the 24-25 string had four, and the 40-17 string had none. Peripheral locations required fewer flow holes for cooling, since the heat flux is lower in these regions; central locations required the largest number, since more heat removal was needed.

The acquisition of analog data at DAEC is best described by referral to Figure 4.3, which shows the flow process for obtaining the data from one LPRM string. The first step is the removal of each detector signal's mean value component which is necessary to prevent overloading at the input of the FM tape recorder. Next the noise signals are amplified through a gain of eight and are routed to the inputs of the Precision Instrument Company Model PI-6200 four channel FM tape recorder. The adjustable second order filter in the tape recorder, serving to suppress the higher frequency components (anti-aliasing filtering) not of interest in the analysis, requires a cutoff frequency setting of 1000 hertz during recording at a tape speed of 3-3/4 ips. The

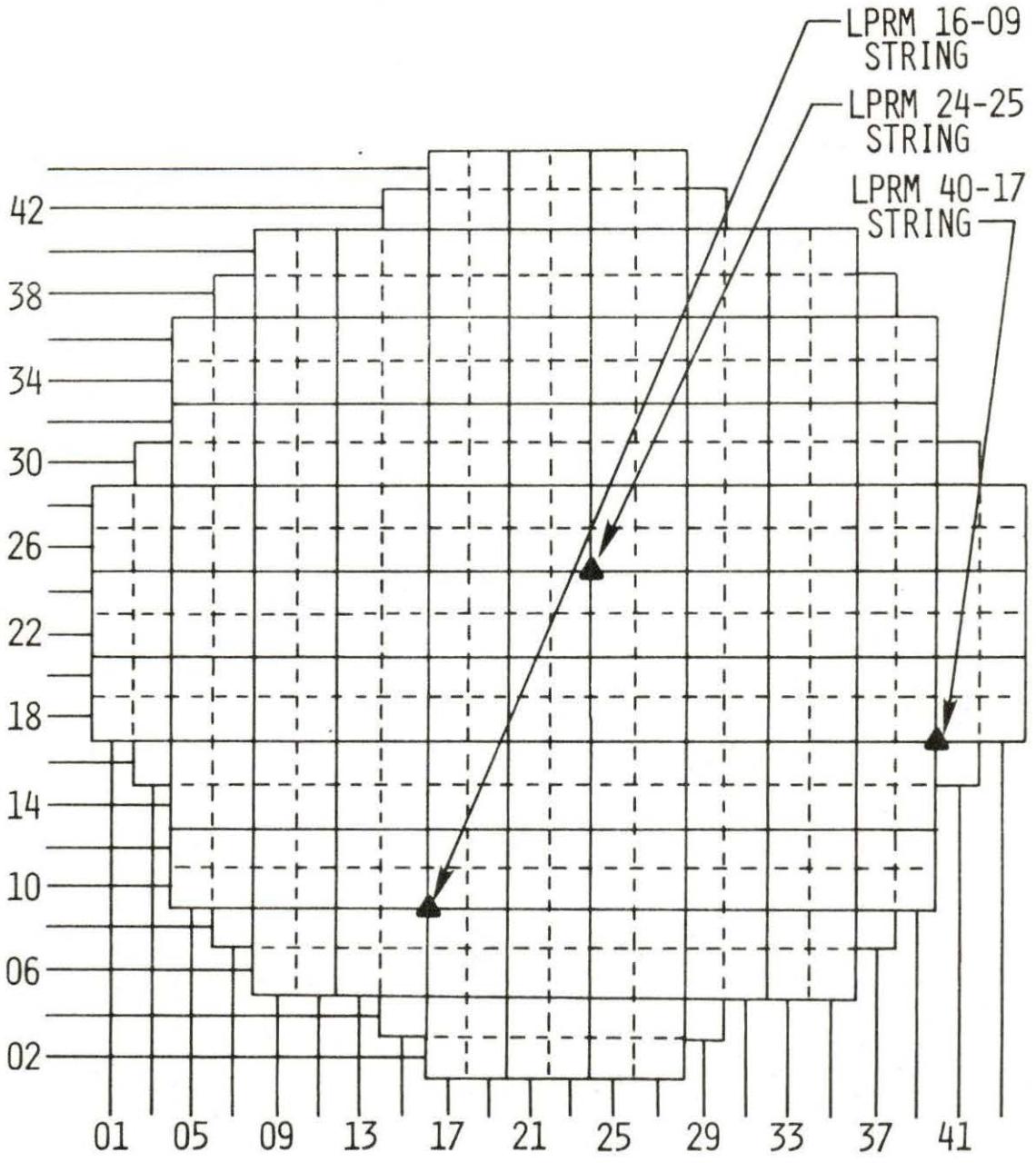

Figure 4.2. DAEC core layout and location of LPRM strings monitored.

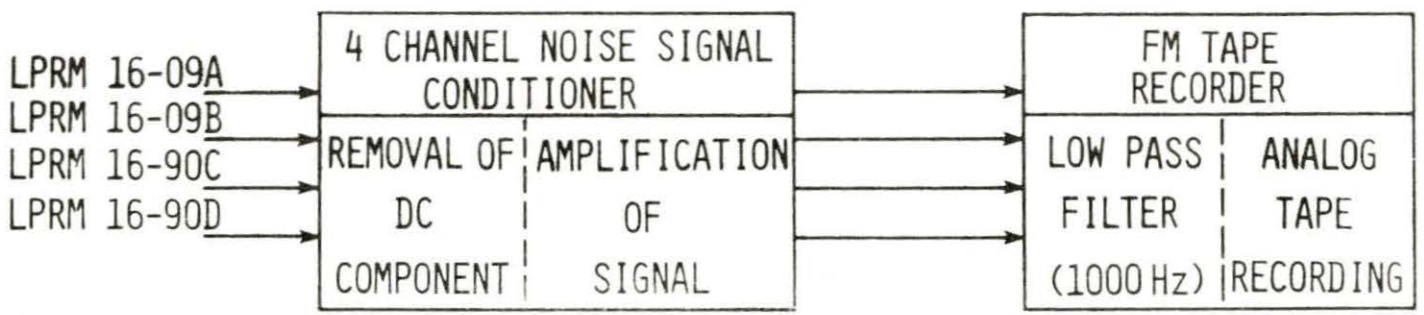

Figure 4.3. Analog noise signal recording.

results of these efforts is an analog tape containing the zero mean neutron noise signals.

2. Analog to digital processing

Since the noise signals recorded on the FM tape recorder are in analog form, conversion to digital format is necessary before computer processing. To analyze the noise signals in this study, the analysis system shown in Figure 4.4 was developed for digital computation.

An analog to digital conversion (ADC) unit, Geoscience Nuclear Company Model 8050, designed for multipurpose applications, was utilized for digitization of noise signals. Input to the unit requires a voltage signal that varies between 0 and 8 volts. Thus an offset potential of 4 volts (with a gain of 1.00) is mandatory for a zero mean noise signal input. The 4 channel noise signal conditioner used in the data acquisition is adequate for this purpose. In addition to the offset circuit a coincidence input which generates the sampling frequency is necessary for the ADC. A tail pulse generator, BNC model BH-1, was used for this purpose.

Selection of a sampling frequency, f_s, requires that it be at least twice the Nyquist frequency, f_N, of the input noise signals. The cutoff frequency, f_c, should be chosen less than the Nyquist frequency and is used to avoid aliasing errors during analog to digital conversion. An optimal value of 2.5 f_c, determined by Lu [19] was used for the sampling frequency.

Choice of the cutoff frequency, f_c, was chosen as 100.0 hertz early in the analysis when only the recorder filter was available and uncertainty of the frequency range to be monitored existed.

Figure 4.4. The complete digital analysis system.

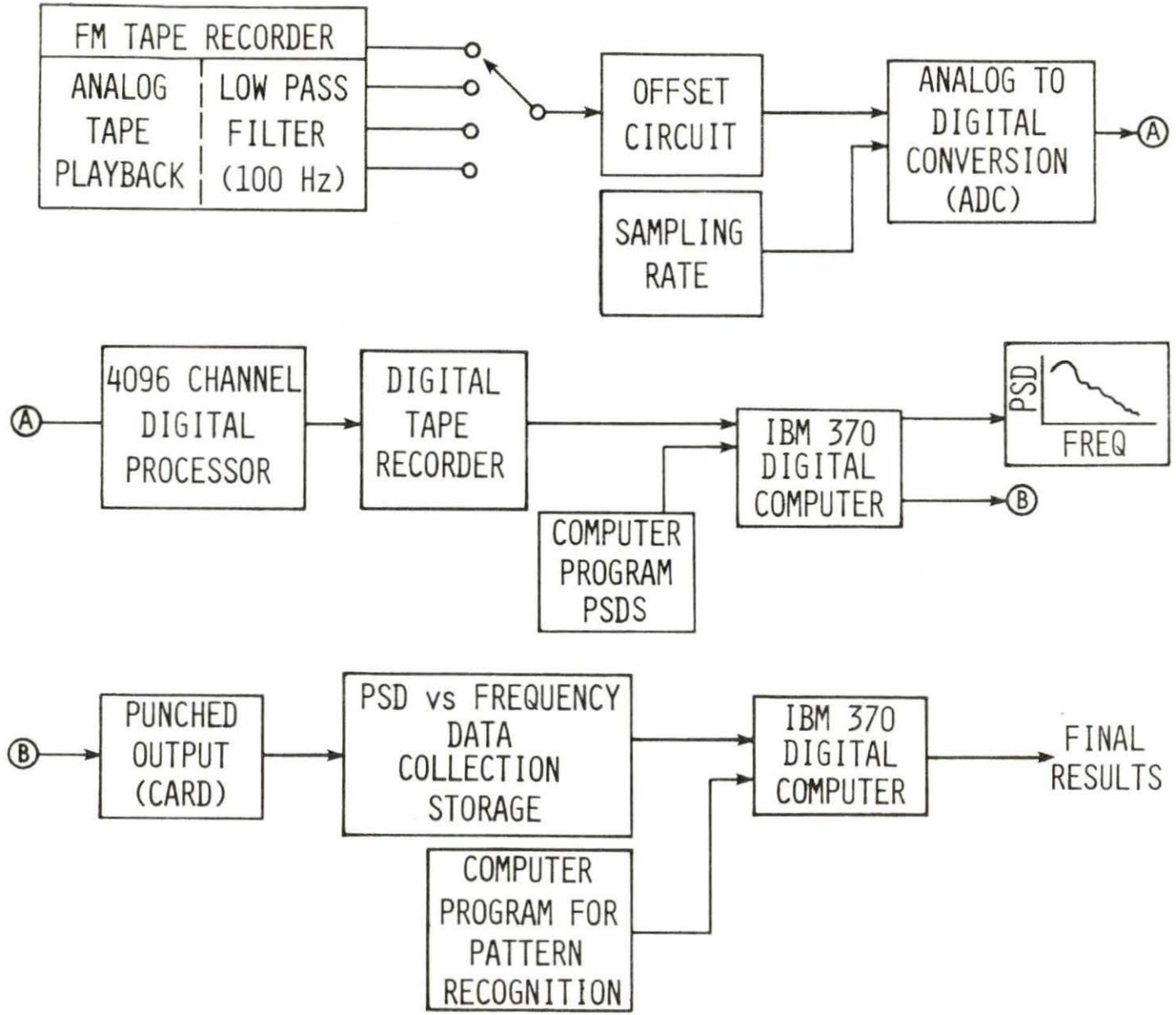
FM TAPE RECORDER
ANALOG TAPE PLAYBACK
LOW PASS FILTER (100 Hz)
OFFSET CIRCUIT
SAMPLING RATE
ANALOG TO DIGITAL CONVERSION (ADC)
A
4096 CHANNEL DIGITAL PROCESSOR
DIGITAL TAPE RECORDER
COMPUTER PROGRAM PSDS
IBM 370 DIGITAL COMPUTER
PSD
FREQ
B
PUNCHED OUTPUT (CARD)
PSD vs FREQUENCY DATA COLLECTION STORAGE
COMPUTER PROGRAM FOR PATTERN RECOGNITION
IBM 370 DIGITAL COMPUTER
FINAL RESULTS

Continued work showed that the actual frequency range for BWR component vibration is approximately 1.0 to 10.0 hertz.

After digitization of the noise signals by the ADC, the data were stored in a digital processor (Geoscience Nuclear Company Model 7000). A two-parameter input and display unit (Geoscience Nuclear Company Model 4000) was used to check the digitized data before and/or after recording.

A magnetic tape controller (Geoscience Nuclear Company Model 5030) and a seven-track digital tape recorder (Peripheral Equipment Corporation, PEC, Model 6860-75) were used to record the digital processor data on half-inch magnetic tape.

The digitized data on the tape were then supplied to the computer program PSDS for evaluation of power spectral densities.

3. The computer program PSDS

The computer program PSDS, written in PL/1 language, was used to calculate the power spectral density functions. Development of the program resulted from a modification of approximately 60 percent of an earlier computer program written by Lu [19]. The program requires digital input from magnetic tape and utilizes the library subroutine FFT (fast Fourier transform) which is in the IBM PL/1 SSP.

The flow diagram of PSDS is shown in Figure 4.5. The first step in the program is to read the number of noise signal groups (ensembles) to be processed and their processing parameters. The PSD sum vector, used in the ensemble averaging procedure, is set to zero.

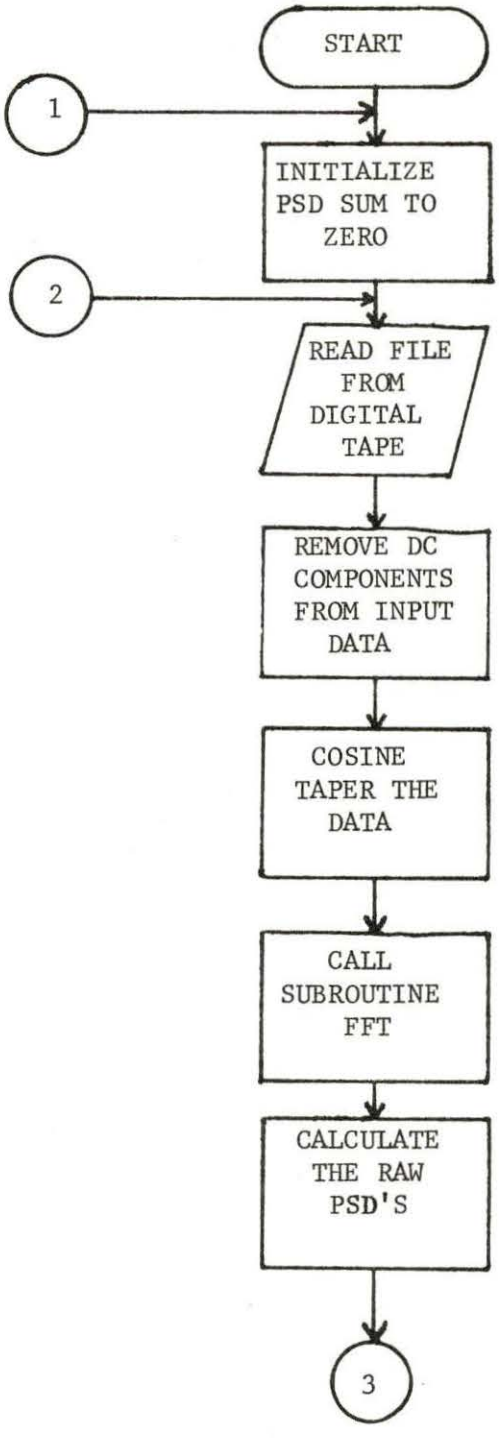

Figure 4.5. Flow diagram of PSDS.

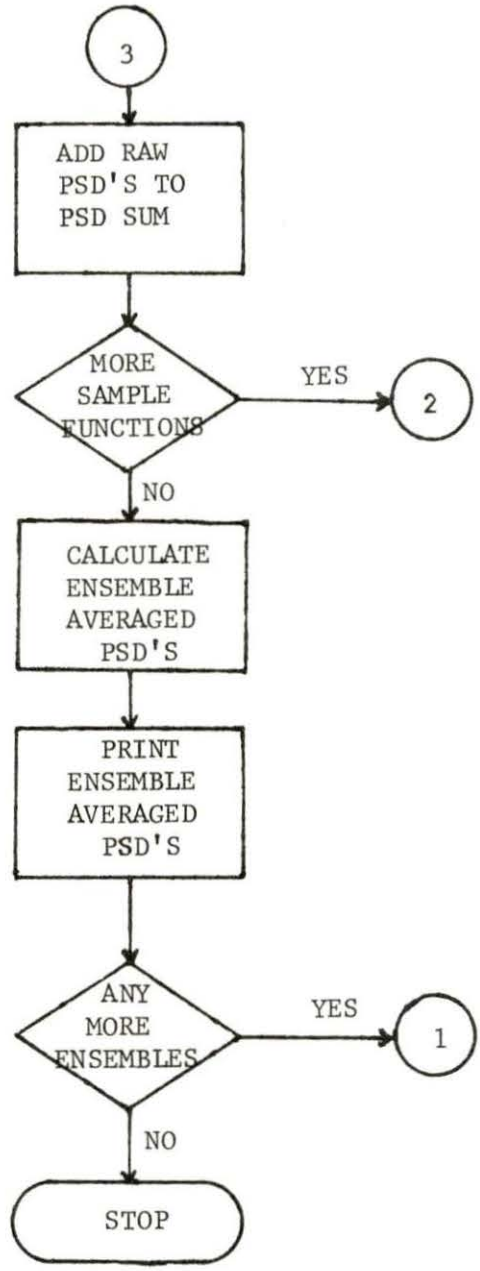

Figure 4.5. Continued.

Once a sample function consisting of 4096 sampled points has been read off of the digital tape, removal of the d-c offset component (introduced during digitization) is performed. Application of a window function to the original random time series at each end is required to reduce side lobe leakage in the FFT. The cosine taper, one of several window functions available, was chosen for use in PSDS because of minimal leakage.

After application of the fast Fourier transform the raw PSD's for each frequency, f_i, are calculated, using the relation [20]

$$PSD(f_i) = \frac{2.0}{f_s \cdot N} \cdot [Re[F(f_i)]^2 + Im[F(f_i)]^2] \cdot \frac{1}{0.875} \qquad (4.1)$$

where f_s is the sampling frequency (hertz), N represents the number of digitized points per sample function (4096), $Re[F(f_i)]$ is the real part of the Fourier transform, $Im[F(f_i)]$ is the imaginary part of the Fourier transform, and 0.875 is a normalizing factor used when a cosine taper has been applied to the data.

The standard error ε, after calculation of the raw PSD, is given by [1]

$$\varepsilon = 1/(B_e \cdot T_r)^{1/2} \qquad (4.2)$$

where B_e is the bandwidth of the estimate and T_r is the finite time interval of the sample function data record. For the fast Fourier transform, B_e is equal to $1/T_r$ so Equation 4.2 becomes

$$\varepsilon = 1/(\frac{1}{T_r} \times T_r)^{1/2} = 1.00$$

yielding a standard error of 100% which is unacceptable for practical applications. Two averaging techniques are available for reducing the standard error. These are ensemble averaging and frequency smoothing. Application of both of these methods results in a standard error given by [1]

$$\varepsilon = 1/(LQ)^{1/2} \tag{4.3}$$

where L represents the number of points frequency smoothed, and Q represents the number of sample functions ensemble averaged. Only ensemble averaging was utilized in PSDS, since different values of L may be used outside the PSDS routine without permanently altering (into unusable form) the PSD vectors.

Following the completion of ensemble averaging the results are printed and punched (option) out.

The program continues to process all the remaining ensembles requested in the above order and terminates upon completion. A complete listing of the PSDS program with control card and data input requirements is found in Appendix B.

4. The noise analysis-pattern recognition interface

After processing neutron noise ensembles with the computer program PSDS, several intermediate steps are required to put the data into a form suitable for use in pattern recognition analysis.

Computer space and time allocations limit the number of PSD values which may be used in a vector to approximately 50. The number of data points available from PSDS in the frequency range of interest

was 152, thus exceeding the desirable limit. The preferable method of data reduction is through the use of frequency smoothing techniques which also decrease the standard error. Averaging of four points was utilized in this analysis which served to decrease the number of PSD values to 38 and also to reduce the standard error by 50%.

Normalization of the PSD's was also done in this intermediate step to remove the reactor power as a variable. Referral to Equation 3.14 shows this to be done by dividing the PSD's by the flux level squared. The values of the relative flux (0.0 to 1.00) for each detector were provided in the "P1" process computer output available at DAEC.

Plots of the noise signatures for each detector were made at this time to allow visual comparison and to provide a crude validity check of the pattern recognition system results obtained later.

5. Pattern recognition processing

The pattern recognition system essentially consists of a main program, the MISODATA subroutine, and two other subroutines. A listing of the complete computer code and its input data formats are found in Appendix C. A maximum of 25 patterns, each with dimensionality of 38 or less, can be analyzed in one computer run.

The MISODATA algorithm listed in Appendix A is used in subroutine ISODAT and comprises most of the pattern recognition code. Subroutine ZIP, used to find cluster center-sample pattern distances, is actually part of the MISODATA algorithm, but is used externally (of ISODAT), since it is required in more than one step of the algorithm.

When successive iterations of the program yield unchanging results, specifically the cluster centers and their respective subsets, the program has calculated the "equilibrium values." The intermediate results are printed out by the program and determination of this equilibrium is easy to check. If the results are still changing at the end of execution (which is determined by the number of iterations requested) and an option in the main program has been used for punching card output of the final cluster centers, these cards may be substituted for the old cluster centers allowing continued execution of the program. For example, if the program needed eleven iterations for equilibrium, and eight had been used, running the program with the punched output would require only three more iterations, as opposed to starting all over again.

Input to the program is brief requiring only the following essential information:

(1) the number of sample patterns to be processed,

(2) the dimensionality of the sample patterns,

(3) the punching option,

(4) an option allowing data corresponding to specific frequencies to be found and normalized,

(5) the sample pattern vectors,

(6) the assumed number of cluster centers and their associated vectors, and

(7) the MISODATA parameters K(KLUSD), θ_N(THETAN), θ_s(THETAS), θ_c(THETAC), L(LCLMAX), and I(ITRNS).

This type of algorithm offers the advantage that it can be used for both unsupervised and supervised pattern recognition. The use of either can be accomplished by tuning the input parameters and selecting specific pattern vector input.

After the initial effort of acquiring a noise signature pattern library (of dimensionality 38), the unsupervised technique was used to create cluster center groupings using a standard error criterion of 1.5ε, where ε was calculated from Equation 4.3. This value of 1.5ε was chosen to allow for pattern differences and standard errors of the pattern data. The easiest method to group the data is to specify each pattern as a cluster center and to adjust the lumping parameter, θ_c(THETAC), so that similar patterns are merged. The use of the Euclidean distance as the criterion for lumping may result in unacceptable standard errors (those greater than 1.5ε) even though the data apparently fits. Figure 4.6 shows the undesirable results obtained when using only Euclidean distance as the criterion for pattern assignment to cluster subsets. Lumping sample patterns such as #1 and #2 in Figure 4.6 always results in a large average standard error and will have standard error components which exceed 100%. A proper assignment is shown in Figure 4.7, in contrast to the previous example.

Although not visually obvious, occurrences of clustering similar to Figure 4.6 are detectable upon examination of the associated average standard error and the standard error vector. The application of supervised pattern recognition techniques by analyzing data for only one cluster subset at a time eliminates the small distance-large

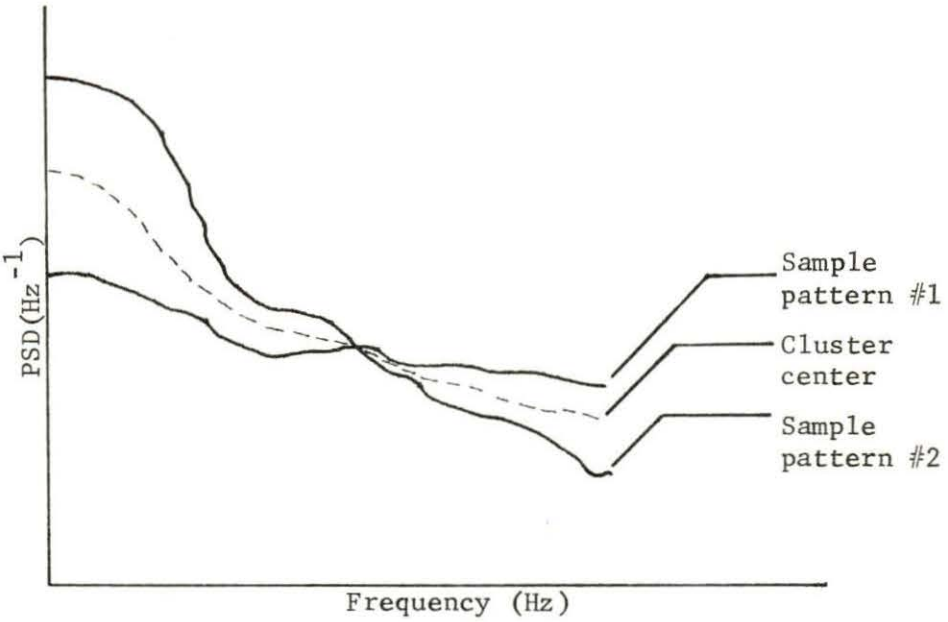

Figure 4.6. Poorly-fitted sample patterns.

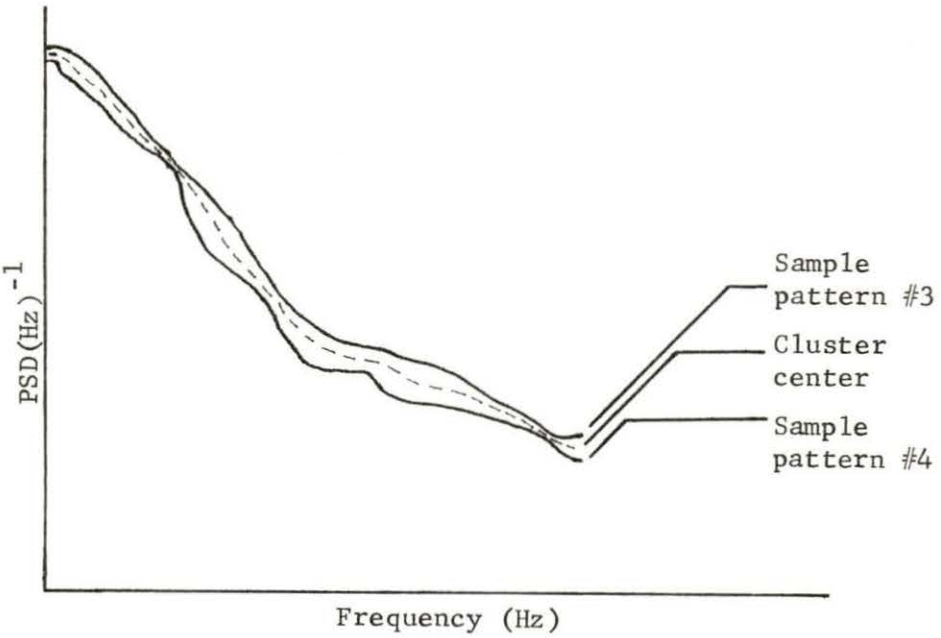

Figure 4.7. Properly-fitted sample patterns.

standard error problem by allowing elimination of subset members which create the large standard errors.

The final results obtained from the pattern recognition process list the following items of interest:

(1) each cluster center derived from its subset,

(2) the cluster's subset members,

(3) the cluster subset to which each sample pattern is assigned,

(4) the average standard error and standard error vector, and

(5) the cluster center-cluster center distances.

The fifth item serves to indicate the degree of similarity between cluster subsets, but it is not necessarily a good measure of data similarity when sample patterns resembling those in Figure 4.6 are analyzed.

B. Analysis Results

1. Noise analysis results

Dates of data recording at DAEC, power levels, and coolant flow rates are listed in Table 4.1. The power level shown is the gross thermal value, which for 100% power is 1593 Mw(th). Axial and radial neutron flux profiles are manipulated by control-rod positioning, so the local power levels at various detector locations are not directly related to the gross thermal power. Table 4.2 summarizes the relative local flux or power values (which vary between 0.0 and 1.0) for the 16-09 LPRM's A, B, C, and D.

Table 4.1. Dates of data recording and reactor operating conditions

Date	Sample number	Gross thermal power level (%)	Coolant flow rate (%)
5-28-75[a]	1	49.28	33.49
6-5-75[a]	2	89.53	90.27
8-29-75	3	64.41	53.92
10-7-75	4	81.04	82.12
10-28-75	5	81.54	89.57
11-11-75	6	68.30	70.67
12-3-75	7	82.17	93.49
12-17-75	8	76.59	85.59
1-14-76	9	85.44	99.96
1-28-76	10	85.62	98.61
2-11-76	11	81.54	100.29
5-11-76[b]	12	61.46	61.84

[a]Before bypass flow hole plugging.

[b]New core loading.

Due to the extensive number of noise signatures processed, only the file for the 16-09C LPRM is included in its entirety. This 16-09C "library" consisting of "normalized" PSD versus frequency is found in Appendix D. Criteria for the selection of the C detector included:

(1) it indicated that small amplitude vibrations were still occurring after bypass flow hole plugging,

Table 4.2. Relative flux levels for the 16-09 LPRM detectors

Date	ϕ_A	ϕ_B	ϕ_C	ϕ_D
5-28-75[a]	0.42	0.47	0.32	0.18
6-5-75[a]	0.46	0.79	0.68	0.41
8-29-75	0.60	0.51	0.42	0.27
10-7-75	0.89	0.60	0.50	0.28
10-28-75	0.80	0.61	0.51	0.29
11-11-75	0.64	0.50	0.46	0.33
12-3-75	0.75	0.60	0.54	0.35
12-17-75	0.66	0.54	0.49	0.34
1-14-76	0.74	0.58	0.56	0.36
1-28-76	0.71	0.61	0.53	0.34
2-11-76	0.61	0.58	0.52	0.35
5-11-76[b]	0.41	0.49	0.40	0.29

[a]Before bypass flow hole plugging.

[b]New core loading.

(2) the detector was near the axial center of the fuel region where two-phase flow occurs, and

(3) results obtained can be visually examined to determine the same distinct pattern classes as calculated in the pattern recognition portion of the system.

It is appropriate to begin the discussion of the noise analysis results with the data obtained prior to bypass flow hole plugging.

The May 28, 1975 data were obtained from "unusual" reactor operating conditions, that is, the power and flow rate levels were extremely low and are rarely, if ever, encountered during normal operation. Nuclear Regulatory Commission deratings based on inadequate information of vibration levels were the reason for the low power operation of the reactor. One would expect a noise signature obtained under these conditions to be very different from normal operation, which was indeed the case.

Of all the data obtained, the June 5, 1975 measurements, taken during a brief testing period at normal operating conditions were the most interesting. Shown in Figures 4.8, 4.9, 4.10, and 4.11 are plots of the noise signatures for the 16-09A, B, C, and D detectors. Data obtained by the reactor vendor at DAEC and other BWR/4's indicated that there were two distinct in-core vibrations occurring (prior to bypass flow hole plugging). Flow-induced vibrations of the in-core LPRM instrument tubes occurred at approximately 2.0 Hz; fuel assembly vibrations induced by instrument tubes impacting against the channel boxes were detectable at approximately 4.0 Hz, although smaller components extended up to 6.0. Table 4.3 compares the values of the two major frequencies of component vibration for the computer program PSDS (four points frequency smoothed) and reactor vendor PSD-frequency measurements (conducted June 3 through June 5, 1975). Only vendor PSD measurements made during reactor operating conditions similar to those of this project's June 5, 1975 signal-measurement period are included in Table 4.3. One can see that the component vibration frequencies measured in this project agree very well with those measured by the

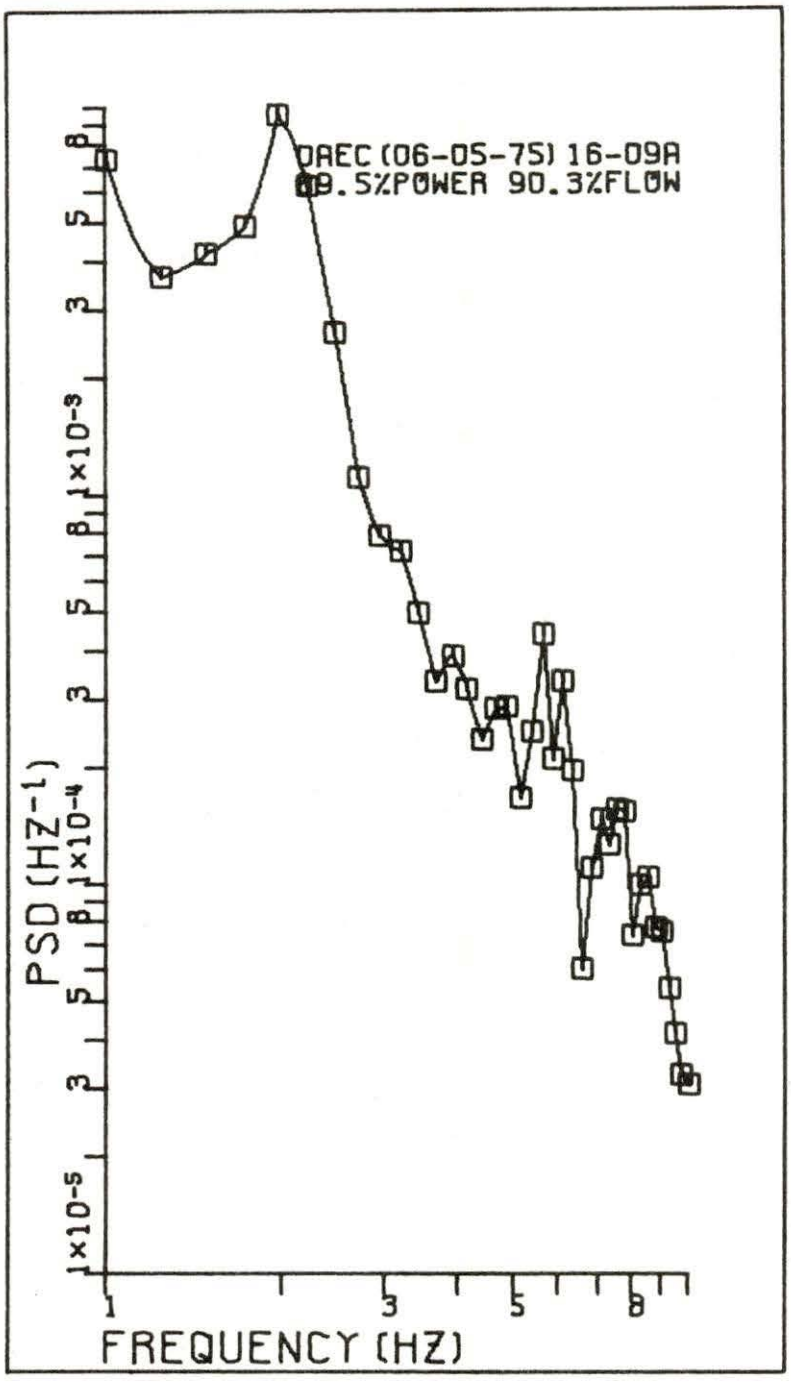

Figure 4.8. Noise signature for the 16-09A LPRM (June 5, 1975).

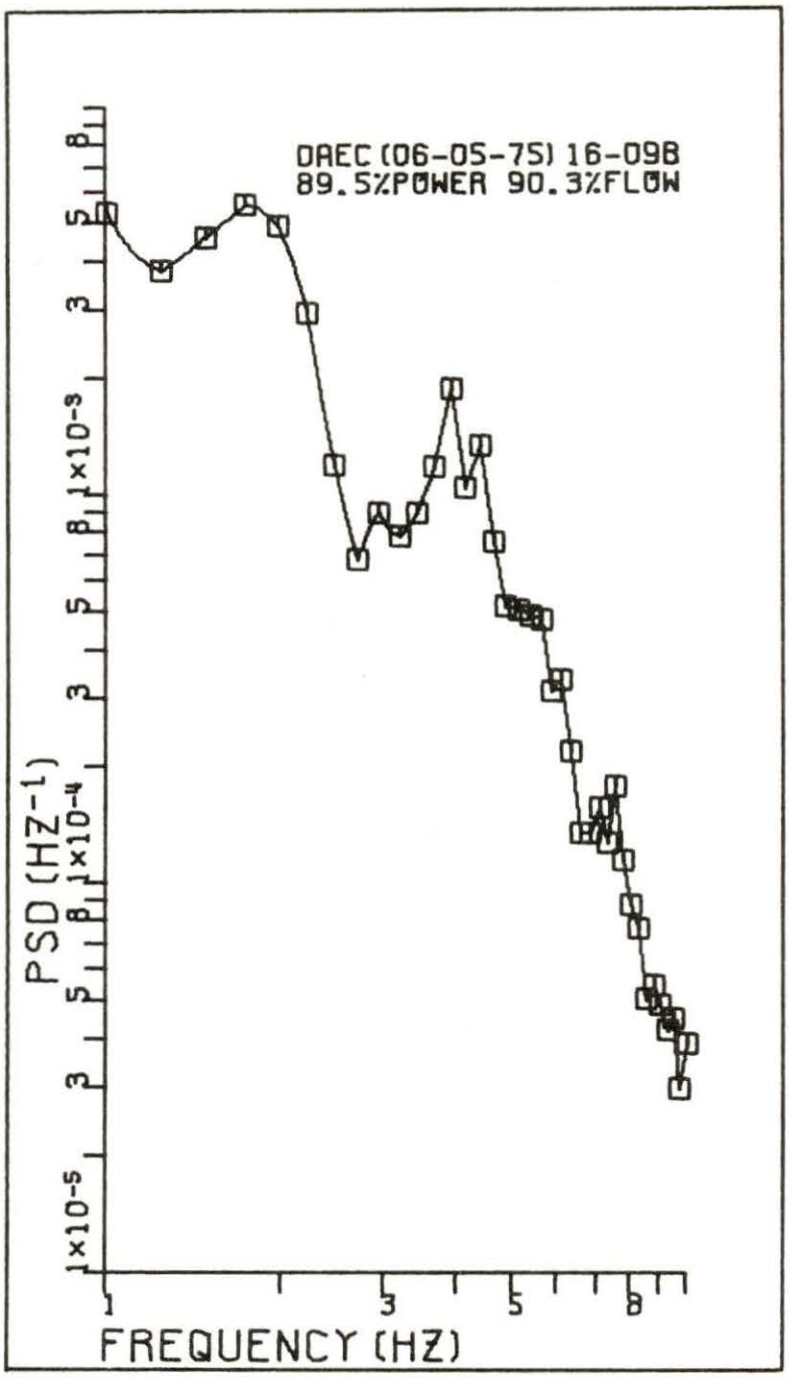

Figure 4.9. Noise signature for the 16-09B LPRM (June 5, 1975).

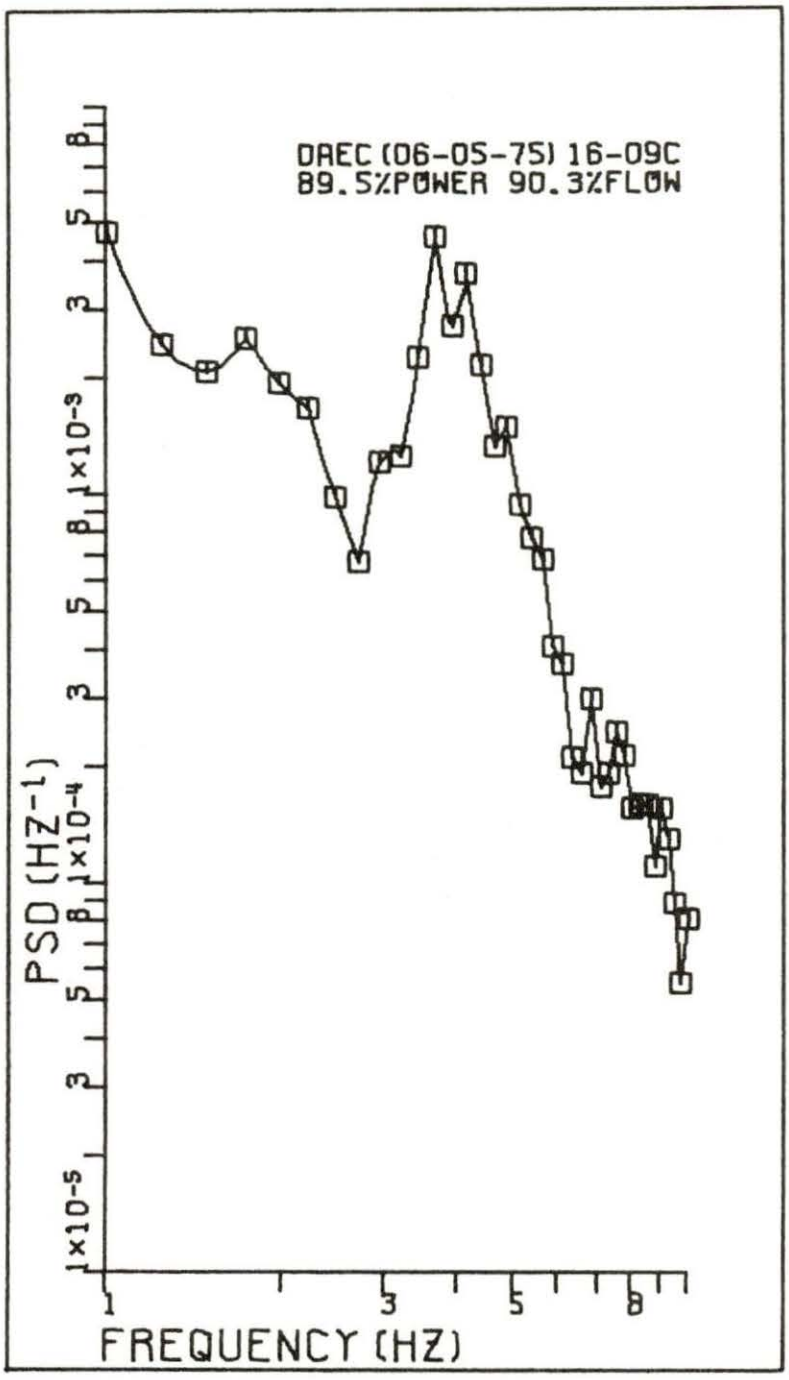

Figure 4.10. Noise signature for the 16-09C LPRM (June 5, 1975).

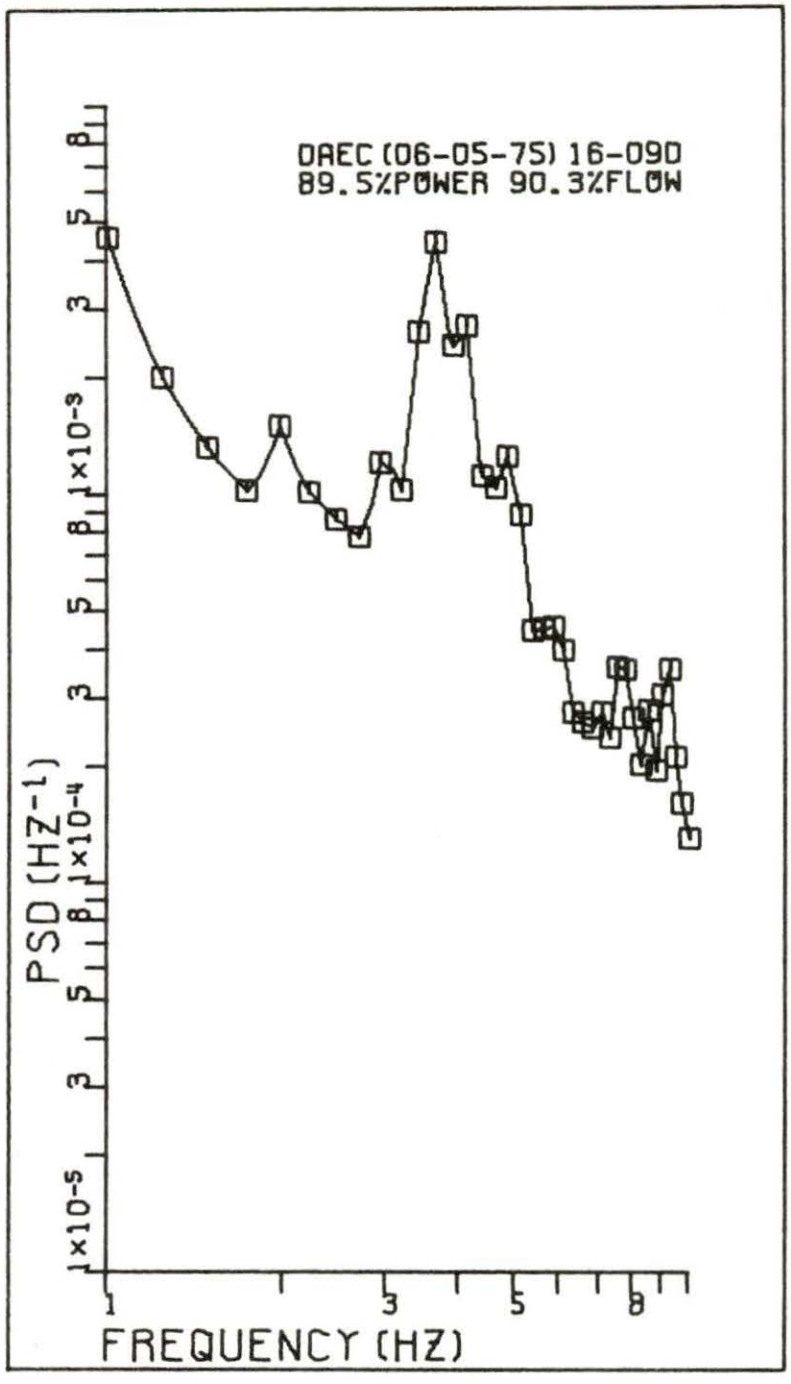

Figure 4.11. Noise signature for the 16-09D LPRM (June 5, 1975).

Table 4.3. Comparison of vibrational frequencies measured in the project to those measured by the reactor vendor prior to bypass flow hole plugging

Measurement date	Power (%)	Coolant flow rate (%)	Standard error, ε	Frequency resolution (Hz)	Vibrational frequencies (Hz) LPRM 16-09A	LPRM 16-09B	LPRM 16-09C	LPRM 16-09D
6-3-75 (vendor)	87	90	0.183	—[a]	—[b]	2.0 4.3	1.8 4.2	—[b]
6-3-75 (vendor)	90	90	0.189	—[a]	2.0 4.1	—[b]	—[b]	—[b]
6-5-75 (PSDS[c])	90	90	0.177	0.24	2.0 4.2, 6.0	1.7 4.2	1.7 4.0	2.0 4.0
6-5-75 (vendor)	90	90	0.189	—[a]	2.2 4.2	1.8 4.0	1.8 4.2	—[b]

[a] Information not available.

[b] Data measurements taken were not available for examination.

[c] Four points frequency smoothed.

vendor. The frequency resolution of the vendor was unavailable, but the 0.244 Hz resolution of this analysis can account for any differences. Mathis et al. [21] obtained results very similar to those in Table 4.3 in noise measurements of other BWR/4's.

One of the interesting trends to note from Figures 4.8 through 4.11 is that the LPRM instrument tube vibration at ~ 2.0 Hz decreases with upward vertical detector position while channel box assembly vibration increases and changes frequency. Mott et al. [22] concluded that an increase in the magnitude of the instrument tube vibration mode does not indicate impacting. When impacting does occur the channel box containing the fuel assemblies vibrates, and this motion is similar to a cantilevered beam attached at the lower core with the largest amplitude in the upper region of the core. Thus when impacting does occur one might expect a decrease in the 2.0 Hz vibrational component.

Another observable trend (common to all BWR's), found from comparison of all four detectors in an LPRM string, is that the slope of the PSD curve flattens or becomes less negative as upward vertical detector position increases. This effect is due to the increase of local noise from steam-bubble formation, i.e. increasing void fraction [9]. This phenomenon is even more apparent when the PSD's are plotted over the frequency range from 0.1 to 100.0 Hz.

From Figures D.1 and D.2 it is apparent that the instrument tube vibration level is highly dependent upon the coolant flow rate. As the flow rate is decreased the level of vibration also decreases. Results obtained by the reactor vendor were in agreement with this.

Ackermann et al. [7] reported similar conclusions from noise measurements taken at other BWR/4's.

Referral to Appendix D and in particular to PSD curves obtained after bypass flow hole plugging indicates a trend of decreasing negative slope (flattening) as the coolant flow rate decreases. This shift from low-to-high frequency noise is probably a function of the steam void content which affects the neutron moderating process.

The phenomenon of global noise being dominant in the frequency range from approximately 0.0 to 2.0 Hz [8] was observable to some extent (even though cross-power spectral density measurements were not made). A sharp change in slope of most Appendix D curves at approximately 1.5 Hz seem to indicate separable global and local noise components. As an example, observations made from overlaying the June 5, 1975 curves show an almost exact shape up to 1.25 Hz, i.e. a large coherence value characteristic of global noise.

Examination of the PSD versus frequency curves presented in Appendix D indicates that the bypass flow hole plugging was successful in removing the high amplitude component vibrations, but that some low amplitude vibrations still occur. The December 3, 1975 data, Figure D.7, represent the highest level vibrations measured (after hole plugging) in this project, however, this level of vibration amplitude is almost insignificant compared to vibrations prior to plugging.

2. Pattern recognition results and interpretation

The results of the pattern recognition study for each of the 16-09 LPRM detectors are summarized in Tables 4.4, 4.5, 4.6, and 4.7.

Table 4.4. Summary of pattern recognition results for the 16-09A LPRM

Cluster subset number	Number of subset members	Sample pattern numbers	Date	Flow rate (%)	Flow rate range (%)	Average standard error
1	1	1[a]	5-28-75	33.49	33.49	0.0000
2	1	2[a]	6-5-75	90.27	90.27	0.0000
3	1	12[b]	5-11-76	61.84	61.84	0.0000
4	2	3	8-29-75	53.92	53.92-70.67	0.2056
		6	11-11-75	70.67		
5	5	4	10-7-75	82.12	82.12-99.96	0.2337
		7	12-3-75	93.49		
		8	12-17-75	85.59		
		9	1-14-76	99.96		
		10	1-28-76	98.61		
6	1	5	10-28-75	89.57	89.57	0.0000
7	1	11	2-11-76	100.29	100.29	0.0000

[a]Before bypass flow hole plugging.

[b]New core loading.

Included in each table are the cluster subset numbers, the number of members in each subset, relevant information about each member, the coolant flow rate range, and the average standard error. The final criterion for pattern classification was based on an average standard error, θ_S, of 1.5¢ (0.2652). Cluster subsets having average standard errors less than this value were considered to be correctly classified.

Examination of all four tables shows each of the first two cluster subsets to contain only one member. As previously stated the May 28, 1975 reactor operating conditions were atypical due to

Table 4.5. Summary of pattern recognition results for the 16-09B LPRM

Cluster subset number	Number of subset members	Sample pattern numbers	Date	Flow rate (%)	Flow rate range (%)	Average standard error
1	1	1[a]	5-28-75	33.49	33.49	0.0000
2	1	2[a]	6-5-75	90.27	90.27	0.0000
3	2	3	8-29-75	53.92	53.92-61.84	0.1755
		12[b]	5-11-76	61.64		
4	7	4	10-7-75	82.12	70.67-100.29	0.2639
		6	11-11-75	70.67		
		7	12-3-75	93.49		
		8	12-17-75	85.59		
		9	1-14-76	99.96		
		10	1-28-76	98.61		
		11	2-11-76	100.29		

[a]Before bypass flow hole plugging.

[b]New core loading.

the low power (and flow rate) deratings. Consequently one would expect sample patterns from this date to be classified into single-member subsets. The second single-member subsets contained the June 5, 1976 sample patterns which were characterized by the high amplitude instrument tube and channel box vibrations. After hole plugging no sample patterns resembled the June 5, 1975 data due to removal of the high amplitude vibrations. Exclusion of the first two abnormal samples leaves ten sample patterns remaining to be classified (nine for the 16-09B LPRM).

Results for the 16-09B detector, shown in Table 4.5, identify one of the most important trends observable in the sample patterns. One

Table 4.6. Summary of pattern recognition results for the 16-09C LPRM

Cluster subset number	Number of subset members	Sample pattern numbers	Date	Flow rate (%)	Flow rate range (%)	Average standard error
1	1	1[a]	5-28-75	33.49	33.49	0.0000
2	1	2[a]	6-5-75	90.27	90.27	0.0000
3	2	3	8-29-75	53.92	53.92-61.84	0.1533
		12[b]	5-11-76	61.84		
4	3	4	10-7-75	82.12	70.67-89.57	0.2134
		5	10-28-75	89.57		
		6	11-11-75	70.67		
5	5	7	12-3-75	91.49	85.59-100.29	0.2354
		8	12-17-75	85.59		
		9	1-14-76	99.96		
		10	1-28-76	98.61		
		11	2-11-76	100.29		

[a]Before bypass flow hole plugging.

[b]New core loading.

can see that the data contained in the normal cluster subsets #3 and #4 group according to the flow rate range. Visual verification of the classification results is possible upon examination (overlaying) of the Appendix D curves. This visual comparison reveals that the PSD values decrease and the slope of the curve becomes less negative with decreasing flow rate. Examination of the cluster center PSD components (from the pattern recognition program output) yield results consistent with those obtained from visual comparison. Similar flow rate range clustering for the 16-09A, C, and D detectors were obtained when the average standard error classification criteria of 2ε was

Table 4.7. Summary of pattern recognition results for the 16-09D LPRM

Cluster subset number	Number of subset members	Sample pattern numbers	Date	Flow rate (%)	Flow rate range (%)	Average standard error
1	1	1[a]	5-28-75	33.49	33.49	0.0000
2	1	2[a]	6-5-75	90.27	90.27	0.0000
3	2	3	8-29-75	53.92	53.92-61.84	0.1368
		12[b]	5-11-76	61.84		
4	4	4	10-7-75	82.12	82.12-99.96	0.2355
		7	12-3-75	93.49		
		9	1-14-76	99.96		
		10	1-28-76	98.61		
5	2	5	10-28-75	89.57	70.67-89.57	0.1606
		6	11-11-75	70.67		
6	2	8	12-17-75	85.59	85.59-100.29	0.2169
		11	2-11-76	100.29		

[a]Before bypass flow hole plugging.

[b]New core loading.

used. Ackermann et al. [7], in noise signature comparisons, also found the PSD values to be a function of flow rate.

The use of 1.5ϵ as the average standard error criterion resulted in splitting of cluster subsets which were unable to meet this more stringent requirement. The 16-09C detector results, summarized in Table 4.6, indicate a PSD dependence upon time or fuel burnup in addition to the flow rate. Again the lower flow rate classification (53.92-61.84%) was maintained, but splitting of the higher flow rate group into two time or fuel burnup classes resulted. Thus one finds

the data from October 7, 1975 through November 11, 1975 being classified into the same cluster subset. Operation of the reactor from December through mid-February required increasing the coolant flow rate to allow criticality to be maintained until refueling. These sample patterns (#7, #8, #9, #10, and #11) were thus representative of fuel burnup near the end of core-life and consequently were classified into the same cluster subset.

Tables 4.4 and 4.7 show what appears to be the combination of flow rate and burnup effects, i.e. the two effects are not easily separated. One might speculate that control rod positioning will cause variations in the flow patterns, since rod-followers are not used in the DAEC BWR, thus resulting in another dependent variable for PSD values.

The curves obtained for the 16-09A and D detectors on February 11, 1976, several days prior to the refueling shutdown, show PSD values less than what would be expected (using the January 28, 1976 data as criteria). Noise signature curves for the 24-25A, 24-25D, 40-17A, and 40-17D LPRM's on February 11, 1976 were consistent with the predicted results, i.e. they were similar to the January 28, 1976 data. Thus it will only be noted that the 16-09A and D PSD values were less than expected, but were correctly classified in the pattern recognition analysis.

In addition to verifying that the pattern recognition and visual classifications were identical, an analysis of the supervised pattern recognition sensitivity to detect abnormal operating conditions was undertaken. The first step in the process was the creation of 24

"statistically normal" sample patterns from an actual sample pattern designated as the cluster center. These simulated sample patterns were created by inducing evenly distributed random variations of 6% of the amplitude in the cluster center PSD components. Creation of an abnormal twenty-fifth pattern containing a simulation of channel box vibrations at DAEC was next undertaken. To adequately describe the vibration simulation procedures, it is convenient to define a "vibration" ratio at frequency f, $R_v(f)$, by

$$R_v(f) = \frac{PSD_v(f)}{PSD_{ex}(f)}$$

where $PSD_v(f)$ corresponds to a measured PSD value (in data containing vibrations) and $PSD_{ex}(f)$ is its expected "no vibration" PSD value which is estimated by linear approximation of the noise signature curve. Reference values of $R_v(f)$ over the channel box vibration frequency range were calculated from the June 5, 1975 data. Before inducing the simulated vibration into the twenty-fifth pattern, it was essentially the same as the first 24 patterns, and each component had a value corresponding to $PSD_{ex}(f)$. Using a 90% vibration amplitude simulation coefficient ($0.90\ R_v(f)$), the $PSD_v(f)$ values for the abnormal twenty-fifth sample pattern were calculated using the relation

$$PSD_v(f) = 0.90\ R_v(f) \cdot PSD_{ex}(f)$$

The simulated sample patterns were analyzed by the pattern recognition system in the supervised mode by running first one pattern, then two, next three, ..., and finally all 25 patterns. In addition to the 90% simulated vibration coefficient, values of 20 and 35% were used to

represent "small" and "moderate" vibration levels. Figures 4.12, 4.13, and 4.14 show plots of how the average standard error changes with the number of samples analyzed and with the level of vibration. As the number of samples in a subset increases (to approximately eight to ten) the average standard error becomes a constant. With less than eight sample patterns the average standard error obtained is not on the "plateau" and consequently indicates a standard error less than ϵ (the measurement standard error), i.e. it overestimates the fit to the cluster center. When the twenty-fifth pattern, containing the simulated vibration, is included a sharp peaking of the standard error curve occurs, thus showing the detection of an abnormal sample pattern. All three simulated cases are easily detected, although the larger coefficient values are more obvious. Thus the sensitivity of the system has been demonstrated in a reference test to show that it is capable of detecting abnormal patterns containing vibration levels as small as 20% of those experienced at DAEC on June 5, 1975.

Cluster subsets of sample patterns from reactor operation are characterized by average standard errors containing two components — a statistical or measurement standard error (ϵ) and a reactor operating conditions' standard error. The second component, the operating standard error, is derived from cluster subsets containing members whose patterns vary (due to differences in such reactor parameters as coolant flow rate or burnup). Analysis of cluster subsets with ten or more members allows pattern recognition based upon only the second component of the average standard error, the reactor operating portion, since the statistical standard error component is a constant (ϵ) located on

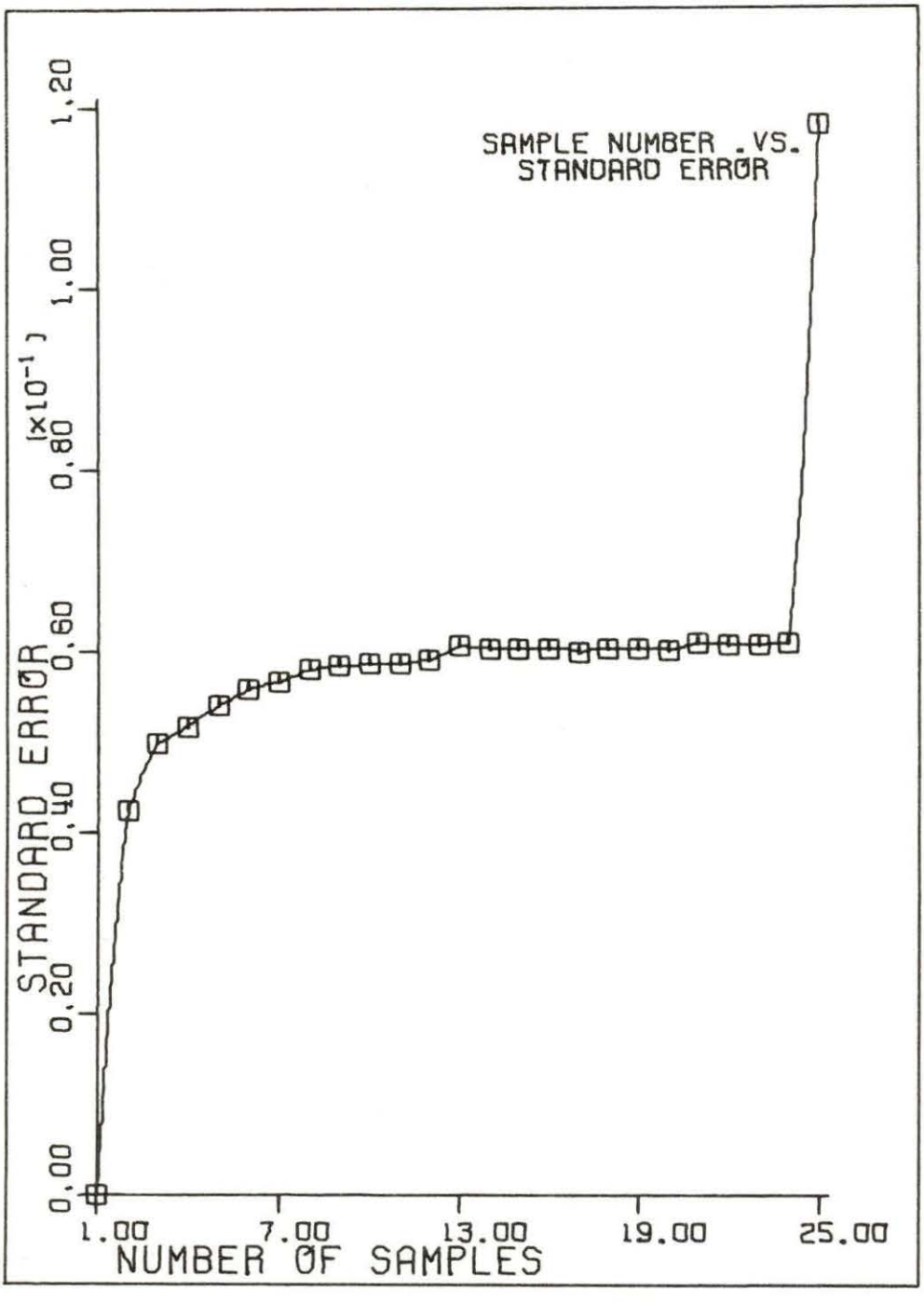

Figure 4.12. Simulated vibration level of 90% of the June 5, 1975 data.

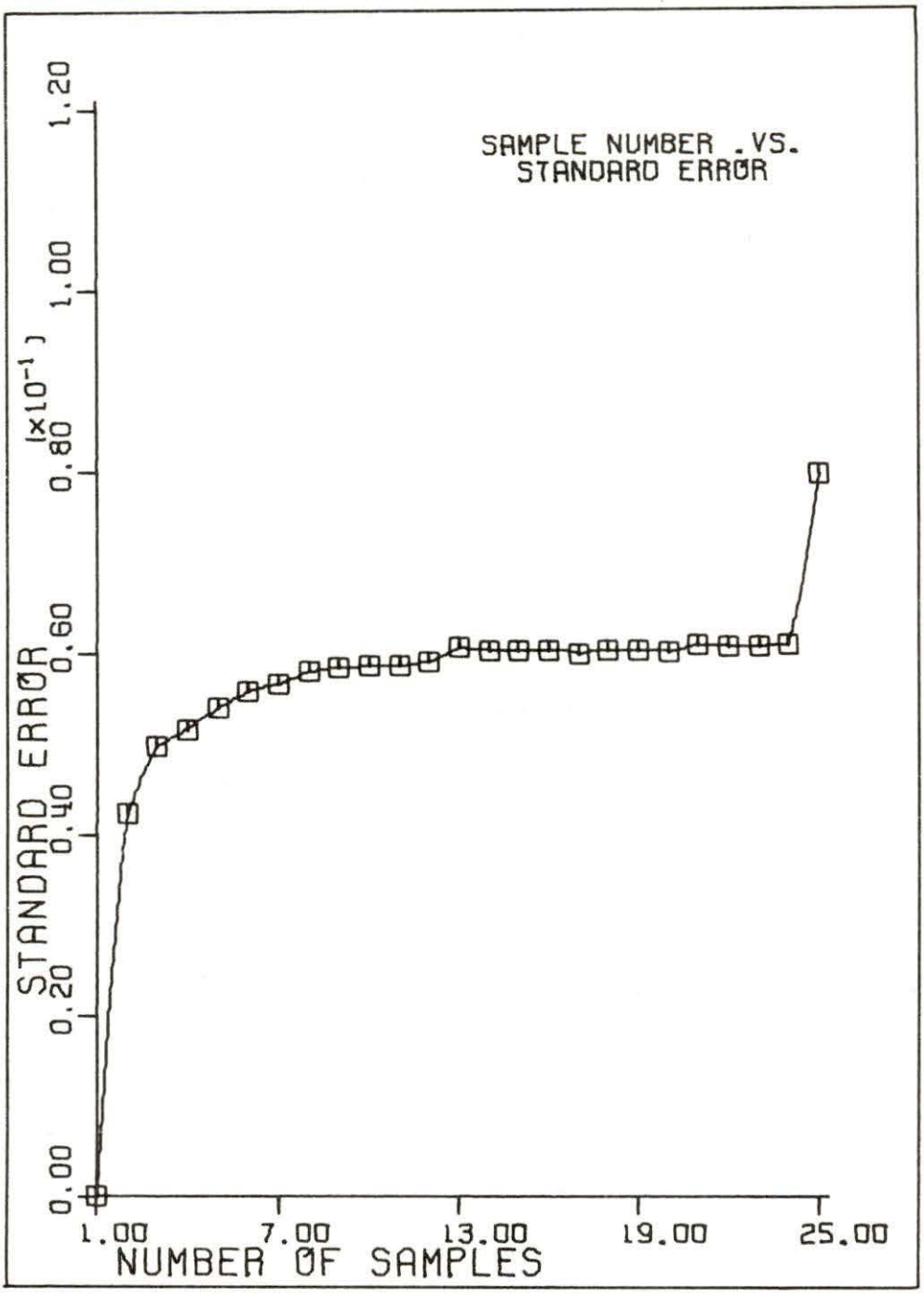

Figure 4.13. Simulated vibration level of 35% of the June 5, 1975 data.

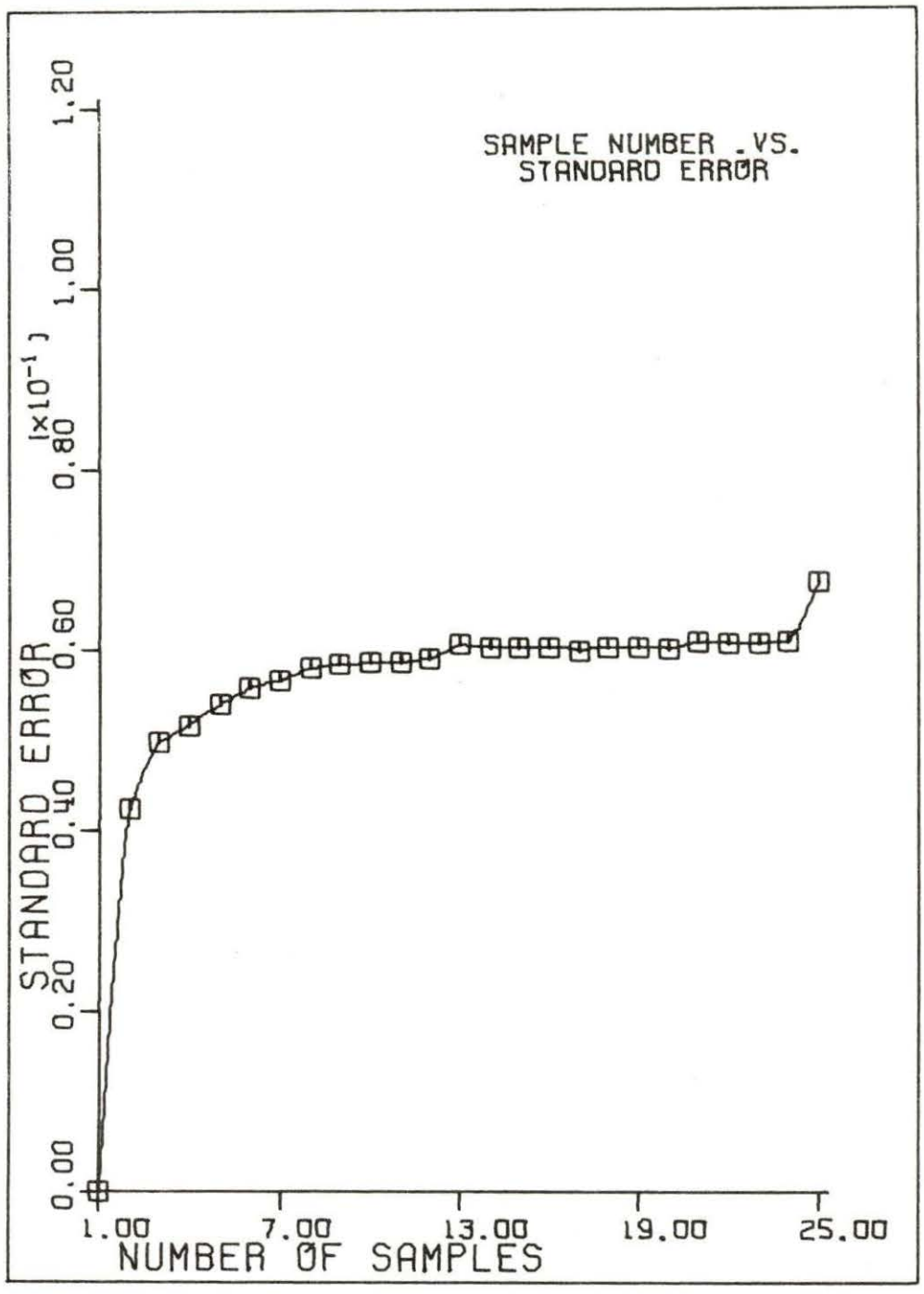

Figure 4.14. Simulated vibration level of 20% of the June 5, 1975 data.

the plateau of the average standard error versus number of samples curve and may be subtracted from the total average standard error. Thus, the choice of 1.5ϵ is a reasonable choice for classification criterion, since it allows a 0.5ϵ variation in the patterns in addition to their statistical distribution.

The plateau obtained in Figures 4.12 through 4.14 indicates that many more sample patterns than those used in this analysis are needed for a reactor monitoring system. Situations may occur where the statistical component of the average standard error is less than ϵ, thus allowing an operational classification criterion greater than 0.5ϵ. For use in a reactor monitoring system used by a utility, there would be no problem of obtaining a library of sample patterns, because continuous access to noise signals is available.

The use of the standard error criterion for classification of sample patterns also offers the potential for use as a monitoring index of reactor behavior. This monitoring index, MI, may be defined by

$$MI = \frac{\left| \overline{\overline{\sigma_E}} - \overline{\overline{\sigma_E}} \right|}{\sigma_{\overline{\sigma}_E}} \tag{4.4}$$

where $\overline{\overline{\sigma_E}}$ is the mean of the average standard error, $\overline{\sigma}_E$ is the measured average standard error which changes with an increasing number of samples, and $\sigma_{\overline{\sigma}_E}$ is the standard deviation of the measured average standard error. Since the average standard error is sensitive to changes in reactor operation, i.e. anomalous reactor behavior, the monitoring index could be used as an input to a diagnostic monitoring

system which would contain an alarm system. The alarm levels could be set at constant values of MI, such as 2.0 or 3.0, to indicate different degrees of abnormal behavior.

V. CONCLUSIONS AND SUGGESTIONS FOR FUTURE WORK

A. Conclusions

The following are important conclusions and observations from this study:

(1) Power spectral density values are dependent upon the coolant flow rate. Cluster centers calculated in the pattern recognition analysis and visual examination of the Appendix D curves reveal that the PSD values decrease and the slope of the curve becomes less negative with decreasing flow rate.

(2) The coolant flow rate is a parameter directly affecting the classification of sample patterns into cluster subsets. As an example, Table 4.5 shows that the normal cluster subsets #3 and #4 are characterized by two different flow rate regimes.

(3) Fuel burnup may be a parameter affecting shapes of the noise signature curves. Table 4.6 reveals that a cluster subset, characteristic of a specific flow rate range, may be further divided and categorized by the date of observation.

(4) Figures D.1 and D.2 indicate that in-core instrument tube and channel box vibration amplitudes were directly related to the coolant flow rate. The lower flow rate of May 28, 1975 removed the high amplitude vibrations experienced at higher flow rates.

(5) Examination of June 5, 1975 data revealed that the channel box vibration amplitude increased significantly and the instrument vibration amplitude decreased as the point of observation was shifted upward (axially).

(6) Bypass flow hole plugging effectively removed the high amplitude vibrations but small amplitude vibrations at the characteristic frequencies still occur.

(7) As the point of observation is shifted upward axially, there is a flattening of the PSD curve, i.e. a decreasing negative slope, caused by a shift from low to high frequency noise. This spectral shift is due to an increasing steam void fraction.

(8) The noise analysis-pattern recognition system is capable of detecting abnormal reactor operating conditions and is sensitive to vibration amplitudes as small as 20% of the relative PSD peak levels experienced June 5, 1975.

(9) Figures 4.12 through 4.14 indicate that approximately eight to ten sample patterns per cluster subset (or class) are required to remove the statistical variation component of the standard error, so that the reactor operation component can be used as the classification criterion.

(10) It is recommended that a large library of sample patterns be obtained for use in a noise analysis-pattern recognition reactor monitoring system.

B. Suggestions for Future Work

The following are suggestions for future work related to this study:

(1) Develop an on-line monitoring system incorporating the data analysis procedures used in this study.

(2) Collect more data thus creating a larger library. The development of a data storage-retrieval system other than punched cards would be desirable.

(3) Investigate the effects on PSD values of control rod positioning and its associated flow pattern changes.

(4) Pursue the development of a reactor monitoring system incorporating the use of the monitoring index described in the pattern recognition results section.

VI. LITERATURE CITED

1. Bendat, J. S., and A. G. Piersol. 1971. Random data: Analysis and measurement procedures. John Wiley & Sons, Inc., New York, N.Y. 407 pp.

2. Uhrig, R. E. 1970. Random noise techniques in nuclear reactor systems. The Ronald Press Co., New York, N.Y. 490 pp.

3. Cooper, G. R., and C. D. McGillem. 1971. Probabilistic methods of signal and system analysis. Holt, Rinehart and Winston, Inc., Chicago, Ill. 258 pp.

4. Cooley, J. W., and J. W. Tukey. 1965. An algorithm for the machine calculation of complex Fourier series. Math. Comp. 19 (90): 297-307.

5. Fry, D. N. 1971. Experience in reactor malfunction diagnosis using on-line noise analysis. Nuc. Technol. 10: 273-282.

6. Fry, D. N., R. C. Kryter, and J. C. Robinson. 1973. On-site noise diagnostics at Palisades nuclear power station. Pages 27-1 – 27-14 in T. W. Kerlin, ed. Power Plant Dynamics Control and Testing an Application Symposium. University of Tennessee, Knoxville, Tennessee.

7. Ackermann, N. J., Jr., D. N. Fry, R. C. Kryter, W. H. Sides, Jr., J. C. Robinson, J. E. Mott, and M. A. Atta. 1975. Diagnosis of in-core instrument tube vibrations in BWR-4's. Am. Nuc. Soc., Trans. 22: 624-625.

8. Fry, D. N., J. C. Robinson, R. C. Kryter, and O. C. Cole. 1975. Core component vibration monitoring in BWR's using neutron noise. Am. Nuc. Soc., Trans. 22: 623-624.

9. Thie, J. A. 1972. Reactor noise monitoring for malfunctions. Reactor Technol. 14 (4): 354-365.

10. Gonzalez, R. C. 1973. On the application of pattern recognition methods to reactor malfunction diagnosis. Pages 25-1 – 25-17 in T. W. Kerlin, ed. Power Plant Dynamics, Control and Testing an Application Symposium. University of Tennessee, Knoxville, Tennessee.

11. Gonzalez, R. C., D. N. Fry, and R. C. Kryter. 1974. Results to the application of pattern recognition methods to nuclear reactor core component surveillance. IEEE Trans. Nuc. Sci. 21 (1): 750-756.

12. Kryter, R. C., D. N. Fry, and R. C. Gonzalez. 1973. Application of pattern recognition methods to reactor core component surveillance. Am. Nuc. Soc., Trans. 17: 379-380.

13. Ball, G. H., and D. J. Hall. 1965. Isodata, a novel method of data analysis and pattern classification. NTIS report AD 699616.

14. Piety, K. R., and J. C. Robinson. 1975. An on-line surveillance algorithm based on multivariate analysis of noise. Pages 15-1 – 15-33 in T. W. Kerlin, ed. Proceedings of the Second Power Plant Dynamics, Control and Testing Symposium. University of Tennessee, Knoxville, Tennessee.

15. Piety, K. R. 1976. On-line reactor surveillance based on multivariate analysis of noise signals. Ph.D. Thesis. University of Tennessee, Knoxville, Tennessee. 123 pp.

16. Albrecht, R. W. 1972. The use of coherence for anomaly detection in nuclear reactors. Nuc. Technol. 14: 208-217.

17. Cohn, C. E. 1960. A simplified theory of pile noise. Nuc. Sci. and Engr. 7: 472-475.

18. Wach, D., and G. Kolsay. 1974. Investigation of the joint effect of local and global driving sources in in-core neutron noise measurements. Atomkernenergie 23 (4): 244-250.

19. Lu, J. T. 1976. Detection of void fluctuations in reactor coolant channels by neutron noise analysis. Ph.D. Thesis. Iowa State University, Ames, Iowa. 99 pp.

20. Otnes, R. K., and L. Enochson. 1972. Digital time series analysis. John Wiley & Sons, Inc., New York, N.Y. 467 pp.

21. Mathis, M. V., D. N. Fry, J. C. Robinson, and J. E. Jones. 1976. Neutron noise measurements to evaluate BWR-4 core modification to prevent instrument tube vibration. Am. Nuc. Soc., Trans 23: 466.

22. Mott, J. E., J. C. Robinson, D. N. Fry, and M. P. Brackin. 1976. Detection of impacts of instrument tubes against channel boxes in BWR-4's using neutron noise analysis. Am. Nuc. Soc., Trans. 23: 465.

A. Additional References

Gopal, R. 1973. Surveillance systems for nuclear power plants. Am. Nuc. Soc., Trans. 17: 378.

Mott, M. E., and J. C. Robinson. 1975. Minicomputer-based surveillance and diagnostics for nuclear power plants. Am. Nuc. Soc., Trans. 22: 289.

Robinson, J. C. 1973. Nuclear power plant noise monitoring. Am. Nuc. Soc., Trans. 17: 376-377.

Seifritz, W. 1970. At-power reactor noise induced by fluctuations of the coolant flow. Atomkernenergie 16 (5): 29-34.

Tou, J. T., and R. C. Gonzalez. 1974. Pattern recognition principles. Addison-Wesley Publishing Co., Inc., Reading, Mass. 377 pp.

VII. ACKNOWLEDGMENTS

The author is indebted to his major professor, Dr. Richard A. Hendrickson, for the support and guidance he provided throughout the investigation and preparation of the thesis. The author also wishes to acknowledge and thank Iowa Electric Light and Power Company, and in particular the Reactor Engineering Group, for providing time and services which allowed signal measurements to be made. The support of Power Affiliates and project funding from the Engineering Research Institute is acknowledged. In addition, the services and facilities provided by Ames Laboratory of the ERDA is highly appreciated.

VIII. APPENDIX A: THE MISODATA ALGORITHM USED IN THE PATTERN RECOGNITION SYSTEM

The algorithm presented in this section utilizes univariate Euclidean distances as the criteria for assigning sample patterns to cluster centers. To process a set of N_p sample patterns , $\{\underline{PSD}, \underline{PSD}_2, \underline{PSD}_3, \ldots, \underline{PSD}_{N_p}\}$, each of dimensionality N_{DIM}, MISODATA consists of the following principal steps.

Step 1. First, specify a set of N_c initial cluster centers, $\{\underline{Z}_1, \underline{Z}_2, \underline{Z}_3, \ldots, \underline{Z}_{N_c}\}$, which is not necessarily equal in number to the desired number of clusters. These initial cluster centers, representing a guess of the results, can be selected by using sample patterns.

Next the following process parameters are specified:

K = number of cluster subsets desired

θ_N = a parameter against which the number of samples in a cluster subset is compared. Cluster subsets containing fewer than this value are eliminated and sample patterns reassigned.

θ_s = the maximum standard error permissable for a cluster subset.

θ_c = a lumping parameter. A cluster center – cluster center distance smaller than this value results in the merger of the two respective cluster subsets.

L_{MAX} = maximum number of pairs of cluster centers which can be lumped during one iteration.

I = number of iterations allowed.

Step 2. Distribute the N_p sample patterns among the present cluster centers using the smallest Euclidean distance as the criteria, that is

$$PSD_i \in S_j \text{ if } D_{ij} < D_{ik}, \qquad k = 1, 2, 3, \ldots, N_c;\ k \neq j$$

where

$$D_{ij} = [\sum_{k=1}^{N} (PSD_{ik} - Z_{jk})^2]^{1/2}$$

for sample pattern i and S_j represents the subset of samples assigned to cluster subset j.

If this is the last iteration go to Step 14.

Step 3. Discard cluster subsets with fewer than θ_N members and reduce N_c by 1.

Step 4. Update each cluster center ($\underline{Z}_j$) by setting it equal to the mean of its corresponding set S_j; that is,

$$\underline{Z}_j = \frac{1}{N_j} \sum_{PSD_i \in S_j}^{N_j} \underline{PSD}_i, \qquad j = 1, 2, 3, \ldots, N_c$$

where N_j is the number of samples in S_j.

Step 5. Compute the average distance $\bar{D}_j$ of samples in cluster subset S_j from their corresponding cluster center, using the relation

$$\bar{D}_j = \frac{1}{N_j} \sum_{PSD_i \in S_j}^{N_j} D_{ij}, \qquad j = 1, 2, 3, \ldots, N_c$$

Step 6. Compute the overall average distance, $\bar{D}$ of the samples from their respective cluster centers using the relation

$$\bar{D} = \frac{1}{N_p} \sum_{j=1}^{N_c} N_j \bar{D}_j$$

Step 7. (a) If this is the last iteration, set $\theta_c = 0$ and go to Step 11. (b) If $N_c \leq (K/2.0)$, go to Step 8. (c) If this is an even-numbered iteration, or if $N_c \geq 2K$, go to Step 11; otherwise continue.

Step 8. Find the components of the standard error vector $\underline{\sigma_E}_j = (\sigma_{E_{j1}}, \sigma_{E_{j2}}, \sigma_{E_{j3}})^T$ for each sample subset, using the relation

$$\sigma_{E_{jk}} = \frac{\sqrt{\frac{1}{N_j} \sum_{\underline{PSD}_i \, \epsilon \, S_j}^{N_j} (PSD_{ik} - Z_{jk})^2}}{Z_{jk}}$$

Next calculate the average standard error for each cluster center using

$$\bar{\sigma}_{E_j} = \frac{1}{N_{DIM}} \sum_{\kappa=1}^{N_{DIM}} \sigma_{E_{jk}} \qquad \text{for } j = 1, 2, 3, \ldots, N_c$$

Step 9. Find the maximum component of each standard error vector and denote it $\sigma_{E_{jmax}}$.

Step 10. If for any $\bar{\sigma}_{E_j}$, $j = 1, 2, 3, \ldots, N_c$, we have $\bar{\sigma}_{E_j} > \theta_s$ and

(a) $\bar{D}_j > \bar{D}$ and $N_j > 2(\theta_N + 1)$

or

(b) $N_c \leq K/2$

then split $\underline{Z}_j$ into two new cluster centers $\underline{Z}_j^+$ and $\underline{Z}_j^-$, delete $\underline{Z}_j$, and increase N_c by 1. $\underline{Z}_j^+$ is formed for each component Z_{jk}^+, using the relation

$$Z_{jk}^+ = [1.0 + 0.5(\sigma_{E\ jk})]Z_{jk}$$

Likewise $\underline{Z}_j^-$ is formed by

$$Z_{jk}^- = [1.0 - 0.5(\sigma_{E\ jk})]Z_{jk}$$

If splitting took place go to Step 2.

Step 11. Compute the cluster center-cluster center distances DD_{ij};

$$DD_{ij} = \left[\sum_{k=1}^{N_{DIM}} (Z_{ik} - Z_{jk})^2\right]^{1/2} \quad \text{for } i = 1, 2, 3, \ldots, (N_c - 1); \quad j = i + 1, \ldots, N_c$$

Step 12. Compare the distances DD_{ij} against the paramater θ_c and arrange the L_{MAX} smallest distances in ascending order.

Step 13. With each distance DD_{ij} there is an associated pair of cluster centers $\underline{Z}_i$ and $\underline{Z}_j$. Starting with the smallest of these distances perform a pairwise lumping operation according to the following rule:

If neither $\underline{Z}_i$ or $\underline{Z}_j$ has been used in lumping in this iteration, merge these two cluster centers using the following relation:

$$\underline{Z}_\ell^* = \frac{1}{N_i + N_j}\left[N_i(\underline{Z}_i) + N_j(\underline{Z}_j)\right]$$

where N_i and N_j represent the number of subset members for clusters i and j. Delete $\underline{Z}_i$ and $\underline{Z}_j$ and reduce N_c by 1.

It is noted that further pair lumping is allowed, but experimental evidence indicates further lumping can produce unsatisfactory results.

Go to Step 2.

Step 14. List final results and terminate execution.

IX. APPENDIX B: THE PSDS COMPUTER PROGRAM

A. Input Data for PSDS

The data input variables and their descriptions for PSDS are:

1. NPLT = the number of noise signal groups (ensembles) to be processed in a job.

2. PUNCH = card punching option (0 = no punched output; 1 = punched output).

3. NPNT = the number of digitized data points per sample function (should always be 4096).

4. H = the time step of data points or sampling period.

   = 1.0/sampling frequency (f_s).

5. NSET = the number of sample functions per ensemble to be averaged.

6. SCLF = an amplitude scale factor.

7. CUTOFF = cutoff frequency (f_c).

The data input formats consist of:

CARD #1: NPLT, PUNCH

CARD #2: NPNT, H, NSET, SCLF, CUTOFF

(There are NPLT of these)

It should be noted that for each ensemble the second card describes how it is to be processed; for NPLT = 3, there would be four input cards (one card #1 and three card #2's).

In addition to data input cards, control cards determining how to read the records off tape are required. As an example, Section B of Appendix B shows data and control card input for PSDS. In this

example one should first note that one ensemble is being processed and that there are eight sample functions in the ensemble. Consequently eight tape control cards are needed — one for each sample function.

Section C of Appendix B lists the computer program PSDS. The output of the program includes a listing of the PSD from approximately 0.0 to 10.0 hertz. Punched output of the same form is also available depending upon the punching option used.

The 4096 real and imaginary pairs returned from FFT cover a frequency range from 0.0 to f_s hertz. Only the range from 0.0 to $f_s/2.0$ hertz are correct, however, due to the Nyquist frequency criteria. Thus for a sampling frequency of 250 hertz only the range from 0.0 to 125.0 hertz is usable. Since the criteria for selection of f_c is $f_c = 2.5\ f_c$, the upper limit is further reduced to 100.0 hertz.

On the third page of the program listing, in the loop calling "OUTPUT," the "DO" parameter may be increased to as high as .40*NPNT if frequency points up to f_c are desired. The value of J = 175 is used to stop the output execution at slightly over 10.0 hz, since this is the frequency range of interest for BWR component vibration when a cutoff of 100.0 hertz is used.

B. Sample Control Cards and Input Data

```
//D317PSDS JOB A0118,'HOLTHAUS'
//S1 EXEC  PL1CG,REGION.GO=128K,TIME.GO=4
//PL1L.SYSIN  DD  *

                    ----- PROGRAM PSDS -----

//GO.CARDS  DD  SYSOUT=B,DCB=(LRECL=80,RECFM=FB,BLKSIZE=80)
//GO.DAPT   DD DCB=(DEN=1,TRTCH=ET,BUFNO=1,RECFM=U,BLKSIZE=1554),
// DISP=(OLD,PASS),UNIT=TAPE7,LABEL=(001,NL,,IN),VOL=SER=KH0002
//           DD DCB=(DEN=1,TRTCH=ET,BUFNO=1,RECFM=U,BLKSIZE=1554),
// DISP=(OLD,PASS),UNIT=TAPE7,LABEL=(002,NL,,IN),VOL=SER=KH0002
//           DD DCB=(DEN=1,TRTCH=ET,BUFNO=1,RECFM=U,BLKSIZE=1554),
// DISP=(OLD,PASS),UNIT=TAPE7,LABEL=(003,NL,,IN),VOL=SER=KH0002
//           DD DCB=(DEN=1,TRTCH=ET,BUFNO=1,RECFM=U,BLKSIZE=1554),
// DISP=(OLD,PASS),UNIT=TAPE7,LABEL=(004,NL,,IN),VOL=SER=KH0002
//           DD DCB=(DEN=1,TRTCH=ET,BUFNO=1,RECFM=U,BLKSIZE=1554),
// DISP=(OLD,PASS),UNIT=TAPE7,LABEL=(005,NL,,IN),VOL=SER=KH0002
//           DD DCB=(DEN=1,TRTCH=ET,BUFNO=1,RECFM=U,BLKSIZE=1554),
// DISP=(OLD,PASS),UNIT=TAPE7,LABEL=(006,NL,,IN),VOL=SER=KH0002
//           DD DCB=(DEN=1,TRTCH=ET,BUFNO=1,RECFM=U,BLKSIZE=1554),
// DISP=(OLD,PASS),UNIT=TAPE7,LABEL=(007,NL,,IN),VOL=SER=KH0002
//           DD DCB=(DEN=1,TRTCH=ET,BUFNO=1,RECFM=U,BLKSIZE=1554),
// DISP=(OLD,PASS),UNIT=TAPE7,LABEL=(008,NL,,IN),VOL=SER=KH0002
//GO.SYSIN  DD  *
  NPLT=1   , PUNCH=1;
  NPNT=4096, H=0.0040, NSET=8,   SCLF=1.000,     CUTOFF=100.;
//
```

C. Listing of the Computer Program PSDS

```
PSDS: PROC OPTIONS(MAIN) REORDER;
/*    NPLT=NUMBER OF ENSEMBLES TO BE PROCESSED                          */
/*    PUNCH=PUNCHING OPTION(0=NO PUNCHED OUTPUT; 1=PUNCHED OUTPUT)      */
/*    NPNT=NUMBER OF DIGITIZED DATA POINTS(4096)                        */
/*    H=SAMPLING PERIOD=1.0/SAMPLING FREQUENCY                          */
/*    NSET=NUMBER OF SAMPLE FUNCTIONS PER ENSEMBLE                      */
/*    SCLF=AMPLITUDE SCALE FACTOR                                       */
/*    CUTOFF=CUTOFF FREQUENCY                                           */
DCL DAPT FILE;
DCL S(2048);
DCL PUNCH FIXED BINARY INIT(0);
DCL PI INIT(3.141592653);
GET DATA(NPLT,PUNCH) COPY;
DO JP=1 TO NPLT;
  PUT PAGE;
  S=0.0;
  GET DATA(NPNT,H,NSET,SCLF,CUTOFF) COPY ;
  TP=NPNT*H;
  IF NPNT ¬= 4096 THEN DO;
    PUT SKIP LIST('***NPNT ¬= 4096***');
    GO TO EXIT;
  END;
  NPND=2*NPNT;
  M=LOG2(NPND);
  DELTA=2.*H/NPNT;
BEGIN   REORDER       ;
DCL ERROR CHAR(1) EXTERNAL;
DCL B(8192);
  ABART=0.0;
  DO J=1 TO NSET;
    B=0.0;
/*      READ REAL-VALUED, DIGITIZED DATA INTO ODD NUMBERED ARRAY
        POSITIONS                                                       */
    GET FILE(DAPT) EDIT((B(K) DO K=1 TO 8192 BY 2))
                        (16(X(18),256 F(6)));
```

```
/*      REMOVE DC COMPONENT                                              */
     ABAR=SUM(B)/4096;
     ABART=ABART+ABAR;
     DO I=1 TO 8192 BY 2;
       B(I)=(B(I)-ABAR)/SCLF;
     END;
/*      COSINE TAPER THE INPUT DATA BEFORE FFT                           */
     DO K=1 TO NPNT/10;
       B(2*K-1)=B(2*K-1)*(COS(5.*PI*(K-NPNT/2)/NPNT))**2;
     END;
     DO K=.9*NPNT TO NPNT;
       B(2*K-1)=B(2*K-1)*(COS(5.*PI*(K-NPNT/2)/NPNT))**2;
     END;
     CALL FFT(B,M,'1');
     IF ERROR ¬= '0' THEN DO;
        PUT LIST('***ERROR IN FFT***');
        GO TO EXIT;
     END;
/*      CALCULATE ENSEMBLE AVERAGED POWER SPECTRAL DENSITIES             */
     DO I=1 TO NPNT/2;
       S(I)=S(I)+DELTA*(B(2*I-1)**2+B(2*I)**2)/0.875;
     END;
   END;
S=S/NSET;
ABART=ABART/NSET;
PUT SKIP LIST('DC-LEVEL MEAN FOR DIGITIZING=',ABART);
END;
BEGIN   RECRDER       ;
DCL F(2048);
   STD=1.0/SQRT(NSET);
   PUT DATA(STD) SKIP(3);
/*      LIST RESULTANT VALUES OF FREQUENCY,PSD, AND ERROR LIMITS         */
   PUT LIST('         FREQUENCY                PSD              PSD+STD' ||
            '              PSD-STD') SKIP(3);
   PUT LIST('         ---------                ---              -------' ||
```

```
          '                -------') SKIP;
  DO J=1 TO .41*NPNT;
    F(J)=J/TP;
      END;
    DO J=1 TO 175;
      CALL OUTPUT(J);
    END;
  OUTPUT:PROC(I);
DCL I FIXED BINARY;
  STDPLUS=S(I)*(1.+STD);
  STDMNUS=S(I)*(1.-STD);
  PUT EDIT(F(I),S(I),STDPLUS,STDMNUS) (4 E(20,6)) SKIP;
IF PUNCH ¬= 0 THEN PUT SKIP FILE(CARDS) EDIT(F(I),S(I),STDPLUS,STDMNUS)
                                                  (4 E(13,6));
  END OUTPUT;
  END;
END;
EXIT:END PSDS;
```

X. APPENDIX C: THE PATTERN RECOGNITION PROGRAM

A. Definitions of the Input Parameters

The parameters required for input to the pattern recognition program are:

1. NDGRPS = the number of sample patterns to be processed.

2. NDIM = the dimensionality of the pattern vectors.

3. IOPT = the processing option. The value of the option is 1 for input of pattern vectors containing frequency-smoothed and normalized components. Punched card output from PSDS may be used as input to the pattern recognition program upon specification of the processing option as 0. The main program finds the frequencies (specified in the FREQ vector) and their associated PSD values and normalizes the data. Omission of frequency smoothing yields higher standard errors in the PSD values. Therefore, use of 0 as the option is not recommended.

4. PUNCH = option for producing punched card output of the cluster centers calculated upon completion of the last iteration (0 = do not punch output; 1 = punch output).

5. FREQLO = lowest frequency point used in sample patterns.

6. FREQHI = highest frequency point used in sample patterns.

7. FREQ = vector containing frequencies used over the range from FREQLO to FREQHI.

8. PSDNOR = vector containing NDGRPS normalization factors for use when IOPT = 0.

9. PSD = a two-dimensional array containing the sample patterns. Two to twenty-five patterns may be used in the program, each with two to 38 dimensions (each dimension corresponding to the a component of FREQ).

10. NSUBC = N_c = an estimation of the number of clusters which will result from the analysis. This value does not necessarily have to be equal to KLWSD.

11. Z = the NSUBC cluster centers initially guessed at. Use of sample patterns to be used is a convenient method for selection of the Z's.

12. KLUSD = K = the number of clusters desired.

13. THETAN = θ_N = a parameter against which the number of samples in a cluster subset is compared. Clusters containing less than this value are eliminated and the sample patterns are reassigned to a different cluster subset. The suggested value of THETAN to be used is 1, thus allowing the identification of an abnormal sample pattern.

14. THETAS = θ_s = the maximum-permissable average standard error for a cluster subset. Selection of a value is dependent upon the standard error of the PSD's (ϵ). A value of 1.5ϵ is recommended. For, ϵ = 0.17678, THETAS should be 0.26517.

15. THETAC = θ_c = a lumping parameter. Cluster center-cluster center distances less than THETAC result in their merger. A typical value is 1.0×10^{-4}. Decreasing the value to 1.0×10^{-10} makes the lumping function inoperable.

16. LCLMAX = L = the maximum number of cluster subsets which can be lumped during one iteration. A value of 1 is strongly recommended.

17. ITRNS = the number of iterations to be executed.

B. Input Data and Formats

There are two possible systems of input to the pattern recognition program, the difference being based upon the processing option, IOPT, specified. For IOPT = 0 the input formats will not be listed because this is a more expensive method yielding larger standard errors. For IOPT = 1 the input data and formats are:

CARD #1: NDGRPS, NDIM, IOPT, PUNCH (4I3)

CARD #2: FREQLO, FREQHI (2F10.0)

CARDS #3: FREQ [NDIM * (E 13.6)]

CARDS #4: PSD_1, PSD_2, PSD_3, ..., PSD_{NDGRPS}

[(NDIM/6) * (6E13.6)]

for each PSD_n

CARD #5: NSUBC (I2)

CARDS #6: Z_1, Z_2, Z_3, ..., Z_{NSUBC}

[(NDIM/6) * (6E13.6)]

for each Z_m

CARD #7: KLUSD, THETAN, THETAS, THETAC, LCLMAX, ITRNS

(2I10, 2E13.6, 2I10)

C. Sample Input Data

```
12 38   1   1
   1.007C8     10.04C3
0.100708E 01
0.125122E 01
0.149536E 01
0.173950E 01
0.198364E 01
0.222778E C1
0.247192E 01
0.271607E 01
0.296021E 01
0.320435E 01
0.344849E C1
0.369263E 01
0.393677E 01
0.418091E 01
0.442505E 01
0.466919E 01
0.491333E 01
0.515747E 01
0.540161E C1
0.564575E 01
0.588989E 01
0.613403E 01
0.637817E 01
0.662231E 01
0.686646E 01
0.711060E 01
0.735474E 01
0.759888E 01
0.784302E 01
0.808716E 01
0.833130E 01
0.857544E C1
0.881958E 01
```

0.906372E 01
0.930786E 01
0.955200E 01
0.979614E 01
0.100403E 02
0.267412E-03 0.192002E-03 0.193196E-03 0.166127E-03 0.173206E-03 0.182772E-03
0.119436E-03 0.210107E-03 0.177570E-03 0.185259E-03 0.205040E-03 0.152331E-03
0.242787E-03 0.188751E-03 0.173644E-03 0.176183E-03 0.219289E-03 0.177577E-03
0.159029E-03 0.173404E-03 0.210839E-03 0.221278E-03 0.183490E-03 0.100483E-03
0.174438E-03 0.189547E-03 0.193937E-03 0.236452E-03 0.145509E-03 0.205472E-03
0.161530E-03 0.200290E-03 0.175998E-03 0.191596E-03 0.131648E-03 0.169201E-03
0.118544E-03 0.157631E-03
0.473771E-02 0.241996E-02 0.206675E-02 0.252049E-02 0.192082E-02 0.165267E-02
0.971798E-03 0.668048E-03 0.120236E-02 0.123889E-02 0.222715E-02 0.459326E-02
0.267852E-02 0.368169E-02 0.214297E-02 0.131973E-02 0.148554E-02 0.933451E-03
0.764561E-03 0.673118E-03 0.401906E-03 0.364250E-03 0.208601E-03 0.189931E-03
0.295586E-03 0.175485E-03 0.191173E-03 0.243833E-03 0.211971E-03 0.155747E-03
0.159052E-03 0.158960E-03 0.110085E-03 0.155700E-03 0.128849E-03 0.879765E-04
0.551387E-04 0.807930E-04
0.759328E-03 0.303835E-03 0.200065E-03 0.182755E-03 0.148587E-03 0.108502E-03
0.112855E-03 0.113603E-03 0.100591E-03 0.796192E-04 0.102462E-03 0.109231E-03
0.876484E-04 0.895847E-04 0.838997E-04 0.996966E-04 0.105785E-03 0.723851E-04
0.639507E-04 0.684263E-04 0.562547E-04 0.685828E-04 0.610411E-04 0.674033E-04
0.725703E-04 0.730248E-04 0.742308E-04 0.505633E-04 0.728175E-04 0.672891E-04
0.651600E-04 0.687714E-04 0.585563E-04 0.512338E-04 0.519163E-04 0.649647E-04
0.674476E-04 0.704974E-04
0.401047E-02 0.152519E-02 0.468689E-03 0.229877E-03 0.186415E-03 0.160444E-03
0.154503E-03 0.164028E-03 0.144038E-03 0.119300E-03 0.141781E-03 0.676298E-04
0.937090E-04 0.100659E-03 0.597499E-04 0.733545E-04 0.398396E-04 0.660747E-04
0.447414E-04 0.564180E-04 0.528998E-04 0.463787E-04 0.479766E-04 0.528791E-04
0.485322E-04 0.529258E-04 0.463269E-04 0.393580E-04 0.373698E-04 0.368261E-04
0.389905E-04 0.393751E-04 0.299359E-04 0.303277E-04 0.342861E-04 0.474925E-04
0.312053E-04 0.284612E-04
0.640218E-02 0.192700E-02 0.746302E-03 0.476224E-03 0.327294E-03 0.347145E-03
0.225540E-03 0.238701E-03 0.210764E-03 0.193512E-03 0.130286E-03 0.179224E-03

0.172899E-03 0.158782E-03 0.942575E-04 0.113391E-03 0.609348E-04 0.961318E-04
0.385270E-04 0.480240E-04 0.592019E-04 0.444066E-04 0.573174E-04 0.473952E-04
0.420142E-04 0.442815E-04 0.292341E-04 0.350532E-04 0.400069E-04 0.460282E-04
0.350182E-04 0.296965E-04 0.339928E-04 0.489786E-04 0.418955E-04 0.295868E-04
0.322557E-04 0.252698E-04
0.182533E-02 0.428775E-03 0.252520E-03 0.238457E-03 0.243989E-03 0.155027E-03
0.143843E-03 0.147102E-03 0.868665E-04 0.101864E-03 0.968681E-04 0.661798E-04
0.963198E-04 0.674321E-04 0.665011E-04 0.540150E-04 0.623958E-04 0.605424E-04
0.355002E-04 0.468743E-04 0.368710E-04 0.364514E-04 0.397566E-04 0.494313E-04
0.314015E-04 0.655779E-04 0.335993E-04 0.356253E-04 0.390842E-04 0.362327E-04
0.289153E-04 0.390974E-04 0.351124E-04 0.461366E-04 0.334314E-04 0.338886E-04
0.357642E-04 0.398133E-04
0.451042E-02 0.183141E-02 0.433208E-03 0.296463E-03 0.221262E-03 0.126761E-03
0.194602E-03 0.193700E-03 0.107019E-03 0.162152E-03 0.149918E-03 0.118874E-03
0.713976E-04 0.879745E-04 0.459739E-04 0.678513E-04 0.600873E-04 0.629824E-04
0.477646E-04 0.552750E-04 0.447062E-04 0.352927E-04 0.230031E-04 0.240793E-04
0.253836E-04 0.263489E-04 0.208198E-04 0.250735E-04 0.190735E-04 0.201521E-04
0.223946E-04 0.178330E-04 0.261852E-04 0.194614E-04 0.160204E-04 0.272822E-04
0.149331E-04 0.217790E-04
0.535386E-02 0.115508E-02 0.544630E-03 0.387540E-03 0.159697E-03 0.264138E-03
0.171593E-03 0.123781E-03 0.117125E-03 0.135704E-03 0.123644E-03 0.828122E-04
0.849100E-04 0.869897E-04 0.689755E-04 0.572078E-04 0.680918E-04 0.752644E-04
0.439334E-04 0.305719E-04 0.345175E-04 0.348514E-04 0.331505E-04 0.282526E-04
0.235430E-04 0.273666E-04 0.304749E-04 0.219498E-04 0.271832E-04 0.241914E-04
0.201783E-04 0.209707E-04 0.274268E-04 0.262536E-04 0.202191E-04 0.206709E-04
0.162689E-04 0.282866E-04
0.569864E-02 0.210087E-02 0.694179E-03 0.483358E-03 0.309452E-03 0.215213E-03
0.151470E-03 0.131907E-03 0.151856E-03 0.979097E-04 0.614881E-04 0.905411E-04
0.835603E-04 0.578585E-04 0.555357E-04 0.611571E-04 0.490333E-04 0.502580E-04
0.433898E-04 0.355754E-04 0.256823E-04 0.268859E-04 0.228508E-04 0.271388E-04
0.310815E-04 0.229268E-04 0.263263E-04 0.210176E-04 0.189479E-04 0.157764E-04
0.178794E-04 0.195674E-04 0.230381E-04 0.162391E-04 0.194295E-04 0.173511E-04
0.125766E-04 0.156543E-04
0.388433E-02 0.969842E-03 0.371192E-03 0.174232E-03 0.177380E-03 0.130628E-03
0.129574E-03 0.975376E-04 0.133676E-03 0.107615E-03 0.827913E-04 0.686139E-04

0.605616E-04 0.377816E-04 0.533074E-04 0.558407E-04 0.345867E-04 0.380118E-04
0.373701E-04 0.347523E-04 0.269262E-04 0.253331E-04 0.212652E-04 0.169952E-04
0.205944E-04 0.226714E-04 0.130589E-04 0.180066E-04 0.139463E-04 0.241148E-04
0.203960E-04 0.164283E-04 0.116033E-04 0.148391E-04 0.169700E-04 0.122377E-04
0.110847E-04 0.130245E-04
0.423316E-02 0.133402E-02 0.596196E-03 0.149900E-03 0.166289E-03 0.209910E-03
0.127358E-03 0.141354E-03 0.142852E-03 0.853933E-04 0.598058E-04 0.104746E-03
0.955286E-04 0.630492E-04 0.719213E-04 0.609216E-04 0.484077E-04 0.413565E-04
0.396618E-04 0.280509E-04 0.269035E-04 0.207209E-04 0.178491E-04 0.198807E-04
0.167501E-04 0.157532E-04 0.111497E-04 0.113037E-04 0.106232E-04 0.151725E-04
0.971828E-05 0.112457E-04 0.943131E-05 0.134077E-04 0.105576E-04 0.980941E-05
0.865054E-05 0.112242E-04
0.212169E-02 0.587968E-03 0.259679E-03 0.126016E-03 0.149380E-03 0.925446E-04
0.827160E-04 0.109169E-03 0.116434E-03 0.833830E-04 0.849520E-04 0.697116E-04
0.705231E-04 0.799710E-04 0.104333E-03 0.951918E-04 0.798806E-04 0.831808E-04
0.841565E-04 0.737193E-04 0.907649E-04 0.510460E-04 0.764885E-04 0.926212E-04
0.681802E-04 0.887731E-04 0.118451E-03 0.109407E-03 0.785197E-04 0.912427E-04
0.102053E-03 0.671464E-04 0.110511E-03 0.107183E-03 0.123651E-03 0.781820E-04
0.849700E-04 0.117123E-03
4
0.267412E-03 0.192002E-03 0.193196E-03 0.166127E-03 0.173206E-03 0.182772E-03
0.119436E-03 0.210107E-03 0.177570E-03 0.185259E-03 0.205040E-03 0.152331E-03
0.242787E-03 0.188751E-03 0.173644E-03 0.176183E-03 0.219289E-03 0.177577E-03
0.159029E-03 0.173404E-03 0.210839E-03 0.221278E-03 0.183490E-03 0.100483E-03
0.174438E-03 0.189547E-03 0.193937E-03 0.236452E-03 0.145509E-03 0.205472E-03
0.161530E-03 0.200290E-03 0.175998E-03 0.191596E-03 0.131648E-03 0.169201E-03
0.118544E-03 0.157631E-03
0.473771E-02 0.241996E-02 0.206675E-02 0.252049E-02 0.192082E-02 0.165267E-02
0.971798E-03 0.668048E-03 0.120236E-02 0.123889E-02 0.222715E-02 0.459326E-02
0.267852E-02 0.368169E-02 0.214297E-02 0.131973E-02 0.148554E-02 0.933451E-03
0.764561E-03 0.673118E-03 0.401906E-03 0.364250E-03 0.208601E-03 0.189931E-03
0.295586E-03 0.175485E-03 0.191173E-03 0.243833E-03 0.211971E-03 0.155747E-03
0.159052E-03 0.158960E-03 0.110085E-03 0.155700E-03 0.128849E-03 0.879765E-04
0.551387E-04 0.807930E-04
0.129233E-02 0.366305E-03 0.226292E-03 0.210606E-03 0.196288E-03 0.131764E-03

```
0.128349E-03 0.130352E-03 0.937287E-04 0.907416E-04 0.996650E-04 0.877054E-04
0.919841E-04 0.785084E-04 0.752004E-04 0.768558E-04 0.840904E-04 0.664637E-04
0.497254E-04 0.676503E-04 0.465628E-04 0.525171E-04 0.503988E-04 0.584173E-04
0.519859E-04 0.693013E-04 0.539150E-04 0.430943E-04 0.559508E-04 0.517609E-04
0.470379E-04 0.539344E-04 0.468343E-04 0.486852E-04 0.426738E-04 0.494266E-04
0.516059E-04 0.551553E-04
0.487043E-02 0.154906E-02 0.550636E-03 0.313942E-03 0.221113E-03 0.207748E-03
0.164948E-03 0.155858E-03 0.143904E-03 0.128798E-03 0.107102E-03 0.101777E-03
0.946379E-04 0.847277E-04 0.643173E-04 0.699604E-04 0.515687E-04 0.614398E-04
0.421983E-04 0.412382E-04 0.386910E-04 0.334099E-04 0.319161E-04 0.309458E-04
0.296998E-04 0.303249E-04 0.253415E-04 0.245375E-04 0.238787E-04 0.260373E-04
0.235107E-04 0.221595E-04 0.230876E-04 0.242153E-04 0.227666E-04 0.234901E-04
0.161393E-04 0.205285E-04
         4           1       3.5E-01     1.0000E-05          1           6
```

D. The Pattern Recognition Code Listing

```
C     ************************************************************************
C     *                                                                      *
C     *      MAIN PROGRAM:  PATTERN RECOGNITION OF VECTORS WITH              *
C     *                     DIMENSIONALITY OF UP TO 38 AND 25 PATTERNS       *
C     *                                                                      *
C     ************************************************************************
      DIMENSION PSD(25,38),PSDNOR(25),FREQ(38)
      DIMENSION Z(25,38)
      INTEGER PUNCH
      COMMON/POWER/PSD,PSDNOR,FREQ
      COMMON/PARAM1/NDGRPS,NDIM,NSUBC,Z
      WRITE(6,5)
    5 FORMAT('1','MAIN PROGRAM INPUT DATA'/' ','---- ------- ----- ----'
     1///)
      READ(5,10) NDGRPS,NDIM,IOPT,PUNCH
   10 FORMAT(10I3)
      IF(NDIM .GE. 2  .AND.  NDIM .LE. 38) GO TO 15
      WRITE(6,12) NDIM
   12 FORMAT(' ','$$$$$$$$$ERROR$$$$$$$$$$',10X,'NDIM=',I2)
      STOP
   15 WRITE(6,20) NDGRPS,NDIM,IOPT,PUNCH
   20 FORMAT(' ','NUMBER OF DATA GROUPS PROCESSED=',I2/' ','DIMENSIONALI
     1TY=',I2/' ','PROCESSING OPTION=',I2,5X,'(0=FIND AND NORMALIZE DATA
     2;  1=DATA ALREADY FOUND AND NORMALIZED)'/' ','PUNCH=',I2,5X,
     3'(0=DO NOT PUNCH OUTPUT;  1=PUNCH OUTPUT)'/)
      READ(5,30) FREQLO,FREQHI
   30 FORMAT(8F10.0)
      WRITE(6,40) FREQLO,FREQHI
   40 FORMAT(' ','DATA ARE PROCESSED OVER A FREQUENCY RANGE FROM ',F7.4,
     1' HZ TO ',F7.4,' HZ'/)
C     READ FREQUENCIES TO BE USED (NUMBER OF DIMENSIONS)
      DO 50 I=1,NDIM
   50 READ(5,60) FREQ(I)
   60 FORMAT(6E13.6)
      DO 65 I=1,NDIM
```

```
   65 WRITE(6,67) I,FREQ(I)
   67 FORMAT(' ','FREQUENCY(',I2,')=',F10.5)
      WRITE(6,69)
   69 FORMAT(' ',///)
      IF(IOPT .EQ. 1) GO TO 110
C     IOPT=0:  FIND AND NORMALIZE PSD'S READ FROM FILES 11 THROUGH 31
C     FIND PSD'S AT GIVEN FREQUENCIES
      NIN=11
      DO 90 IP=1,NDGRPS
      DO 80 JP=1,NDIM
   70 READ(NIN,60) FREQR,PSDR
      IF(ABS(FREQR-FREQ(JP))/FREQ(JP) .GE. 1.0E-04) GO TO 70
   80 PSD(IP,JP)=PSDR
   90 NIN=NIN+1
      DO 92 I=1,NDGRPS
   92 WRITE(6,95) I,(PSD(I,J),J=1,NDIM)
   95 FORMAT(' ','PSD(',I2,')=',6E13.6/' ',8X,6E13.6/' ',8X,6E13.6/' ',
     18X,6E13.6/' ',8X,6E13.6/' ',8X,6E13.6/' ',8X,6E13.6/' ',8X,2E13.6/)
      WRITE(6,69)
C     NORMALIZE DATA
      DO 100 J=1,NDGRPS
      READ(5,30) PSDNOR(J)
      WRITE(6,97) J,PSDNOR(J)
   97 FORMAT(' ','PSD NORMALIZATION FACTOR(',I2,')=',F4.2)
  100 CALL NORM(J,NDIM)
      CALL ISODAT
      IF(PUNCH .NE. 1) STOP
      DO 105 I1=1,NDGRPS
  105 WRITE(7,120) (PSD(I1,J1),J1=1,NDIM)
      DO 107 I=1,NSUBC
  107 WRITE(7,120) (Z(I,J),J=1,NDIM)
      STOP
C     IOPT=1:  READ NORMALIZED DATA FROM FILE 5
  110 DO 130 I=1,NDGRPS
      READ(5,120) (PSD(I,J),J=1,NDIM)
```

```
  120 FORMAT(6E13.6)
  130 WRITE(6,95) I,(PSD(I,J),J=1,NDIM)
      WRITE(6,69)
      CALL ISODAT
      IF(PUNCH .NE. 1) STOP
      DO 140 I=1,NSUBC
  140 WRITE(7,120) (Z(I,J),J=1,NDIM)
      STOP
      END


      SUBROUTINE NORM(I,NDIM)
C     ***********************************************************************
C     *                                                                     *
C     *     NORMALIZE POWER SPECTRAL DENSITIES                              *
C     *                                                                     *
C     ***********************************************************************
      DIMENSION PSD(25,38),PSDNOR(25),FREQ(38)
      COMMON/POWER/PSD,PSDNOR,FREQ
      DO 10 J=1,NDIM
   10 PSD(I,J)=PSD(I,J)/PSDNOR(I)**2
      RETURN
      END


      SUBROUTINE ISODAT
C     ***********************************************************************
C     *                                                                     *
C     *     MODIFIED ITERATIVE SELF-ORGANIZING DATA ANALYSIS                *
C     *     TECHNIQUE A (MISODATA)                                          *
C     *                                                                     *
C     ***********************************************************************
      DIMENSION PSD(25,38)
```

```
      DIMENSION Z(25,38),D(25,25),DBAR(25),DD(25,25)
      DIMENSION IPSDST(25),ISET(25),ISIGMX(25)
      DIMENSION SIGSD(25,38),SIGMAX(25)
      DIMENSION ASORT(601)
      DIMENSION ICRSA(300),ICRSB(300),ICRSC(25),ICRSD(25)
      DIMENSION IJOIN(50),IELIM(25)
      DIMENSION AVESE(25)
      INTEGER THETAN
      COMMON/POWER/PSD
      COMMON/PARAM1/NDGRPS,NDIM,NSUBC,Z,D,IPSDST,ISET
C
C     NDGRPS=NUMBER OF SAMPLES(PSD VECTORS) TO BE ANALYZED
C     NDIM=NUMBER OF DIMENSIONS(MAXIMUM=38)
C     NSUBC=NUMBER OF CLUSTER CENTERS
C     Z(KCH,J)=CLUSTER CENTER KCH
C     KLUSD=NUMBER OF CLUSTER CENTERS DESIRED
C     THETAN=A PARAMETER AGAINST WHICH THE NUMBER OF SAMPLES IN A
C            CLUSTER DOMAIN IS COMPARED TO DETERMINE IF THE CLUSTER
C            CENTER IS TO BE ELIMINATED
C     THETAS=STANDARD ERROR PARAMETER
C     THETAC=LUMPING PARAMETER CORRESPONDING TO CLUSTER CENTER-CLUSTER
C            CENTER DISTANCES
C     LCLMAX=MAXIMUM NUMBER OF PAIRS OF CLUSTER CENTERS WHICH CAN BE
C            LUMPED DURING ONE ITERATION
C     ITRNS=NUMBER OF ITERATIONS ALLOWED
C     D(KCH,I)=DISTANCE FROM CLUSTER CENTER KCH TO SAMPLE I
C     ISET(KCH)=NUMBER OF SAMPLES IN CLUSTER CENTER KCH
C     IPSDST(I)=CLUSTER CENTER TO WHICH SAMPLE I IS ASSIGNED
C     ITRN=NUMBER OF ITERATIONS EXECUTED-1
C     SIGSD(KCH,N)=STANDARD ERROR VECTOR OF KCH'TH CLUSTER CENTER OF
C                  N'TH DIMENSION
C     SIGMAX(KCH)=MAXIMUM STANDARD ERROR COMPONENT IN KCH'TH CLUSTER
C                 CENTER
C
      READ(5,10) NSUBC
```

```
   10 FORMAT(I2)
      DO 20 I=1,NSUBC
   20 READ(5,30) (Z(I,J),J=1,NDIM)
   30 FORMAT(6E13.6)
C
C     ++++++++++++++++++++++++++++++++++++++++++++++++++++++++++++++++++++
C     +  STEP 1 MISODATA:  SPECIFY PARAMETERS                            +
C     ++++++++++++++++++++++++++++++++++++++++++++++++++++++++++++++++++++
C
      READ(5,40) KLUSD,THETAN,THETAS,THETAC,LCLMAX,ITRNS
   40 FORMAT(2I10,2E13.6,2I10)
      ITRN=0
      KLUB=1
C     LIST INPUT PARAMETERS
      WRITE(6,45)
   45 FORMAT('1',25X,'INPUT PARAMETERS'/' ',25X,'----- ----------'///)
      WRITE(6,50) NDGRPS,NSUBC,KLUSD,THETAN,THETAS,THETAC,LCLMAX,ITRNS
   50 FORMAT(' ','NDGRPS=',I2/' ','NSUBC=',I2/' ','KLUSD=',I2/' ','THETA
     1N=',I2/' ','THETAS=',E12.4/' ','THETAC=',E12.4/' ','LCLMAX=',
     2I2/' ','ITRNS=',I2)
      WRITE(6,51) NDIM
   51 FORMAT(' ','NUMBER OF DIMENSIONS=',I2///)
      DO 52 K=1,NSUBC
   52 WRITE(6,54) K,(Z(K,J),J=1,NDIM)
      WRITE(6,1000)
   54 FORMAT(' ','Z(',I2,')=',6E13.6/' ',6X,6E13.6/' ',6X,6E13.6/' ',6X,
     16E13.6/' ',6X,6E13.6/' ',6X,6E13.6/' ',6X,2E13.6/)
 1000 FORMAT(' ',10X//)
      DO 56 I=1,NDGRPS
   56 WRITE(6,58) I,(PSD(I,J),J=1,NDIM)
   58 FORMAT(' ','PSD(',I2,')=',6E13.6/' ',8X,6E13.6/' ',8X,6E13.6/' ',
     18X,6E13.6/' ',8X,6E13.6/' ',8X,6E13.6/' ',8X,2E13.6/)
      WRITE(6,59)
   59 FORMAT('1',10X,'INTERMEDIATE RESULTS'/' ',10X,'------------ ------
     1-'///)
```

```
C
C     ++++++++++++++++++++++++++++++++++++++++++++++++++++++++++++++++
C     +  STEP 2 MISODATA:  DISTRIBUTE NDGRPS SAMPLES AMONG PRESENT    +
C     +                    CLUSTER CENTERS AND DETERMINE IF LAST      +
C     +                    ITERATION                                  +
C     ++++++++++++++++++++++++++++++++++++++++++++++++++++++++++++++++
C
   60 ITRN=ITRN+1
      IF(ITRN .GT. ITRNS  .AND.  KLUB .NE. 0) GO TO 575
      CALL ZIP(0)
      NCHECK=0
      WRITE(6,61) ITRN
   61 FORMAT(' ',20X,'*****STEP 2*****',10X,'ITRN=',I2)
      DO 62 I=1,NDGRPS
   62 WRITE(6,63) I,IPSDST(I)
   63 FORMAT(' ',' I=',I2,5X,'IPSDST=',I2)
      DO 64 I=1,NSUBC
   64 WRITE(6,65) I,ISET(I)
   65 FORMAT(' ',' I=',I2,5X,'ISET=',I2)
C
C     ++++++++++++++++++++++++++++++++++++++++++++++++++++++++++++++++
C     +  STEP 3 MISODATA:  DISCARD SAMPLE SUBSETS WITH FEWER THAN     +
C     +                    THETAN MEMBERS AND REDUCE NSUBC BY ONE FOR +
C     +                    EACH OCCURRANCE                            +
C     ++++++++++++++++++++++++++++++++++++++++++++++++++++++++++++++++
C
  100 K=1
  110 IF(ISET(K) .LT. THETAN) GO TO 120
  115 K=K+1
      IF(K .GT. NSUBC) GO TO 200
      GO TO 110
C
C     SHIFT ALL DATA DOWN TO (NSUBC-1) LEVELS
C
  120 DO 150 I=1,NDGRPS
```

```
      IF(IPSDST(I) .LT. K) GO TO 150
      IF(IPSDST(I) .GT. K) GO TO 140
C     FIND SAMPLES MEMBER OF CLUSTER CENTER BEING ELIMINATED AND
C     REDISTRIBUTE
      IF(K .EQ. 1) GO TO 125
      DMIN=D(1,I)
      IP=1
      GO TO 128
  125 DMIN=D(2,I)
      IP=2
  128 DO 130 IKCH=2,NSUBC
      IF(D(IKCH,I) .GE. DMIN) GO TO 130
      IF(IPSDST(I) .EQ. IKCH) GO TO 130
      DMIN=D(IKCH,I)
      IP=IKCH
  130 CONTINUE
      IPSDST(I)=IP
      ISET(IPSDST(I))=ISET(IPSDST(I))+1
      IF(IPSDST(I) .LT. K) GO TO 150
  140 IPSDST(I)=IPSDST(I)-1
  150 CONTINUE
      NSUBC=NSUBC-1
      IF(K .GE. NSUBC) GO TO 115
      DO 180 KCH=K,NSUBC
      ISET(KCH)=ISET(KCH+1)
      DO 160 I=1,NDGRPS
  160 D(KCH,I)=D((KCH+1),I)
      DO 170 J=1,NDIM
  170 Z(KCH,J)=Z((KCH+1),J)
  180 CONTINUE
      GO TO 115
C
C     ++++++++++++++++++++++++++++++++++++++++++++++++++++++++++++++++
C     +  STEP 4 MISODATA:  UPDATE EACH CLUSTER CENTER Z(I,J)         +
C     ++++++++++++++++++++++++++++++++++++++++++++++++++++++++++++++++
```

```
C
C       INITIALIZE EACH CENTER AS ZERO VECTOR
  200 DO 210 I1=1,NSUBC
      DO 210 J1=1,NDIM
  210 Z(I1,J1)=0.0
C       SUM COMPONENTS OF CLUSTER CENTERS
      DO 220 I2=1,NDGRPS
      DO 220 J2=1,NDIM
  220 Z(IPSDST(I2),J2)=Z(IPSDST(I2),J2)+PSD(I2,J2)
C       DIVIDE SUM OF COMPONENTS BY NUMBER OF SAMPLES IN CLUSTER
      DO 230 ICK=1,NSUBC
      DO 230 JCK=1,NDIM
  230 Z(ICK,JCK)=Z(ICK,JCK)/ISET(ICK)
      KLUB=KLUB+1
      WRITE(6,231)
  231 FORMAT(' ',20X,'*****STEP 4*****')
      DO 232 I=1,NSUBC
  232 WRITE(6,233) I,(Z(I,J),J=1,NDIM)
  233 FORMAT(' ',' I=',I2,5X,'Z=',10E12.4/' ',11X,10E12.4/' ',11X,10E12.4
     1/' ',11X,8E12.4/)
      DO 234 K=1,NDGRPS
  234 WRITE(6,235) K,IPSDST(K)
  235 FORMAT(' ','K=',I2,5X,'IPSDST=',I2)
      DO 236 I=1,NSUBC
  236 WRITE(6,65) I,ISET(I)
      IF(ITRN .GT. ITRNS) GO TO 575
C
C       ++++++++++++++++++++++++++++++++++++++++++++++++++++++++++++++++
C       +  STEP 5 MISODATA:  COMPUTE THE AVERAGE DISTANCE OF SAMPLES IN  +
C       +                    CLUSTER CENTER DOMAIN FROM THEIR            +
C       +                    CORRESPONDING CLUSTER CENTER                +
C       ++++++++++++++++++++++++++++++++++++++++++++++++++++++++++++++++
C
C       COMPUTE NEW CLUSTER CENTER-SAMPLE DISTANCES
  240 CALL ZIP(1)
```

```
C
C      COMPUTE AVERAGE CLUSTER CENTER-SAMPLE DISTANCES, DBAR(KCH)
C
       DO 250 IX=1,NSUBC
  250  DBAR(IX)=0.0
       DO 260 IY=1,NDGRPS
  260  DBAR(IPSDST(IY))=DBAR(IPSDST(IY))+D(IPSDST(IY),IY)
       DO 270 IZ=1,NSUBC
  270  DBAR(IZ)=DBAR(IZ)/ISET(IZ)
       WRITE(6,271)
  271  FORMAT(' ',20X,'*****STEP 5*****')
       DO 272 I=1,NSUBC
  272  WRITE(6,273) I,DBAR(I)
  273  FORMAT(' ','I=',I2,5X,'DBAR=',E13.6)
C
C      ++++++++++++++++++++++++++++++++++++++++++++++++++++++++++++++++
C      +  STEP 6 MISODATA:  COMPUTE THE OVERALL AVERAGE DISTANCE OF THE +
C      +                    SAMPLES FROM THEIR RESPECTIVE CLUSTER       +
C      +                    CENTERS (DBART)                             +
C      ++++++++++++++++++++++++++++++++++++++++++++++++++++++++++++++++
C
C
  280  DBART=0.0
       DO 290 JU=1,NSUBC
  290  DBART=DBART+ISET(JU)*DBAR(JU)
       DBART=DBART/NDGRPS
       WRITE(6,291)
  291  FORMAT(' ',20X,'*****STEP 6*****')
       WRITE(6,692) DBART
  692  FORMAT(' ','DBART=',E13.6)
C
C      ++++++++++++++++++++++++++++++++++++++++++++++++++++++++++++++++
C      +  STEP 7 MISODATA:  CONDITIONAL BRANCHING                      +
C      ++++++++++++++++++++++++++++++++++++++++++++++++++++++++++++++++
C
```

```
  295 IF(ITRN .LT. ITRNS) GO TO 300
      THETAC=0
      GO TO 400
  300 IF(FLOAT(NSUBC) .LE. FLOAT(KLUSD)/2.0) GO TO 310
      IF(NSUBC .GE. 2*KLUSD  .OR.  (ITRN/2)*2 .EQ. ITRN) GO TO 400
C
C     ++++++++++++++++++++++++++++++++++++++++++++++++++++++++++++++++++++
C     +  STEP 8 MISODATA:  FIND STANDARD ERROR VECTOR                    +
C     ++++++++++++++++++++++++++++++++++++++++++++++++++++++++++++++++++++
C
C     INITIALIZE SIGSD(KCH,N) TO ZERO
  310 DO 320 KCH=1,NSUBC
      DO 320 N=1,NDIM
  320 SIGSD(KCH,N)=0.0
C     SUM SQUARES OF COMPONENTS; IPSDST(I) TRANSFORMS TO KCH
      DO 330 N=1,NDIM
      DO 330 I=1,NDGRPS
  330 SIGSD(IPSDST(I),N)=SIGSD(IPSDST(I),N)+(PSD(I,N)-Z(IPSDST(I),N))**2
C     CALCULATE SIGSD
      DO 340 KCH=1,NSUBC
      DO 340 NN=1,NDIM
      SIGSD(KCH,NN)=SQRT(SIGSD(KCH,NN)/ISET(KCH))
  340 SIGSD(KCH,NN)=SIGSD(KCH,NN)/Z(KCH,NN)
      WRITE(6,341)
  341 FORMAT(' ',20X,'*****STEP 8*****')
      DO 342 I=1,NSUBC
  342 WRITE(6,343) I,(SIGSD(I,J),J=1,NDIM)
  343 FORMAT(' ','SIGSD(',I2,')=',10E12.4/' ',10X,10E12.4/' ',10X,
     110E12.4/' ',10X,8E12.4/)
      DO 345 IKH=1,NSUBC
      AVESE1=0.0
      DO 344 JKH=1,NDIM
  344 AVESE1=AVESE1+SIGSD(IKH,JKH)
      AVESE(IKH)=AVESE1/NDIM
  345 WRITE(6,346) IKH,AVESE(IKH)
```

```
  346 FORMAT(' ','AVERAGE STANDARD ERROR(',I2,')=',F7.4/)
C
C     ++++++++++++++++++++++++++++++++++++++++++++++++++++++++++++++++++++++
C     +  STEP 9 MISODATA:  FIND MAXIMUM COMPONENT OF EACH SIGSD(KCH)    +
C     ++++++++++++++++++++++++++++++++++++++++++++++++++++++++++++++++++++++
C
  350 DO 360 KCH=1,NSUBC
      SIGMAX(KCH)=SIGSD(KCH,1)
      ISIGMX(KCH)=1
      DO 360 NM=2,NDIM
      IF(SIGMAX(KCH) .GE. SIGSD(KCH,NM)) GO TO 360
      SIGMAX(KCH)=SIGSD(KCH,NM)
      ISIGMX(KCH)=NM
  360 CONTINUE
      WRITE(6,361)
  361 FORMAT(' ',20X,'*****STEP 9*****')
      DO 362 I=1,NSUBC
  362 WRITE(6,363) I,ISIGMX(I),SIGMAX(I)
  363 FORMAT(' ','I=',I2,5X,'ISIGMX=',I2,5X,'SIGMAX=',E13.6)
C
C     ++++++++++++++++++++++++++++++++++++++++++++++++++++++++++++++++++++++
C     +  STEP 10 MISODATA:  SPLIT Z(KCH) INTO Z+ AND Z- IF CONDITIONS    +
C     +                     WARRANT.  LET GAMMA=0.5                       +
C     ++++++++++++++++++++++++++++++++++++++++++++++++++++++++++++++++++++++
C
  370 KCH=1
  375 IF(AVESE(KCH) .GT. THETAS  .AND.  ((DBAR(KCH) .GT. DBART  .AND.
     1ISET(KCH) .GT. 2*(THETAN+1))   .OR.   FLOAT(NSUBC) .LE. FLOAT(KLUS
     2D)/2.0)) GO TO 380
      KCH=KCH+1
      IF(KCH .LE. NSUBC) GO TO 375
      GO TO 400
C     SPLIT Z(KCH) IN TO Z+ AND Z-; Z+ IS FIRST; Z- IS SHIFTED TO NSUBC+1
  380 WRITE(6,381) KCH
  381 FORMAT(' ',20X,'*****STEP 10*****'/' ','CENTER BEING SPLIT=',I2)
```

```
      DO 385 KDIM=1,NDIM
  385 Z(KCH,KDIM)=Z(KCH,KDIM)+0.5*SIGSD(KCH,KDIM)*Z(KCH,KDIM)
      NSUBC=NSUBC+1
      DO 390 JDIM=1,NDIM
  390 Z(NSUBC,JDIM)=Z(KCH,JDIM)/(1.0+0.5*SIGSD(KCH,JDIM))-0.5*SIGSD(KCH,
     1JDIM)*Z(KCH,JDIM)/(1.0+0.5*SIGSD(KCH,JDIM))
      KLUB=0
      DO 391 IS=1,NSUBC
  391 WRITE(6,233) IS,(Z(IS,IT),IT=1,NDIM)
      GO TO 60
C
C     ++++++++++++++++++++++++++++++++++++++++++++++++++++++++++++++++
C     +  STEP 11 MISODATA:  COMPUTE CLUSTER CENTER-CLUSTER CENTER    +
C     +                     DISTANCES DD(KCH,JCH)                    +
C     ++++++++++++++++++++++++++++++++++++++++++++++++++++++++++++++++
C
C     INITIALIZE DD TO ZERO
  400 DO 410 KCH=1,NSUBC
      DO 410 JCH=1,NSUBC
  410 DD(KCH,JCH)=0.0
C     CALCULATE DISTANCES
      IF(NSUBC .EQ. 1) GO TO 450
      JOCK=NSUBC-1
      DO 440 KCH=1,JOCK
      KCH1=KCH+1
      DO 430 JCH=KCH1,NSUBC
      DO 420 MDA=1,NDIM
  420 DD(KCH,JCH)=DD(KCH,JCH)+(Z(KCH,MDA)-Z(JCH,MDA))**2
      DD(KCH,JCH)=SQRT(DD(KCH,JCH))
  430 CONTINUE
  440 CONTINUE
      WRITE(6,441)
  441 FORMAT(' ',20X,'*****STEP 11*****')
      DO 442 I=1,NSUBC
  442 WRITE(6,443) I,(DD(I,J),J=I,NSUBC)
```

```
  443 FORMAT(' ',' I=',I2,5X,'DD=',10E12.4/' ',12X,10E12.4/' ',12X,
     110E12.4)
C
C     ++++++++++++++++++++++++++++++++++++++++++++++++++++++++++++++++
C     +  STEP 12 MISODATA:  COMPARE DD(KCH,JCH) AGAINST THETAC AND   +
C     +                     ARRANGE LCLMAX SMALLEST DISTANCES LESS   +
C     +                     THAN THETAC IN ASCENDING ORDER           +
C     ++++++++++++++++++++++++++++++++++++++++++++++++++++++++++++++++
C
  450 IF(LCLMAX .LE. 0  .OR.  NSUBC .EQ. 1) GO TO 570
      WRITE(6,461)
  461 FORMAT(' ',20X,'*****STEP 12*****')
      ICOUNT=1
      NSUBC1=NSUBC-1
      DO 460 KCH=1,NSUBC1
      KCH1=KCH+1
      DO 460 JCH=KCH1,NSUBC
      IF(DD(KCH,JCH) .GE. THETAC) GO TO 460
      ICRSA(ICOUNT)=KCH
      ICRSB(ICOUNT)=JCH
      ICOUNT=ICOUNT+1
  460 CONTINUE
      IF(ICOUNT .EQ. 1) GO TO 570
C     ARRANGE LCLMAX SMALLEST DISTANCES IN ASCENDING ORDER USING LIBRARY
C     SUBROUTINE ABSRT
      LCL=ICOUNT-1
      DO 462 JAKL=1,LCL
  462 WRITE(6,463) JAKL,ICRSA(JAKL),ICRSB(JAKL)
  463 FORMAT(' ',' I=',I2,5X,'ICRSA=',I3,5X,'ICRSB=',I3)
      DO 470 IA=1,LCL
  470 ASORT(IA)=DD(ICRSA(IA),ICRSB(IA))
      DO 471 ICK=1,LCL
  471 WRITE(6,472) ICK,ASORT(ICK)
  472 FORMAT(' ',' I=',I2,5X,'ASORT=',E13.6)
      CALL ABSRT(LCL,ASORT)
```

```
      NMAXL=LCLMAX
      WRITE(6,473) NMAXL
  473 FORMAT(' ','NMAXL=',I2)
      IF(LCL .LT. LCLMAX) NMAXL=LCL
      WRITE(6,473) NMAXL
      DO 490 IB=1,NMAXL
      DO 480 KCH=1,NSUBC
      KCH1=KCH+1
      DO 480 JCH=KCH1,NSUBC
      IF(DD(KCH,JCH) .NE. ASORT(IB)) GO TO 480
      ICRSC(IB)=KCH
      ICRSD(IB)=JCH
      GO TO 490
  480 CONTINUE
  490 CONTINUE
      DO 491 I=1,NMAXL
  491 WRITE(6,492) I,ICRSC(I),ICRSD(I),DD(ICRSC(I),ICRSD(I))
  492 FORMAT(' ','I=',I2,5X,'DD(',I2,',',I2,')=',E13.6)
C
C     ++++++++++++++++++++++++++++++++++++++++++++++++++++++++++++++++++
C     +  STEP 13 MISODATA:  LUMP CLUSTER CENTERS FOR SMALLEST DD'S     +
C     ++++++++++++++++++++++++++++++++++++++++++++++++++++++++++++++++++
C
      WRITE(6,495)
  495 FORMAT(' ',20X,'*****STEP 13*****')
  500 INEXT=1
      JNEXT=1
      DO 540 KJIB=1,NMAXL
      IF(KJIB .EQ. 1) GO TO 520
      KCH2=INEXT-1
      DO 510 KBUG=1,KCH2
      IF(ICRSC(KJIB) .EQ. IJOIN(KBUG)  .OR.  ICRSD(KJIB) .EQ.
     1IJOIN(KBUG)) GO TO 540
  510 CONTINUE
  520 IJOIN(INEXT)=ICRSC(KJIB)
```

```
      WRITE(6,521) INEXT,IJOIN(INEXT)
  521 FORMAT(' ','IJOIN(',I2,')=',I2)
      INEXT=INEXT+1
      IJOIN(INEXT)=ICRSD(KJIB)
      WRITE(6,521) INEXT,IJOIN(INEXT)
      INEXT=INEXT+1
      IELIM(JNEXT)=ICRSD(KJIB)
      JNEXT=JNEXT+1
C     CALCULATE LUMPED CLUSTER CENTERS
      DO 530 LAZY=1,NDIM
  530 Z(ICRSC(KJIB),LAZY)=(ISET(ICRSC(KJIB))*Z(ICRSC(KJIB),LAZY)+ISET(IC
     1RSD(KJIB))*Z(ICRSD(KJIB),LAZY))/(ISET(ICRSC(KJIB))+ISET(ICRSD(KJIB
     2)))
      WRITE(6,532) (Z(ICRSC(KJIB),IFT),IFT=1,NDIM)
  532 FORMAT(' ','Z=',10F10.5)
  540 CONTINUE
C     ELIMINATE CENTERS ALREADY USED IN LUMPING AND SHIFT DATA DOWN
C     TO (NSUBC-(JNEXT-1)) LEVELS
      KNEXT=JNEXT-1
      DO 560 LDOG=1,KNEXT
      I1=IELIM(LDOG)
      I2=NSUBC-1
      DO 550 ISTEP=I1,I2
      DO 550 IDIM=1,NDIM
  550 Z(ISTEP,IDIM)=Z((ISTEP+1),IDIM)
  560 NSUBC=NSUBC-1
      NCHECK=1
C
C     ++++++++++++++++++++++++++++++++++++++++++++++++++++++++++++++++
C     +  STEP 14 MISODATA:  OUTPUT FINAL RESULTS                     +
C     ++++++++++++++++++++++++++++++++++++++++++++++++++++++++++++++++
C
  570 WRITE(6,571)
  571 FORMAT(' ',20X,'*****STEP 14*****')
      DO 572 I=1,NSUBC
```

```
  572 WRITE(6,233) I,(Z(I,J),J=1,NDIM)
      GO TO 60
C     JOB FINISHED-WRITE RESULTS
  575 IF(NCHECK .EQ. 1) CALL ZIP(0)
      WRITE(6,580)
  580 FORMAT('1','CLUSTER CENTERS'/' ','------- -------'///)
      DO 590 KCH=1,NSUBC
  590 WRITE(6,600) KCH,(Z(KCH,J),J=1,NDIM)
  600 FORMAT(' ','Z(',I2,')=',10E12.4/' ',6X,10E12.4/' ',6X,10E12.4/' ',
     16X,8E12.4/)
      WRITE(6,610)
  610 FORMAT('1','SAMPLE NUMBER',10X,'CLUSTER CENTER'/' ','------ ------
     1',10X,'------- ------'///)
      DO 620 KCH=1,NDGRPS
  620 WRITE(6,630) KCH,IPSDST(KCH)
  630 FORMAT(' ',I8,22X,I4)
      WRITE(6,640)
  640 FORMAT('1','CLUSTER CENTER',10X,'NUMBER OF MEMBERS',10X,'AVERAGE S
     1TANDARD ERROR'/' ','------- ------',10X,'------ -- -------',10X,
     2'------- -------- -----'///)
      DO 650 KCH=1,NSUBC
  650 WRITE(6,660) KCH,ISET(KCH),AVESE(KCH)
  660 FORMAT(' ',6X,I2,24X,I2,25X,F6.4)
      RETURN
      END
```

```
      SUBROUTINE ZIP(IGO)
C     ***************************************************************
C     *                                                             *
C     *     CALCULATE CLUSTER CENTER(KCH)-SAMPLE(I) DISTANCES WITH  *
C     *     OPTION OF ASSIGNING SAMPLES TO CLUSTER SUBSET           *
C     *                                                             *
C     ***************************************************************
      DIMENSION PSD(25,38)
      DIMENSION Z(25,38),D(25,25)
      DIMENSION IPSDST(25),ISET(25)
      COMMON/POWER/PSD
      COMMON/PARAM1/NDGRPS,NDIM,NSUBC,Z,D,IPSDST,ISET
      DO 20 KCH=1,NSUBC
      DO 20 I=1,NDGRPS
      D(KCH,I)=0.0
      DO 10 LDUCK=1,NDIM
   10 D(KCH,I)=D(KCH,I)+(PSD(I,LDUCK)-Z(KCH,LDUCK))**2
   20 D(KCH,I)=SQRT(D(KCH,I))
      IF(IGO .GT. 0) RETURN
C     ASSIGN EACH SAMPLE TO A CLUSTER CENTER USING THE LEAST MEAN
C     SQUARE DISTANCE
      DO 30 I=1,NDGRPS
      IPSDST(I)=1
      IF(NSUBC .EQ. 1) GO TO 30
      DMIN=D(1,I)
      DO 25 KCH=2,NSUBC
      IF(D(KCH,I) .GE. DMIN) GO TO 25
      IPSDST(I)=KCH
      DMIN=D(KCH,I)
   25 CONTINUE
   30 CONTINUE
C     DETERMINE THE NUMBER OF SAMPLES IN EACH CLUSTER CENTER
      DO 40 J=1,NSUBC
   40 ISET(J)=0
      DO 50 I=1,NDGRPS
```

```
50  ISET( IPSDST( I ))=ISET( IPSDST( I ))+1
    WRITE(6,55)
55  FORMAT('-',25X,'*****ZIP*****')
    DO 60  J=1,NDGRPS
60  WRITE(6,70)  J,(D( I,J),I=1,NSUBC)
70  FORMAT(' ','D(',I2,')=',10E12.4/' ',6X,10E12.4/' ',6X,10E12.4/' ',
   16X,8E12.4/)
    RETURN
    END
```

XI. APPENDIX D: NORMALIZED NOISE SIGNATURES (SAMPLE PATTERNS) FOR THE 16-09C LPRM

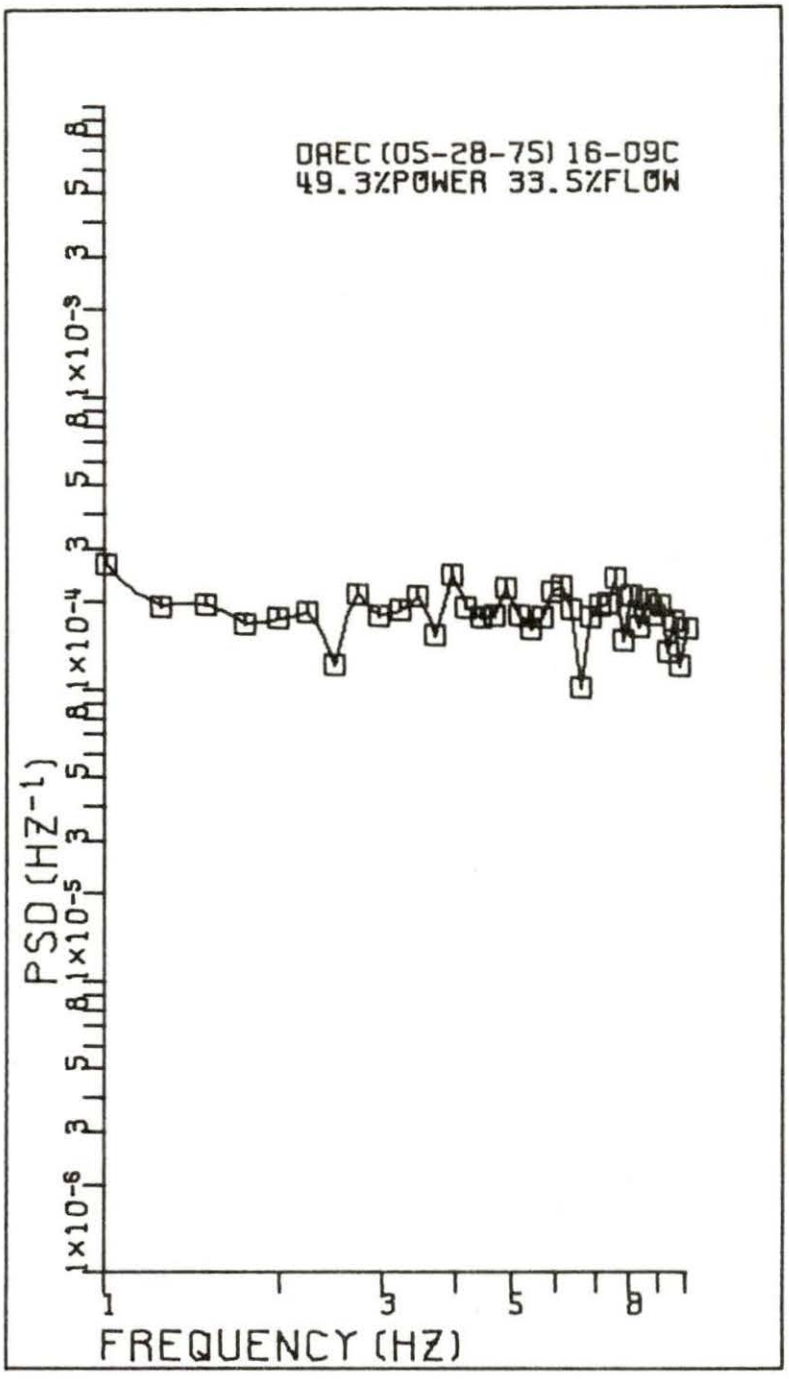

Figure D.1. Sample pattern #1 (May 28, 1975).

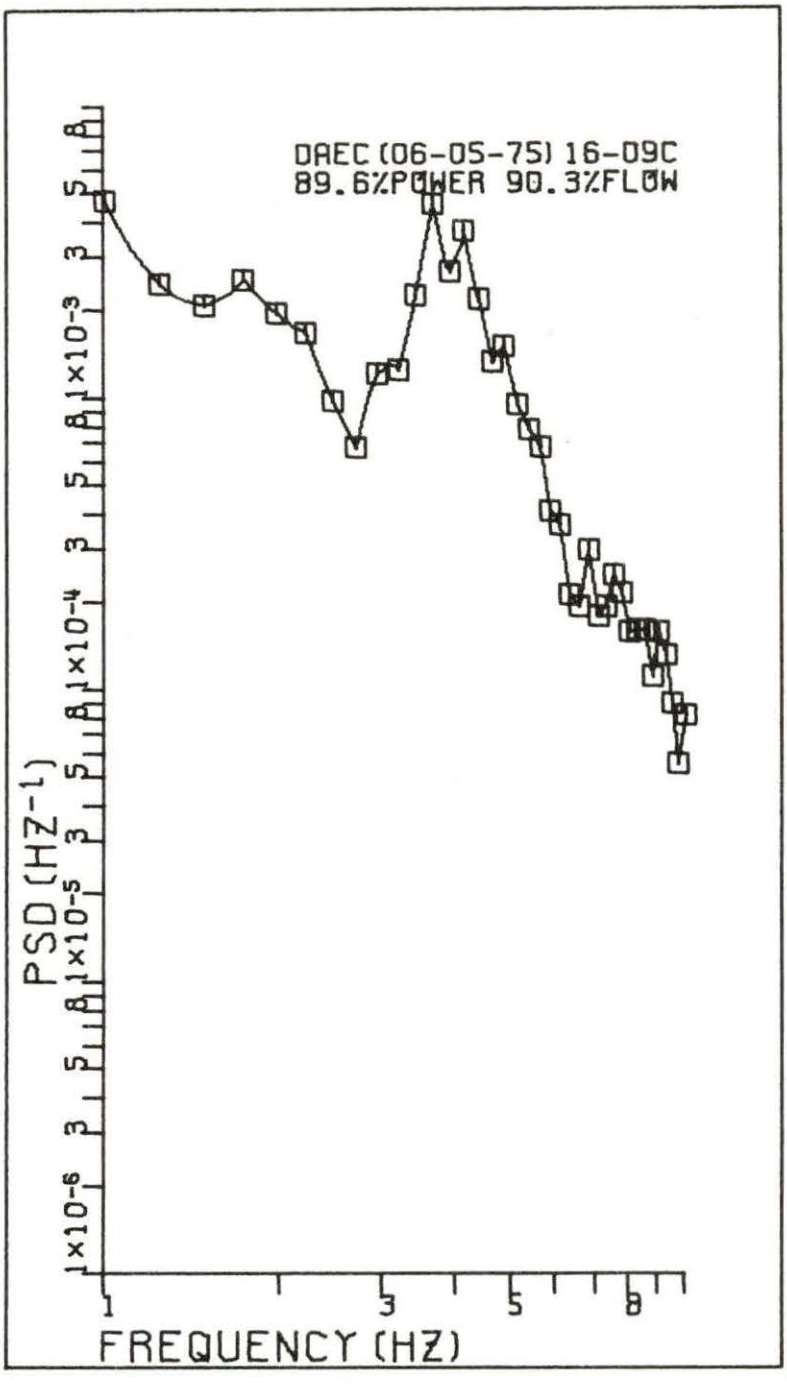

Figure D.2. Sample pattern #2 (June 5, 1975).

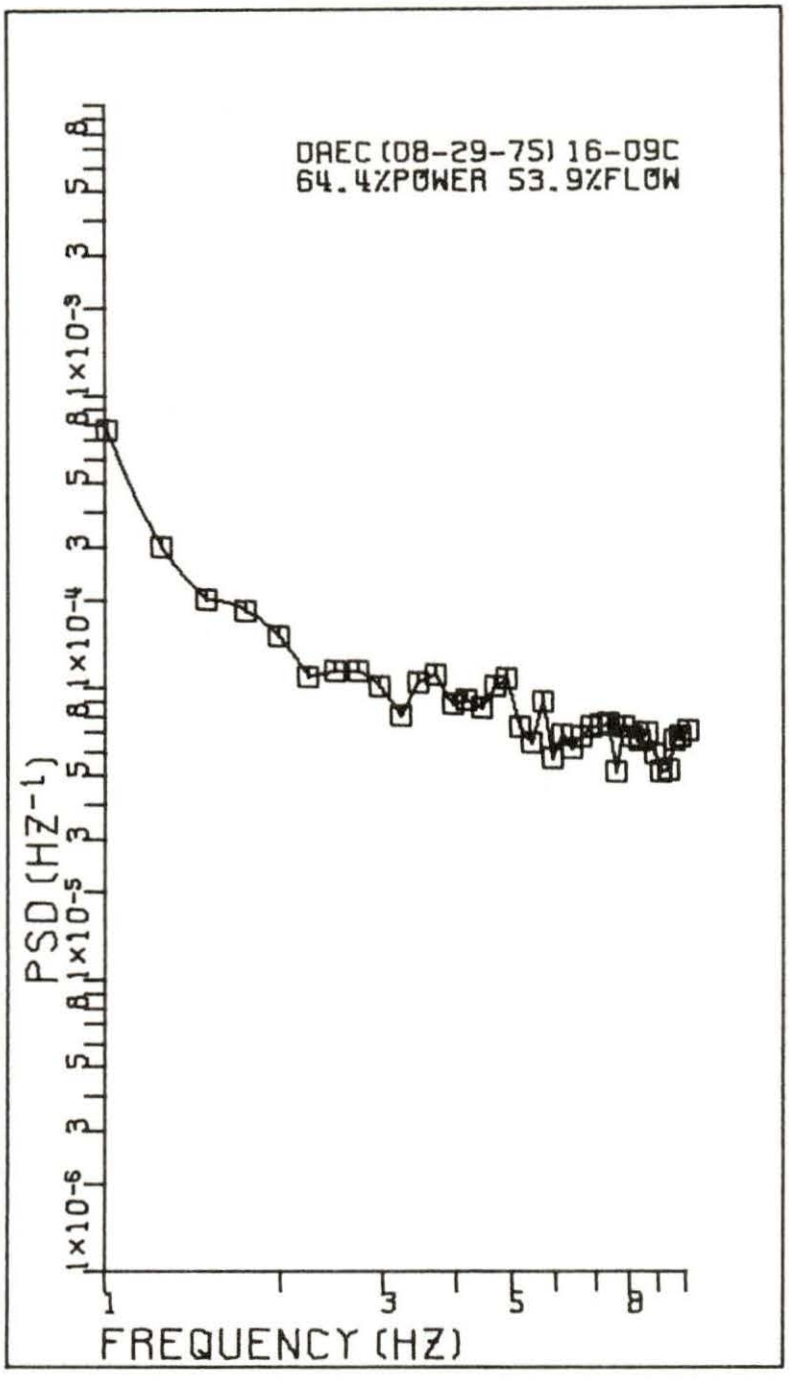

Figure D.3. Sample pattern #3 (August 29, 1975).

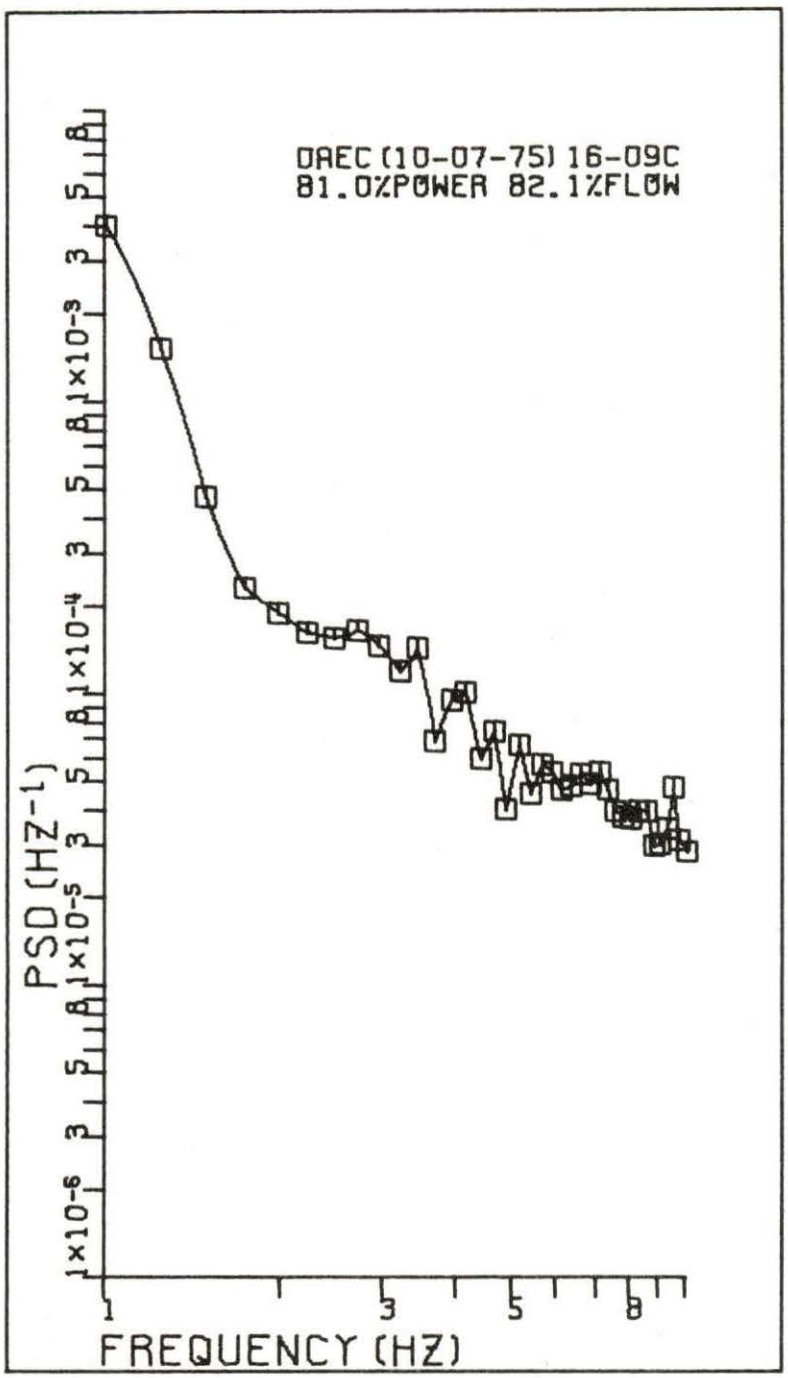

Figure D.4. Sample pattern #4 (October 7, 1975).

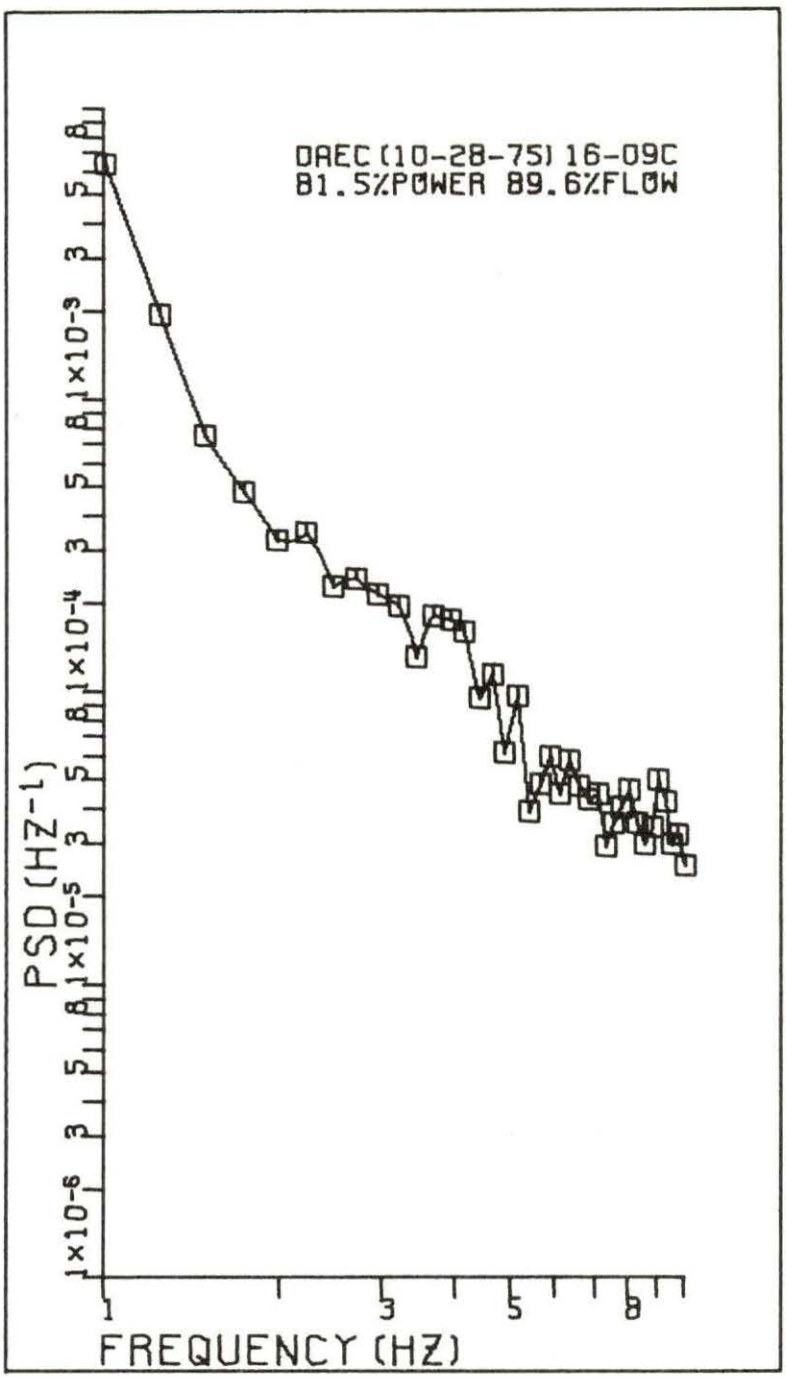

Figure D.5. Sample pattern #5 (October 28, 1975).

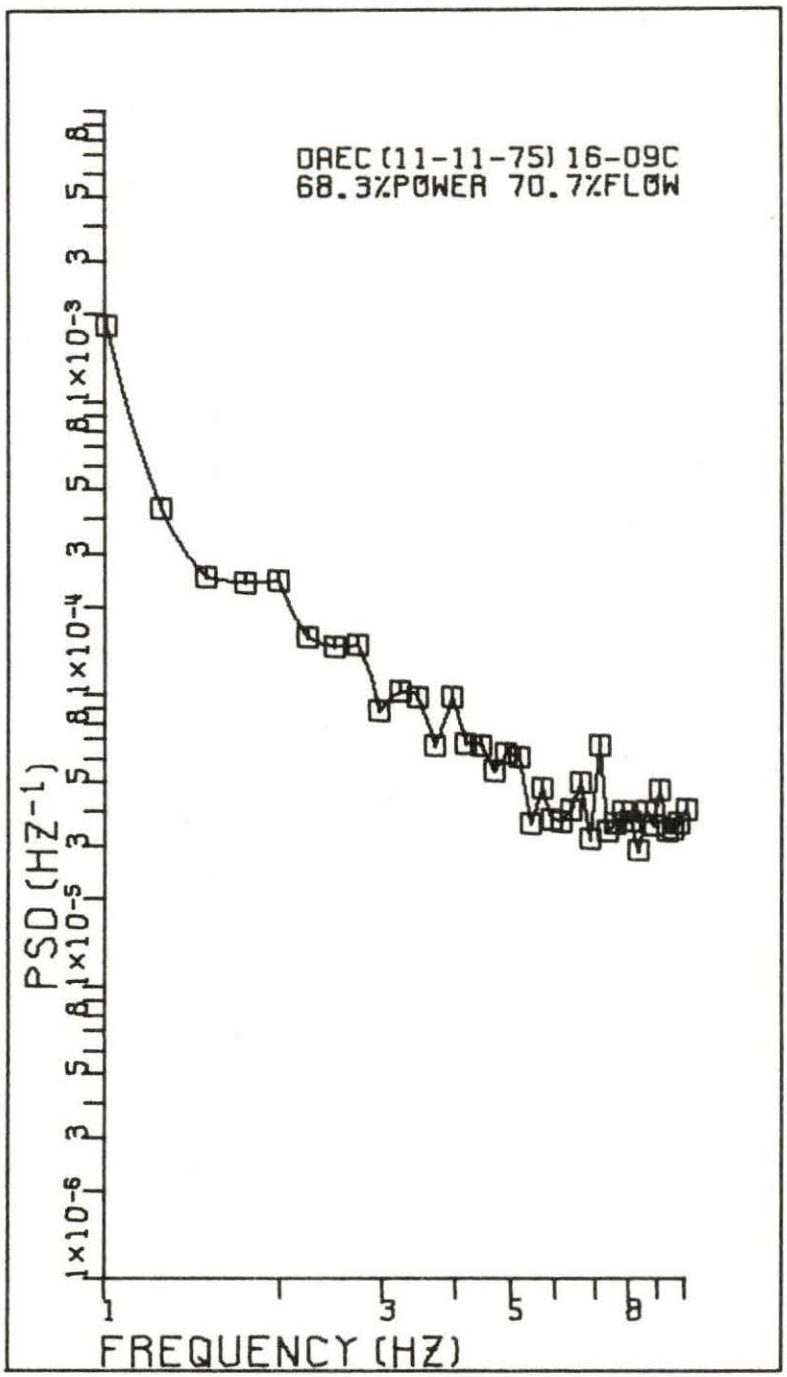

Figure D.6. Sample pattern #6 (November 11, 1975).

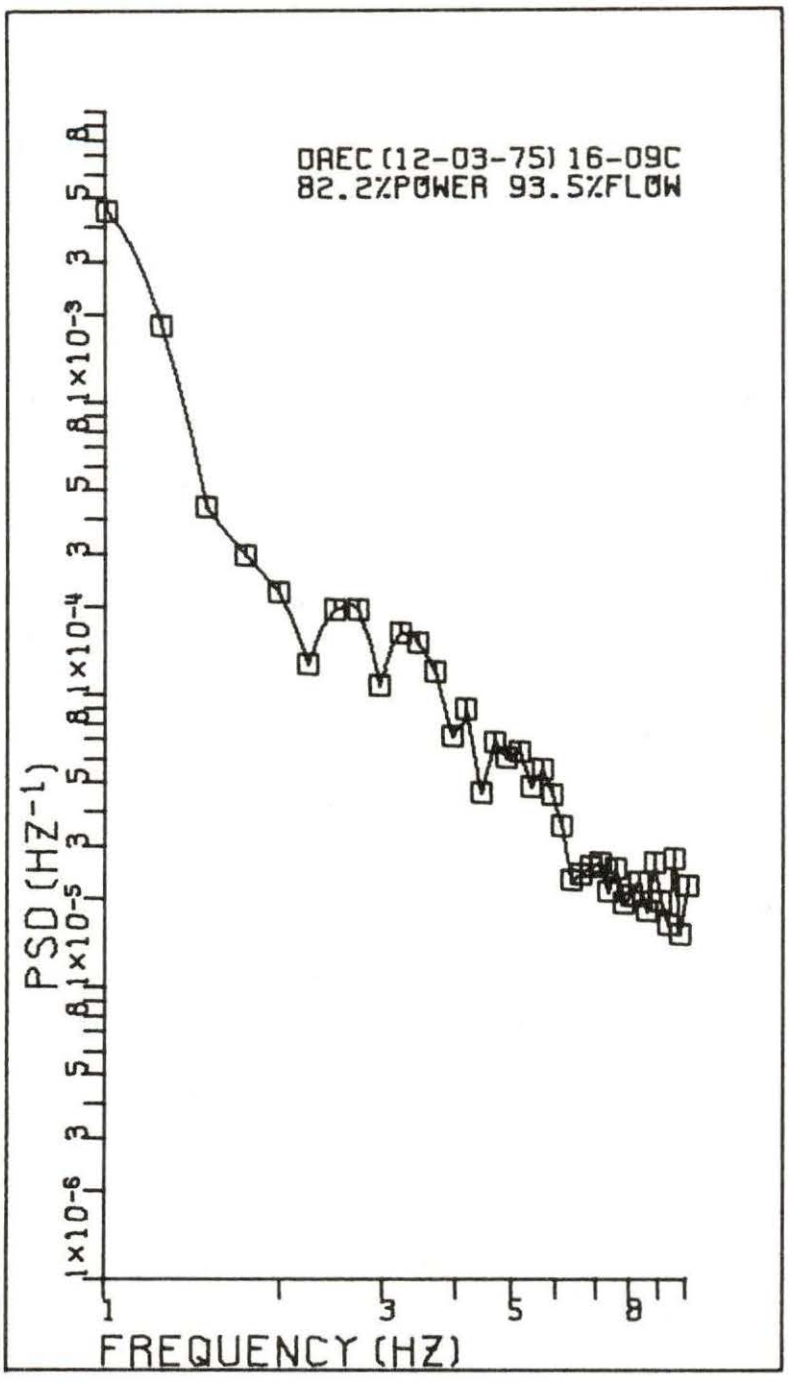

Figure D.7. Sample pattern #7 (December 3, 1975).

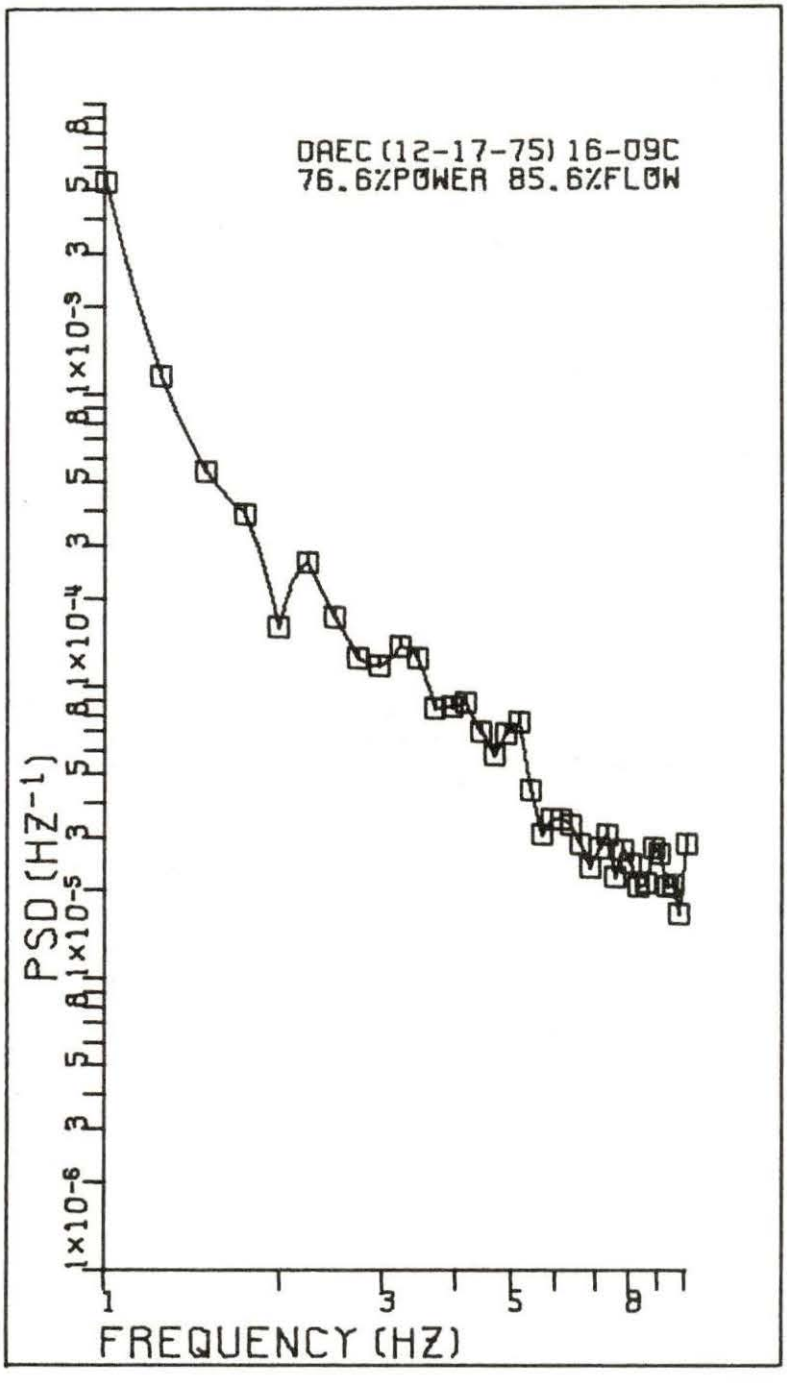

Figure D.8. Sample pattern #8 (December 17, 1975).

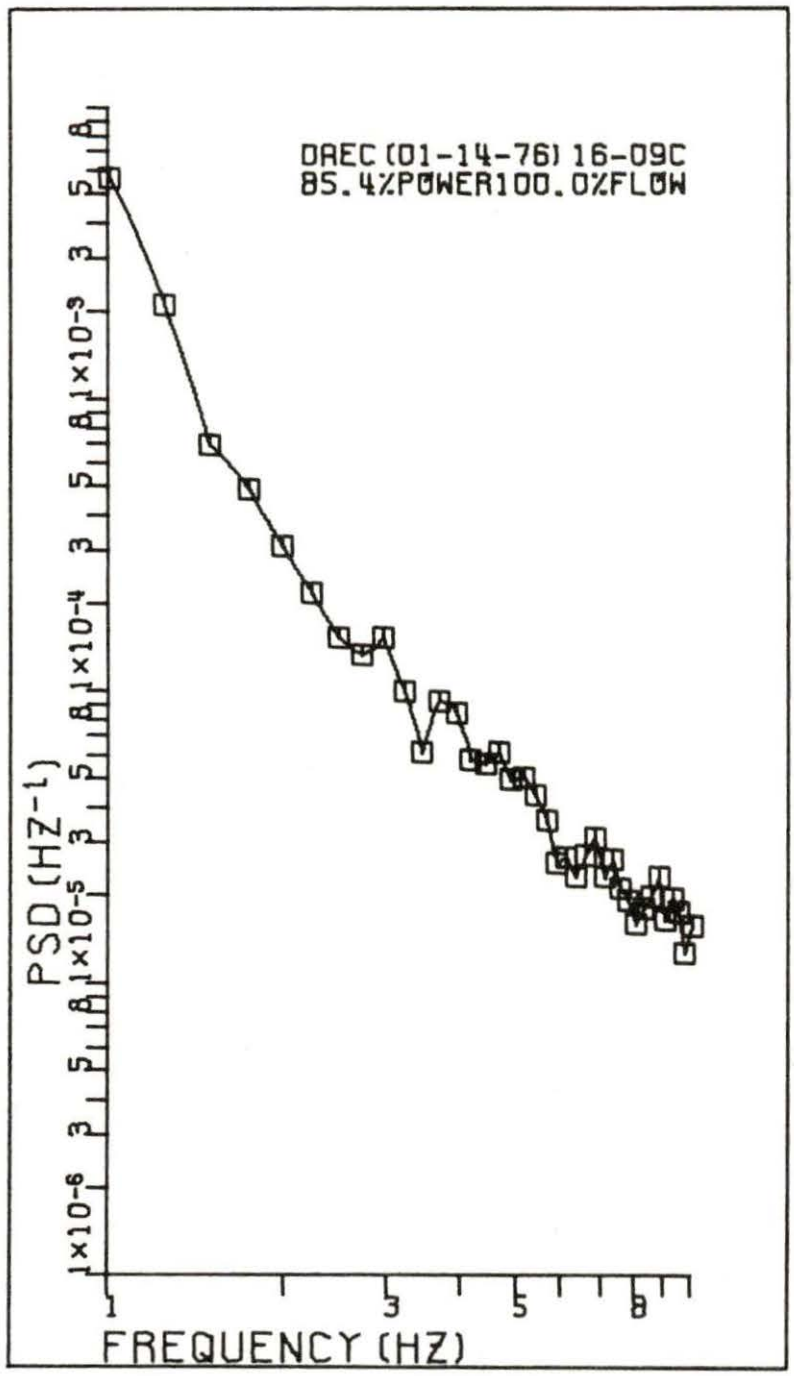

Figure D.9. Sample pattern #9 (January 14, 1976).

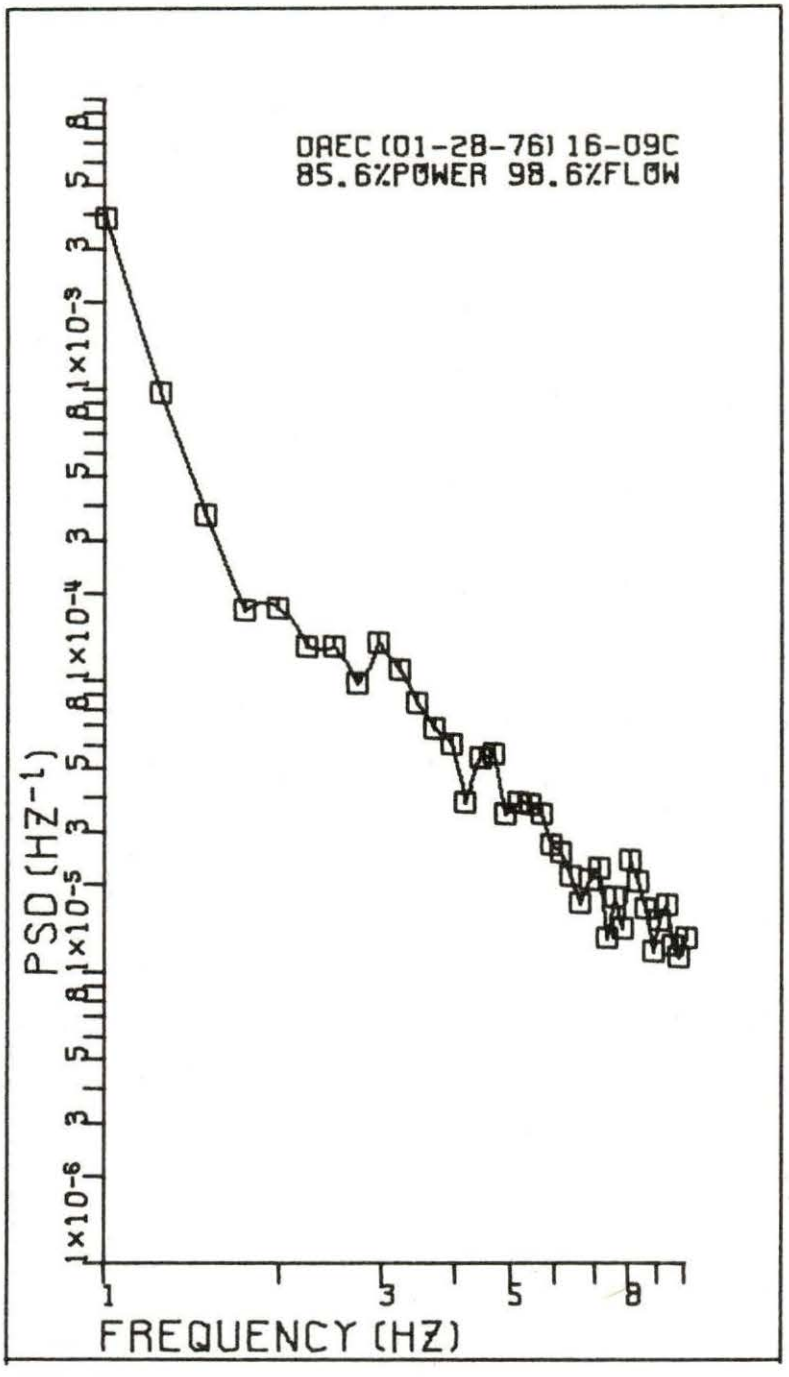

Figure D.10. Sample pattern #10 (January 28, 1976).

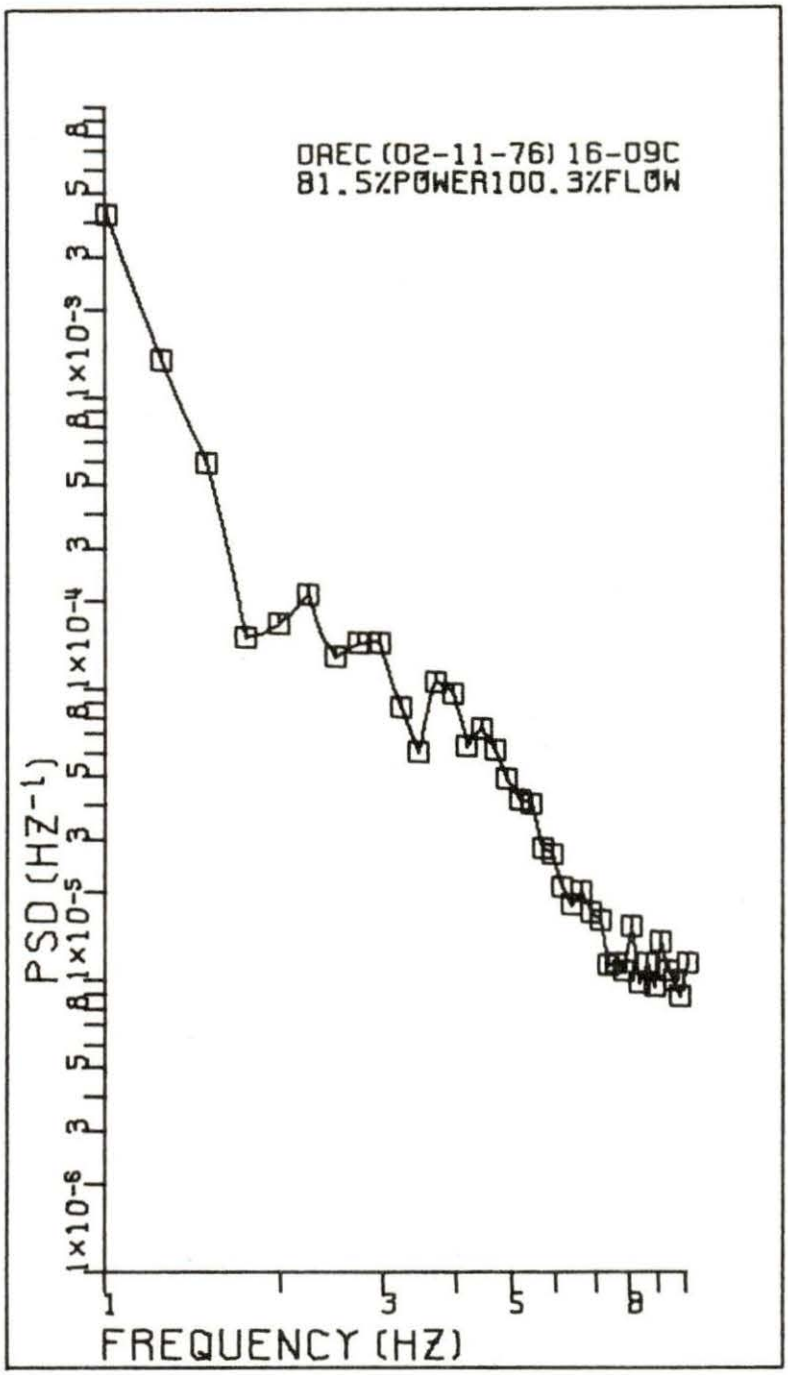

Figure D.11. Sample pattern #11 (February 11, 1976).

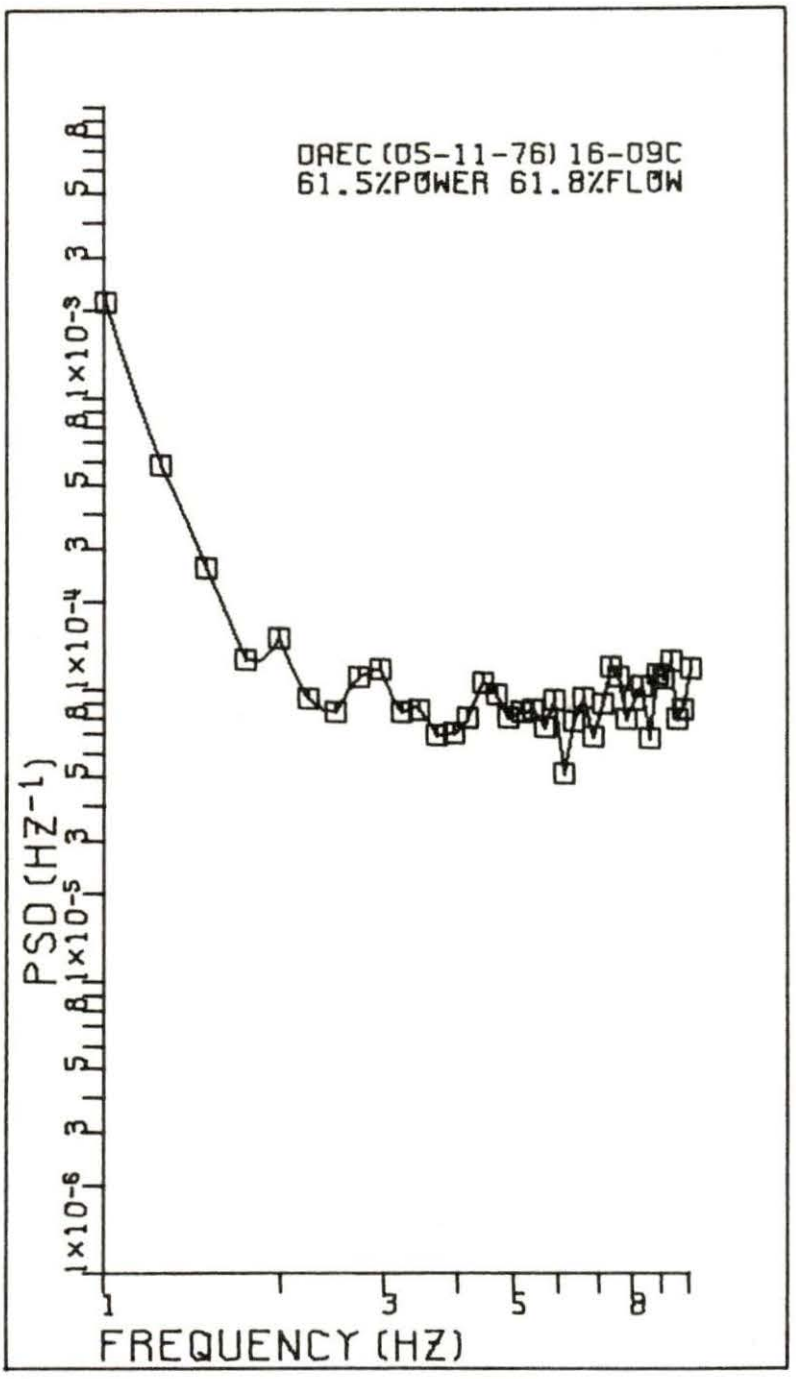

Figure D.12. Sample pattern #12 (May 11, 1976).